Mixed Rossby-Gravity waves and their association with the intrusion of extratropical disturbances

विद्या वाचस्पति की
उपाधि की अपेक्षाओं की आंशिक पूर्ति में प्रस्तुत शोध प्रबंध

A thesis submitted in partial fulfillment of the requirements of the degree of Doctor of Philosophy

द्वारा / By

श्रेया केशरी/ Shreya Keshri

पंजीकरण सं. २०१८३६०८/ Registration No.: 20183608

शोध प्रबंध पर्यवेक्षक : सुहास एट्टम्मल
/ Thesis Supervisor : Suhas Ettammal

IISER PUNE

भारतीय विज्ञान शिक्षा एवं अनुसंधान संस्थान पुणे
INDIAN INSTITUTE OF SCIENCE EDUCATION AND RESEARCH PUNE

2024

Declaration by Student

Name of Student : Shreya Keshri

Reg. No. : 20183608

Thesis Supervisor(s) : Dr. Suhas Ettammal

Department : Earth and Climate Science
Date of joining program : 01 August 2018

Date of Pre-Synopsis Seminar : 08 February 2024

Title of Thesis : Mixed Rossby-Gravity waves and their association with the intrusion of extratropical disturbances

I declare that this written submission represents my idea in my own words and where others' ideas have been included; I have adequately cited and referenced the original sources. I declare that I have acknowledged collaborative work and discussions wherever such work has been included. I also declare that I have adhered to all principles of academic honesty and integrity and have not misrepresented or fabricated or falsified any idea/data/fact/source in my submission. I understand that violation of the above will be cause for disciplinary action by the Institute and can also evoke penal action from the sources which have thus not been properly cited or from whom proper permission has not been taken when needed.

The work reported in this thesis is the original work done by me under the guidance of

Dr./Prof. : Suhas Ettammal

Date : 09 August 2024

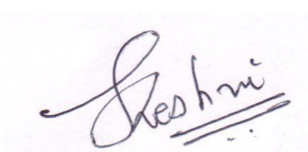

Signature of student

CERTIFICATE

Certified that the work incorporated in the thesis entitled "Mixed Rossby-Gravity waves and their association with the intrusion of extratropical disturbances"

Submitted by Shreya Keshri was carried out by the candidate, under my supervision. The work presented here or any part of it has not been included in any other thesis submitted previously for the award of any degree or diploma from any other University or institution.

(Supervisor)

Date: 9/8/2024

Acknowledgements

I wish to convey my profound appreciation to everyone who has contributed to the successful completion of this dissertation.

This thesis was made possible through the unconditional, consistent, and devoted support of my supervisor, Dr. Suhas Ettammal. I extend my deepest and most sincere gratitude for his mentorship, knowledge, and expertise. Sir's guidance and insightful critiques have profoundly influenced the direction and realization of this research. In challenging times, he was my greatest supporter, directing me towards the right path. More than just a mentor, he has been a life coach, guiding me with patience and care, introducing me to great literature that expanded my horizons, and teaching me invaluable lessons in punctuality, responsibility, and honesty. His belief in me has been the foundation of my achievements, and for that, I am forever grateful.

I would also like to thank the members of my research advisory committee, Dr. Joy Merwin Monteiro and Dr. Sabin Thazhe Purayil, for their constructive feedback and encouragement. I wish to express my gratitude to Dr. Neena Joseph Mani for her support, guidance, and positivity throughout my Ph.D. journey. I am also deeply thankful to Prof. B. N. Goswami for his time during his visits to Pune, offering support and encouragement whenever possible. His insightful feedback and comments, filled with the wisdom of his experience, were always delivered with positivity and humility.

My gratitude extends to my academic peers and lab mates in the Department of Earth and Climate Science for creating a stimulating and enjoyable working environment. Their camaraderie has made this demanding journey both memorable and fulfilling.

I am also thankful for the inspiration and support from many friends at IISER Pune and beyond, including Arpit Goel, Aakansha Negi, Dipal Jain, Pragyant Behera, Madhura Bhattacharjee, Sugandha Negi, Venugopal Kella, Amy Binny Philip, and Risabh Sinha, who have provided both professional and personal support.

Lastly, I would like to express my deepest gratitude to my parents and my sister, Simran, for their unwavering love and support. Mummy and Simran, I love you both dearly. Thank you for always being there and providing me with all the love and encouragement I needed. I could not have achieved any of this without you.

Contents

Acknowledgements 4

Contents 6

Abstract 8

1 Introduction 10

2 A survey of intrusion episodes of the extratropical disturbances into the tropics 17

2.1. Introduction 17

2.2. Data and Methodology 22

2.3. Results and Discussions 24

2.4. Summary and Conclusions 30

3 MRG waves and their association with the intrusion of extratropical disturbances 32

3.1. Introduction 32

3.2. Data and Methodology 36

3.3. Results and Discussions 42

3.4. Summary and Conclusions 55

4 Doppler shifted eastward propagating MRG waves 59

4.1. Introduction 59

4.2. Data and Methodology 65

4.3. Results and Discussions 68

4.4. Summary and Conclusions 79

5 Summary and Conclusions **81**

6 References **84**

7 Published papers **100**

Abstract

Mixed Rossby-Gravity waves and their association with the intrusion of extratropical disturbances

Mixed Rossby-gravity (MRG) waves are tropical synoptic-scale disturbances which exhibit mixed properties of low frequency Rossby waves and high frequency gravity waves. A comprehensive understanding on the major factors that aid the growth and maintenance of the MRG waves is crucial for improving the weather and subseasonal forecast skills in the tropics. Based on the location of its origin, the physical processes that cause the occurrence of MRG waves are generally classified into two groups, in situ and external forcing mechanisms. Extratropical disturbances are considered as the major external forcing that impacts the occurrence of MRG waves. Despite many modeling and observational studies that suggest extratropical disturbances as a crucial element in the genesis of MRG waves, its contribution in the growth and maintenance of the MRG waves are not known.

In the current study, as a first step to address this important issue, we primarily focus on quantifying the association between the intrusion of extratropical disturbances and the occurrence of the MRG waves. Since both the intrusion of extratropical disturbances and MRG waves exhibit episodic character, identification of both the disturbances as events is critical for quantifying their possible association. The episodes of the intruding extratropical disturbances are identified based on potential vorticity (PV) on 350 K isentropic surface. We exploit the PV conservation principle to identify the air of extratropical origin in the tropics. We have identified 3584 extratropical disturbances that intruded into tropics for the period 1979-2022. A major fraction of such events is observed in the central-east Pacific and Atlantic Ocean domains when the westerly ducts are observed. While the intruding extratropical disturbances predominantly propagate eastward, 25% of the intruding extratropical disturbances exhibit westward propagation and such disturbances are observed mainly during summer season.

Because the intrusion of extratropical disturbances is mainly confined to the upper troposphere, MRG wave events at 200 hPa are identified using equatorial meridional wind as the key variable by following the wave fitting method. We have identified 2390 MRG events for the

period 1979-2019 and 37% of them are associated with the intrusion of extratropical disturbances (such MRG events are labeled as intrusion MRG events). It is noteworthy that nearly 70% of the intrusion MRG events occurred in the winter hemisphere where the westerly wind ducts are well developed. Over the central–east Pacific during boreal winter, it is observed that the intrusion MRG wave events have a bigger amplitude and have a larger meridional extent compared to non-intrusion MRG wave events. They also exhibit a similar spatial scale as the extratropical disturbances implying that resonant interactions may be a primary mechanism for the genesis of MRG wave events.

In addition to the intrinsic westward propagating MRG waves, eastward propagating MRG wave-like disturbances are observed in the Western Hemisphere. Theoretical studies showed that the large-scale zonal winds can modulate the MRG waves by modifying its restoring force and causing a shift in its intrinsic frequencies. MRG waves that undergo such modulation by the large-scale winds are named as Doppler shifted MRG waves. Detailed analyses show that the eastward propagating MRG-like disturbances are indeed the Doppler shifted eastward propagating MRG (E-MRG) waves. We have identified 730 E-MRG wave events using the Empirical Mode Decomposition (EMD) method. As expected, 75% of the E-MRG wave events occurred when the large-scale winds were westerly. It is intriguing to note the occurrence of E-MRG wave events when the large-scale winds were easterly. Further analysis revealed that the westerly phase of the Kelvin waves is instrumental in setting up the conducive environment for the MRG wave event to undergo the Doppler shifting. The westerly phase of the Kelvin waves explained more than 75% of the E-MRG wave events that occurred when the large-scale winds were easterly.

Chapter I

Introduction

Mixed Rossby-Gravity (MRG) waves are westward propagating equatorial disturbances, exhibiting periodicity and zonal wavelength in the range of 3 to 10 days and horizontal scales of 2000 to 10000 km respectively. MRG waves belong to the class of tropical synoptic-scale variability and it exerts notable influence in determining the distribution of convection, cloudiness, and precipitation. Studies suggest that MRG waves are integral to tropical cyclogenesis, the modulation of Madden-Julian Oscillations, the Quasi-Biennial Oscillations, and the organization of deep convection in the tropical atmosphere (Kang et al., 2020; Kang & Chun, 2021; Takasuka et al., 2019; Takasuka & Satoh, 2020, 2021; Takayabu et al., 2016; Yanai et al., 2000; Zangvil & Yanai, 1981; Zhou & Wang, 2007). Further, analyses of longitude-height distribution of zonal winds of MRG waves suggest that upper tropospheric MRG waves may serve as a significant source for lower tropospheric and lower stratospheric MRG wave activity (Suhas et al., 2020). In short, MRG waves are important elements of the tropical atmospheric variability, and it is critical for shaping the large-scale circulation, contributing notably to the persistence and development of tropical weather systems (Dominguez et al., 2020; Kiladis et al., 2009; Schlueter et al., 2019). MRG waves were theoretically outlined through linear perturbation analysis of the beta-plane approximated shallow water model (Matsuno, 1966). The MRG waves were first discovered in the observations in 1966 using radiosonde meridional wind data in the Pacific's lower stratosphere by Yanai and Maruyama. As a result, these waves are also commonly referred to as “Yanai waves”. The advancements in satellite technology revealed the coupling between MRG waves and convection, suggesting the possibility of potential feedback between dynamical and convective fields which is crucial for organizing convective activities. This makes the MRG waves influencing tropical precipitation patterns, potentially modulating synoptic-scale convection (Hendon & Liebmann, 1991; Kiladis et al., 2009; Takayabu, 1994a, 1994b; Wheeler et al., 2000; Wheeler & Kiladis, 1999).

The MRG waves stand out among other tropical atmospheric disturbances essentially due to the unique blend of the characteristics of both high-frequency, fast-moving gravity waves and low-frequency, slow-moving Rossby waves. In the mid-latitude atmosphere, motions can be distinctly categorized into low and high-frequency modes but in the tropics; modes like MRG waves and Kelvin waves defy straightforward classification as either gravity or Rossby types, and it makes the tropical weather prediction difficult. Thus, entirely negating the influence of gravity waves while initialization of numerical weather forecasting models is not possible in the tropics. The horizontal structure of MRG waves exhibit a strong cross-equatorial meridional flow and embodies features of both equatorial Rossby waves which are dominantly rotational and gravity waves, marked by their convergent and divergent characteristics. The rotational nature of MRG waves positions them as potential initiators of tropical cyclone-formation (Zhou and Wang, 2007). Recent studies have recognized the crucial role of MRG waves as important precursors to tropical cyclonic activity, which can enhance the predictability of cyclones up to two weeks in advance (X. Feng et al., 2023). Additionally, the associated convergent and divergent wind fields of MRG waves can trigger synoptic-scale tropical convection. The signature of disturbances with propagation characteristics and scales similar to MRG waves are also found in the Intertropical Convergence Zone (ITCZ), which is indicative of the crucial role of these waves in large- scale convective organization over the tropics (Takayabu, 1994a, 1994b). Studies suggest that MRG dynamics is important for the initiation and propagation of Madden-Julian Oscillation (MJO) activity, (Takasuka & Satoh, 2020, 2021). Since, MRG waves also propagate vertically, they play a significant role in vertical zonal momentum transport, influencing the phases of the Quasi-Biennial Oscillation (QBO) between its easterly and westerly periods (Kang et al., 2020; Kang & Chun, 2021; Lin et al., 2019). The complex nature of MRG waves, embodying both convergent-divergent and rotational motions, as well as the connection of MRG waves to various atmospheric scales highlights their multifaceted influence in the tropics. A profound comprehension of the factors that excite and maintain the MRG wave activity is imperative for improving the understanding of other tropical modes of variability.

Various mechanisms have been proposed to explain the excitation and variability of MRG waves, which can be primarily classified as in-situ and external forcing mechanisms. The major in-situ forcing mechanisms include hydrodynamic and convective instabilities, boundary forcing (SST), wave-wave interaction, wave-mean flow interaction. The conditional instability of the second kind (CISK) concept was introduced to examine the impact of tropical convection and latent heat release in exciting MRG waves (Hayashi, 1970; Lindzen, 1974). Though the CISK theory reproduced the spatial structure, it failed to explain the scale selection of the MRG waves.

Radiative heating was considered as another candidate that could excite the MRG waves in the atmosphere (Hayashi, 1976; Itoh, 1978). Based on a diagnostic analysis of tropospheric circulation and sea surface temperature (SST), Hendon and Liebmann 1991, hypothesized that the SST configuration over the central Pacific may be responsible for the seasonal phase locking and excitation of the MRG waves. Diabatic heating associated with tropical convection was considered as one of the sources of lower stratospheric MRG waves (Garcia & Salby, 1987; Salby, 1984). Non-linear interaction among equatorial waves was considered as another factor that could excite MRG waves in the atmosphere (Ripa, 1983). It was found that the energy exchange among Rossby waves, long Kelvin waves and a quasi-geostrophic basic state under the influence of tropical convection led to the selection of 4 days period and 4-5 zonal wavenumber scale MRG waves. Model experiments showed that lateral forcing together with latent heat release associated with tropical convection helped in selecting the horizontal scale of the MRG waves (Itoh & Ghil, 1988; Wilson & Mak, 1984). Since a comprehensive understanding of the feedback between large-scale circulation and small-scale convective motion is largely elusive, the reliability of an idealized representation of diabatic heating employed in models and its subsequent interaction with circulation is questionable. And it makes the in-situ generated MRG waves through the convection mechanism a debatable issue. The inclusion of convection makes the tropical atmosphere divergent and it thereby prohibits the application of the shallow water model in representing the tropical atmosphere.

The conceptual and technical issues associated with the in-situ MRG wave excitation mechanism motivates the possibility of exploring the role of external forcing mechanisms in exciting MRG waves. Tropical scale analysis suggests that, for large- scale non-precipitating motions in the tropics, the vertical scale is smaller, and rate of change of temperature along with horizontal temperature advection are minimal. In scenarios lacking precipitating motions, temperature fluctuations are nearly non-existent in tropical large-scale motions, with an average change of about 0.3K/day. Without the heating from condensation, tropical synoptic-scale motions show very slow vertical motions (around 0.3 cm/s), leading to the conclusion that their contribution to the momentum equations is minimal. Hence, large- scale tropical motions can be considered quasi-nondivergent and quasi-barotropic in nature. The primary mechanisms that can potentially energize and sustain these motions include barotropic instability of the mean zonal flow or through interactions with disturbances from higher latitudes (Charney, 1963).

Multiple observational as well as modeling studies have documented the role of lateral forcing form the higher latitudes in exciting tropical synoptic-scale motions especially over the western hemisphere when the upper tropospheric regions of east Pacific and Atlantic ocean are characterized by strong westerly winds called westerly winds ducts that can act as pathways for tropical-extratropical interaction (Hoskins & Ambrizzi, 1993; Webster & Chang, 1988; Webster & Holton, 1982). The significant contribution of extratropical Rossby waves in sustaining the momentum and energy balance between temperate and colder latitudes via eddy transport is well documented (Held & Hoskins, 1985; Hoskins & Karoly, 1981). In addition to maintaining this balance, extratropical Rossby waves can play a crucial role in triggering synoptic convective activity in the tropical regions. Riehl (1945) highlighted the frequent occurrence of polar air intrusions into the tropics and speculated on their potential impact in forcing tropical convection. A modeling study by (Mak, 1969a), utilizing a two-layer model for the tropics with independent and identically distributed stochastic forcing at the northern and southern hemispheric boundaries at 30°N and 30°S, demonstrated that such forcing could trigger or amplify meridional perturbations in MRG wave scales. (Riehl 1977a ; 1977b) further provided evidence of disturbances from the extratropics triggering rainfall over Venezuela during the northern hemisphere (NH) summer. Numerous studies, (Kousky, 1979; Streten, 1973; Trenberth, 1976) found observational evidence linking wave trains from the extratropics in the southern hemisphere (SH) with tropical convective activity in the South Pacific convergence zone. Research into tropical-extratropical interactions was further propelled by findings from (Arkin & Webster, 1985), who observed peaks in perturbation kinetic energy in the upper troposphere over the East Pacific and Atlantic, coinciding with westerly ducts. The advection of positive isentropic potential vorticity from the extratropics to the tropics can initiate convective anomalies, decrease atmospheric stability, and lead to the formation of frontal systems, akin to baroclinic wave developments in midlatitudes. Several past studies (Cheng et al., 2022; Huaman et al., 2020; Kiladis & Weickmann, 1992a, 1992b; Straub & Kiladis, 2003), underscores the impact of intruding extratropical disturbances on equatorial disturbances, further supported by (Sakaeda & Roundy, 2014; Suhas et al., 2020).

Since MRG waves are dominantly rotational and episodic in nature, and exhibit spatial-temporal scale matching with extratropical Rossby waves, several modeling and observational studies have tried to understand the detailed mechanism behind the excitation of, MRG waves by the extratropical disturbances (Bennett & Young, 1971; Itoh & Ghil, 1988; Webster & Holton, 1982; Zhang & Webster, 1989, 1992). The concept of lateral forcing of MRG waves by the extratropical disturbances was first introduced by (Mak, 1969a). Idealized model experiments showed that the extratropical forcing was not critical for the excitation of MRG waves. However, several observational works like (Zangvil & Yanai, 1981) first displayed the association of MRG activity with extratropical disturbances by analyzing the eddy momentum flux. (Randel, 1992), formulated a hypothesis based on a case study that the upper Tropospheric MRG waves in the East Pacific are mostly dry waves characterized by larger periodicity (6 to 10 days) and likely to be forced by extratropical disturbances. Diagnostic analysis based on reanalysis data revealed that the MRG waves can get amplified when the extratropical disturbances intrude into the domain of MRG waves suggesting a resonant interaction (Kiladis et al., 2016; Magaña & Yanai, 1995; Suhas et al., 2020; G. Yang & Hoskins, 2016). Although previous research has emphasized the significance of extratropical forcing in the development of MRG waves, these studies primarily employ regression or correlation-based approaches to analyze the extratropical influence. Such methodologies, while useful, fall short in quantifying the relative contribution of extratropical disturbances forcing in triggering MRG waves. This gap in the understanding forms the central focus of the thesis, aiming to quantify the association between intruding extratropical disturbances and MRG waves by resorting to an event-based analysis.

Given the identified gaps in previous research and aiming to elucidate the impact of intruding extratropical disturbances on MRG waves in the tropical atmosphere, the current thesis sets forth three primary objectives:

1. Conduct a survey of intrusion episodes of the extratropical disturbances into the tropics.
2. Identify MRG waves in the upper troposphere and quantify their association with the intrusion of extratropical disturbances.
3. Explore the role of westerly wind ducts and large scale Kelvin waves in realizing the Doppler shifted eastward propagating MRG waves.

To quantify the association between the intruding extratropical disturbances and MRG waves, it is essential to first quantify the frequency of synoptic-scale extratropical intrusion events that are realized in the tropical atmosphere. As the foundation of our analysis, we revisit global climatology of the intrusion of extratropical disturbances into the tropics in the second chapter using a long record of data. This necessitates the utilization of the conservation of potential vorticity (PV) and the development of a PV based identification method to categorize the episodes of extratropical disturbances. The goal is to determine whether the number of PV intrusions from the extratropical to the tropical region are significant enough to find a possible association with the MRG wave events. Should the frequency of these intrusion events prove to be minimal, it would undermine the relevance of further exploring the main thesis question. The characteristics of PV intrusions are documented in detail, including their amplitude, longitudinal width, direction, magnitude of zonal phase speed, and the duration of events.Such a comprehensive assessment would set the stage for examining the relative contribution of the extratropical intrusions to the overall dynamics of MRG waves.

The third chapter quantifies the association between the intrusion of extratropical disturbances and MRG waves. The first part of the study seeks to characterize the upper tropospheric MRG waves, focusing on their dynamical wave properties in relation to geographical distribution and seasonality (Hendon & Liebmann, 1991; Suhas et al., 2020; Takayabu et al., 2016; Wheeler & Kiladis, 1999). To achieve this, an event-based methodology (Au-Yeung & Tam, 2018) is employed to track the MRG wave episodes both spatially and temporally. This approach enables the real-time calculation of amplitude, wave number, phase speeds, trapping scale and duration of each MRG wave event, thereby reducing biases associated with previous Fourier-based identification techniques. Given the significant role of the background zonal flow in tropical-extratropical interactions, an investigation will be conducted to determine if it exhibits seasonal and geographical phase locking akin to variations in the background mean flow. In the latter part of this chapter, the identified upper tropospheric MRG wave events will be categorized based on their association with high PV values in proximity to the events preceding the peak MRG wave activity into MRG with intrusion and MRG without intrusion. Diagnostic analyses will be conducted to examine the horizontal structures of the MRG wave events associated with and without PV intrusions, that may provide further insights into their respective characteristics. The study will then compare the local wave properties between the two categories of MRG wave events to ascertain the robustness of the classification technique and verify if the results comply with that implied by theories of tropical-extratropical interactions (Webster & Holton, 1982; Zhang, 1993; Zhang & Webster, 1992).

In the final chapter, the focus is on investigating the presence of eastward spectral power in the synoptic wavenumber and frequencies within the symmetric component of the meridional wind at 200 hPa. While previous studies have noted the existence of eastward-propagating synoptic-scale disturbances in the tropics, these disturbances have not been associated with any linear shallow water modes (Huaman et al., 2020; Kiladis & Weickmann, 1992c; G. Yang & Hoskins, 2016; G.-Y. Yang et al., 2003, 2007a, 2007b). This chapter documents the eastward propagating Doppler shifted MRG waves and explores the potential contribution of Doppler-shifted Mixed Rossby Gravity (E-MRG) waves to the overall synoptic-scale variability in the upper troposphere. The study aims to identify individual episodes of E-MRG wave events utilizing the empirical mode decomposition (EMD) method. The notable advantage of this technique is its independence from predefined basis functions, as well as its ability to operate without assuming a linear relationship among various wave modes. The research will delve into uncovering the potential roles played by westerly wind ducts and large-scale transient disturbances in sustaining E-MRG waves over the western hemisphere. By dissecting the dynamics of the E-MRG wave events and exploring their association with distinct atmospheric features in the tropics and extratropics, the study aims to enhance our understanding of the mechanisms driving synoptic-scale variability in the upper troposphere.

Chapter II

A survey of intrusion episodes of the extratropical disturbances into the tropics

2.1 Introduction

The interaction of extratropical Rossby waves in the tropics has garnered attention for their key role in influencing tropical synoptic-scale convection and equatorial waves (Charney, 1963; Funatsu & Waugh, 2008; Huaman et al., 2020; Mak, 1969a; Straub & Kiladis, 2003; Webster & Holton, 1982; G. Yang & Hoskins, 2016; G.-Y. Yang & Hoskins, 2013; Zangvil & Yanai, 1981). Linear theory elucidates that Rossby waves invariably propagate westward relative to their underlying mean flow and require advection by the background westerlies for the eastward-moving Rossby waves in low latitudes to penetrate through regions of westerly winds during the northern winter over the Pacific and Atlantic Oceans (Charney, 1969; Hoskins & Ambrizzi, 1993; Tomas & Webster, 1994; Webster & Holton, 1982). When the amplitude of the extratropical Rossby waves become very large and their zonal phase speed is proportional to the prevailing background flow, Rossby wave breaking (RWB) events take place. These events facilitate the transport of wave energy towards the equatorial region and momentum poleward, playing a crucial role in shaping large-scale atmospheric circulation (Strong & Magnusdottir, 2008; Woollings et al., 2008) and triggering synoptic-scale motions in the tropical regions (Kiladis, 1998; Kiladis & Weickmann, 1992a; Vishnupriya et al., 2022). RWB involves the distortion and eventual breaking of large-scale waves in the atmosphere (Hoskins et al., 1985; McIntyre & Palmer, 1983), which leads to the redistribution of momentum, heat, and moisture. RWB can affect the strength and position of jet streams, contributing to the development of extreme weather events such as heatwaves and heavy precipitation (Barnes & Hartmann, 2012; Moore et al., 2019). They also play a vital role in stratosphere-troposphere exchange (Scott & Cammas, 2002), influencing ozone distribution and surface weather patterns (Thomas et al., 2023). Additionally, RWB is essential in the formation of atmospheric blocking patterns

(Berrisford et al., 2007; Pelly & Hoskins, 2003), which can cause prolonged weather conditions like droughts or floods.

Instances of RWB events can be identified by examining maps of PV, which acts as a Lagrangian tracer due to its conservation property along isentropic surfaces, for adiabatic, frictionless flows, making it an effective tool for tracking air mass transport (Hoskins et al., 1985; McIntyre & Palmer, 1983). Literature suggests two prominent mechanisms through which extratropical RWB may influence tropical synoptic-scale disturbances. Firstly, via resonant interaction, the convergence of eddy momentum flux from the higher latitudes can remotely interact with the meridional structure of tropical waves (Cheng et al., 2022; Straub & Kiladis, 2003), commonly observed during NH summer. Secondly, a local forcing mechanism that involves extratropical Rossby waves to propagate into the tropics through westerly wind ducts and predominantly excite tropical cloud plumes through quasi-geostrophic forcing, typically observed during NH winter (Huaman et al., 2020; Kiladis, 1998; Kiladis & Weickmann, 1992b). The nature of the tropical response is heavily influenced by the background zonal wind structure (Hoskins and Yang, 2016), with easterly flow hindering direct Rossby wave propagation but enabling resonant forcing.

(Postel & Hitchman, 1999) offered a succinct summary of RWB occurrences near the subtropical tropopause but overlooked an in-depth analysis of the extent to which these events penetrate into the tropics. The study revealed a seasonal pattern mirroring the strength and location of the mid-latitude jet streams, with a peak in the events during summer. (Waugh & Polvani, 2000) conducted a global climatology of PV intrusion events penetrating up to 10°N and 10°S, but used a high PV threshold of 2 Potential Vorticity Unit (PVU; 1 PVU =

$10^{-6}\, m^{2} s^{-1} kg^{-1}$). The PV intrusion events showed peak in seasonality during the NH winter months over the east Pacific and Atlantic ocean domains. However, PV values exceeding even 1 PVU at tropical latitudes may not be exclusively tropical in origin and could originate from the extratropical stratosphere. A recent study by (Vishnupriya et al., 2022) demonstrate a mechanism through which stratospheric PV intrusions exceeding a threshold of 1 PVU during summer at 20°N can induce vortex seeds in the low levels through adiabatic lifting, triggering monsoon low-pressure systems over the northwestern Pacific. Therefore, using a very high PV threshold and setting the latitude circle cutoff deep into the tropics can result in some events being missed.

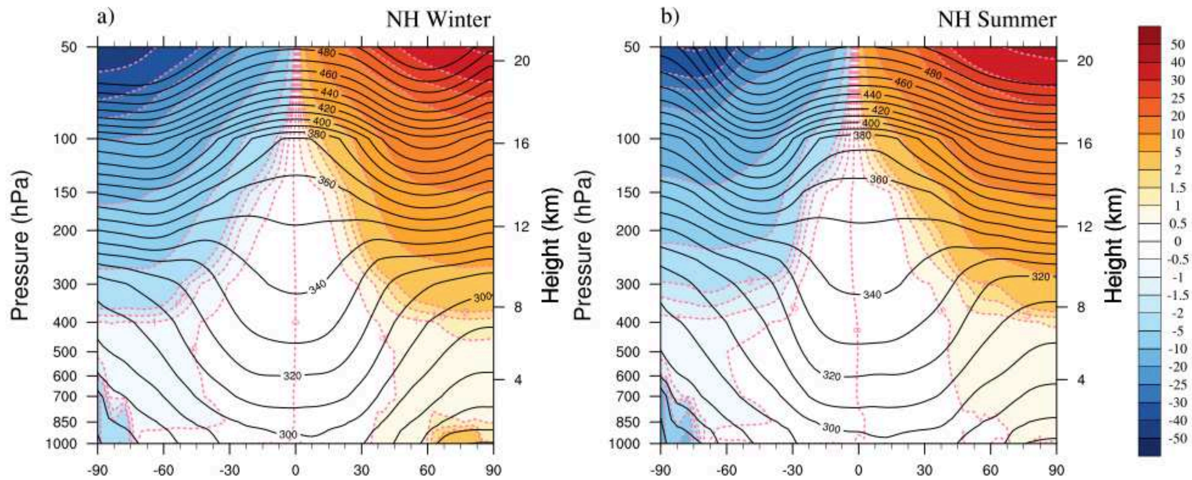

Figure 2.1. Vertical distribution of zonally averaged potential vorticity (PVU) (coloured contour) and isentropic surface (black solid lines) as a function of latitude for a) northern hemispheric (NH) winter and b) northern hemispheric (NH) summer. The pink dotted lines mark the boundary of the potential vorticity values.

(Wernli & Sprenger, 2007) and (Fröhlich & Knippertz, 2008) also identified PV streamers and upper tropospheric troughs, utilizing a high threshold value of 2 PVU and a dataset of limited size. However, their method primarily considered only the meridional extent of the intrusion events and lacked focus on the zonal scale and propagation direction of the intruding disturbances. (Albers et al., 2016) demonstrated that SSWs are closely linked to enhanced upper tropospheric PV intrusion activity, especially over the Pacific, and that these intrusions can significantly impact the tropical upper troposphere and lower stratosphere through their influence on convection and trace gas mixing. In the context of the tropical-extratropical interaction resonant mechanism proposed (Webster & Holton, 1982; G. Yang & Hoskins, 2016), it is essential to concentrate on extratropical disturbances that exhibit spatial and temporal scales comparable to tropical synoptic-scale motions. Apart from the findings of (Fröhlich & Knippertz, 2008), which highlight a notable peak in the occurrence of PV intrusions during the NH summer over the north-central Pacific, even when the upper tropospheric ambient flow over the western hemisphere is easterly or weak westerly, the seasonal pattern of PV intrusion events aligns with the prevalence of westerly wind duct during the NH winter months, as indicated in previous climatologies. But, multiple studies have reported diagnostic association of extratropical intrusions with tropical synoptic-scale motions during NH summer as well (Kiladis, 1998; Kiladis & Weickmann, 1992b; Magaña & Yanai, 1995; Straub & Kiladis, 2003; Suhas et al., 2020; Zangvil & Yanai, 1981). The discrepancy in climatological studies underestimating NH summertime PV intrusion activity may be attributed to the use of high PV thresholds and the choice of latitude levels confined to the deep tropics. Consequently, there is a compelling need to conduct a comprehensive global survey of PV intrusion events in the tropics using a lower PV threshold and a more extensive and recent dataset that can influence synoptic-scale motions in the tropics.

To quantify the impact of PV intrusions on MRG wave activity, we employ an event-based analysis. This method would help us understand how often PV intrusion events occur in the tropics and their potential to affect synoptic-scale movements. The current chapter aims at creating a robust database of PV intrusion events occurring globally that have the potent-

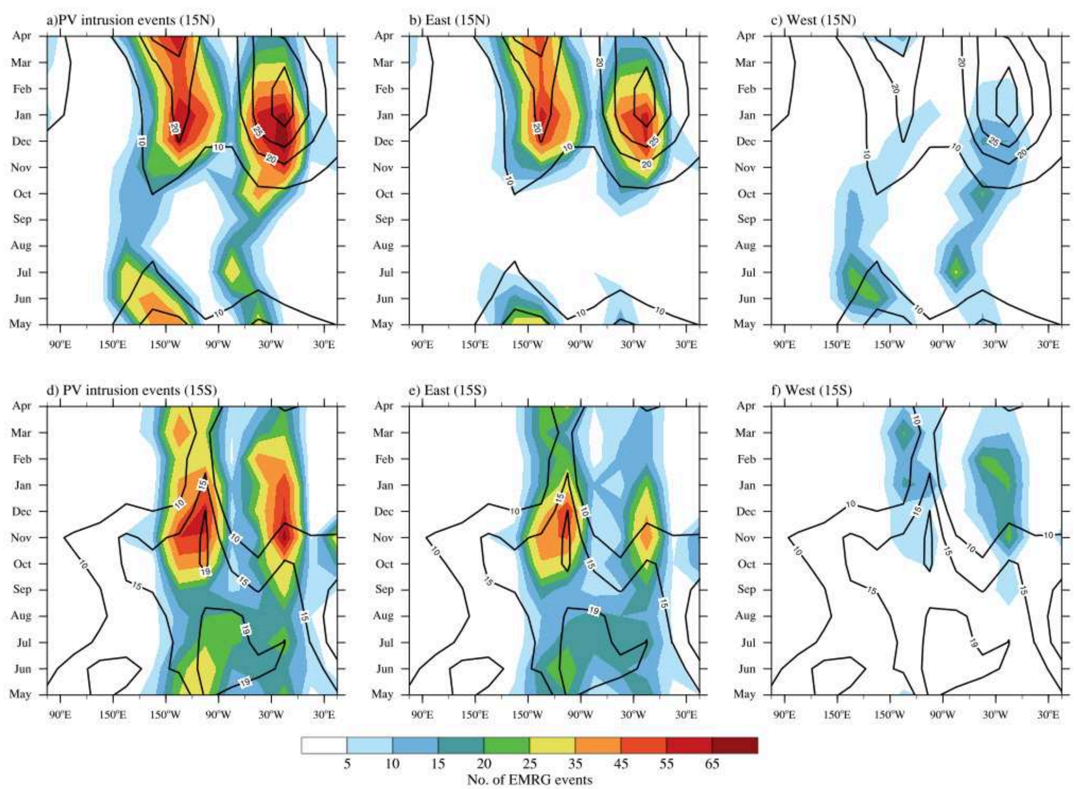

Figure 2.2. Number of occurrences of PV intrusion events (coloured contour) as fiction of month and longitudinal bins at 15 N latitude a) total events, b) eastward propagating events, c) westward propagating events, at 15 S latitude d) total events, e) eastward propagating events and f) westward propagating events. The overlaid block contour lines represent climatological zonal mean winds values calculated by averaging over 12.5°N to 17.5°N and 12.5°S to 17.5°S.

ial of influencing tropical synoptic-scale motions. The significance of the choice of the 350 K isentropic level in the present analysis lies in its alignment with the 200 hPa pressure level, where regions of strong westerly winds extending from the extratropics to the tropics are typically observed (figure 2.1). The 350 K level aids in capturing the dynamics of upper-level atmospheric processes with minimum seasonal contrast, particularly during NH summers and winters (figure 2.1). In the current study, a latitude threshold of 15°N and 15°S and a PV threshold of 1.5 PVU are implemented. PV values crossing a threshold of 1.5 PVU at this level, delineate the dynamic tropopause, and demarcate the extratropical stratospheric air (characterized by high PV) from the tropical tropospheric air (characterized by low PV, due to low planetary rotation). This approach aims to capture events that are not too far from the deep tropics, while also ensuring that the events penetrating deep into the tropics are not overlooked, thereby optimizing the event capture rate.

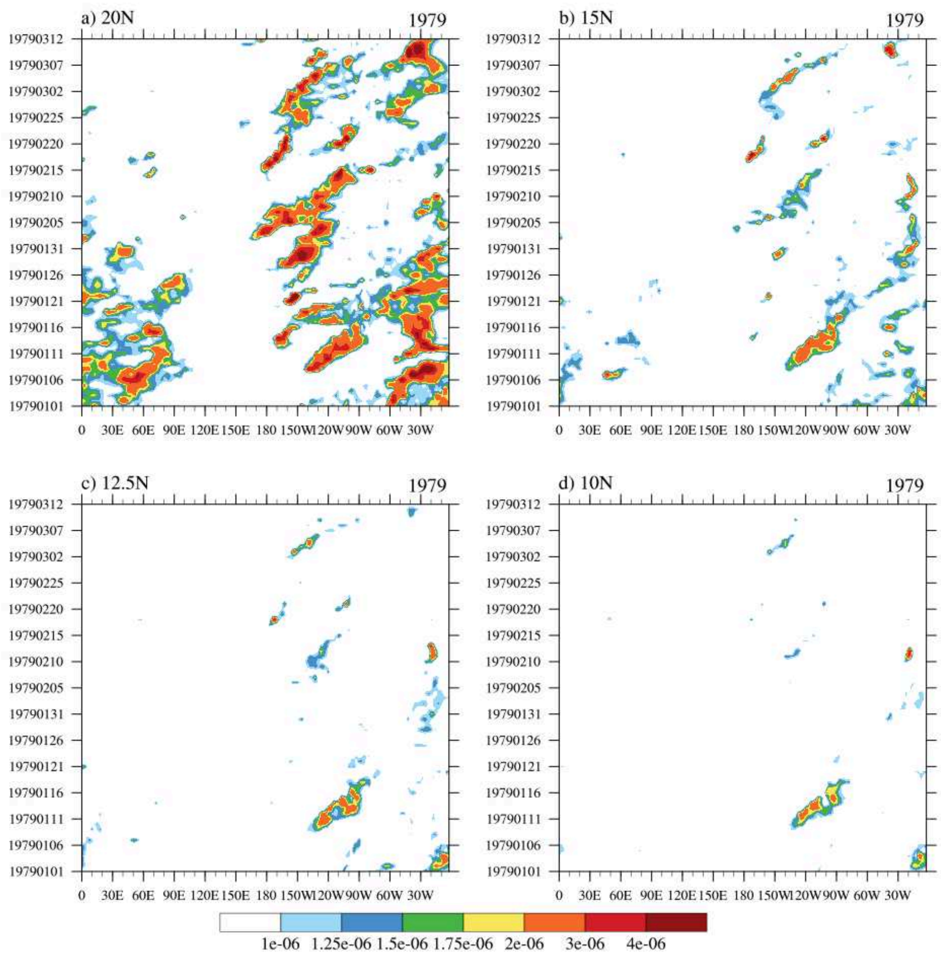

Figure 2.3. Hovmoller plots for the PV at 350 K isentropic surface (PVU) from 1st Jan 1979 to 12 March 1979 at a) 20°N, b) 15°N, c) 12.5°N and d) 10°N.

2.2 Data and Methodology

We use the ECMWF ERA5 reanalysis PV at 350 K isentropic surface from 1979 to 2022 for a period of 44 years. The data is regridded to a horizontal resolution of 2.5° x 2.5° from 0.5° x 0.5° and averaged to daily resolution from 3 hourly since we are interested in capturing synoptic-scale intrusion events. To identify potential PV intrusion events, first, the latitude is set at either 15°N or 15°S and the first day (time step) is fixed. Next, the longitudes where the Potential Vorticity (PV) value exceeds a threshold of 1.5 PVU is recorded. The location where the PV values surpass the threshold extend across a longitude range of 10° or more are noted and the

algorithm proceeds forward to the next time step. For the subsequent time step, a temporary window is created which spans 10° west of the initial longitude values from the previous day and 10° east from the last longitude of the previous day. Within this new interval, the PV values are analyzed to determine the length of longitudes with values exceeding the threshold in the successive time step. If this length exceeds 10°, these locations and the time step are recorded before moving to the next time frame. This iterative process is continued until a time step is reached where the PV values within the temporary interval no longer exceed the threshold over a 10° longitude range. If this threshold criteria persists for a PV cluster over a period exceeding two days, the event is classified as a "PV intrusion event". This systematic approach allows for the detailed identification and tracking of PV intrusion events that are capable of influencing synoptic-scale tropical motions based on specific criteria and consecutive time steps.

To systematically track the PV intrusion events across latitudes, we commence by analyzing each event identified at 15°N. The spatial and temporal locations of the event are recorded. Subsequently, whether a particular event propagates to 12.5°N or not is scrutinized by recording the day (time step) and the longitude on which the event initiates and ends at 15°N. The reference start day is recorded as the day of initiation of the event and the western most longitude on that day is recorded as the reference start longitude. The reference end day is recorded as the day of the end of the event and the easternmost longitude on that day is recorded as the reference end longitude. An analytical framework is established, comprising a temporal and longitudinal window spanning the event's duration plus two additional days, bounded by five degrees west and east of the recorded start and end longitudes. By evaluating PV values within

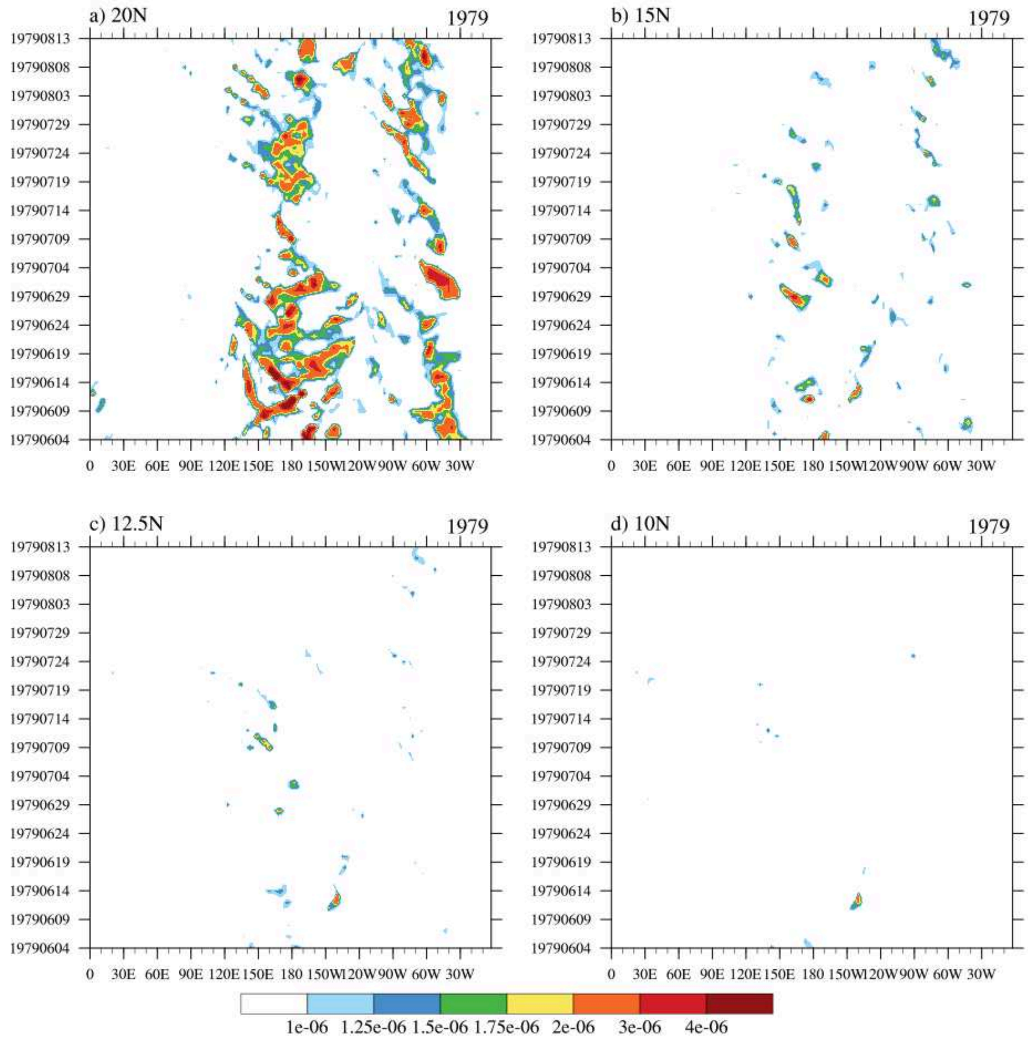

Figure 2.4. Hovmoller plots for the PV at 350 K isentropic surface (PVU) from 4th June 1979 to 13 August 1979 at a) 20°N, b) 15°N, c) 12.5°N and d) 10°N.

prescribed interval, the PV intrusion event exceeding five degrees longitude for a minimum of two days signifies extension to the subsequent latitude. Such events are Conversely, if the above criteria is not met the PV intrusion denotes confinement to 15°N, designating the event as a latitudinally shallow propagating phenomenon. This rigorous methodology is iterated for lower latitudes, such as 12.5°N, 10°N, employing a reduced PV threshold of 1.25 PVU and 1 PVU respectively for enhanced sensitivity. Similar, procedure is used for identifying events in the SH. The number of events is sensitive to the PV threshold but does not change the results and statistics, with a lower value just yielding a larger number of events.

The start and the end day for which the PV event is identified, marks the entire duration of the event. The maximum value of the PV during the entire event is recorded and the corresponding longitudinal location and day marks the lon 0 and day 0 of the PV intrusions event, respectively. The local zonal mean corresponding to individual wave event is calculated by taking a window of ± 2.5° centered at the mean latitude at which the event is identified, a longitudinal window length of ± 15° from the lon 0 location and the time window taken to be ±10 days from the day 0 location. The values of the zonal mean are not sensitive to the length of the time window varying between ± 7 days to ± 15 days. The local phase speed of each event is calculated by taking the mean value of the phase propagation of the easternmost and westernmost longitudinal location in time. A centered finite difference scheme is used to calculate the phase speeds. The longitudinal extent of the event on the day 0 is recorded as the longitudinal width of the event.

2.3 Results and Discussions

The 350 K isentropic surface serves as a key reference level for monitoring the migration of air masses from the extratropics to the tropics. Figure 2.1 illustrates the potential vorticity distribution across various isentropic surfaces as a function of height versus latitude. At the 200 hPa level, where westerly wind ducts are strongest and tropical-extratropical interactions are most prominent, the 350 K isentropic surface closely aligns, highlighting its importance in studying these interactions. The 1.5 PVU cutoff line demarcates a tropopause-like boundary, separating warm tropospheric air from dry stratospheric air. In tropical latitudes, the 350 K isentropic surface resides in the troposphere, transitioning to the stratosphere in extratropical regions. The stable stratification in the stratosphere results in higher PV air masses, which, through the conservation of adiabatic PV, can penetrate the tropics along an isentropic surface of constant potential temperature. Given the fact that the 350 K surface shows minimal seasonality in the subtropical and tropical latitudes during NH summer and winter, it minimizes the impact of seasonal variations on identified PV intrusions events.

A total of 1845 and 1739 extratropical intrusion events were identified globally, both in space and time, at 15° latitude in the NH and SH, respectively. Slightly higher number of PV intrusion events were observed in the NH compared to the SH. For further analysis, the distribution of these events based on day 0 time and longitudinal locations were examined. The number of events occurring in individual months and within longitudinal bins of 30° were tallied, and the frequency of occurrence was visually represented in Figure 2.2. The coloured contours in Figure 2.2 (a) to (c) depict the NH data, while in Figure 2.2 (d) to (f), the SH data is illustrated. The overlaid contours in the plots represent the climatological zonal mean wind values for different months and longitudinal domains. The zonal mean wind is calculated by averaging zonal wind at 200 hPa over specified latitudinal ranges (12.5°N - 17.5°N for NH and 12.5°S - 17.5°S for SH). The 50th percentile value of the zonal mean wind values falling into each monthly and 30 degrees longitudinal bin is assigned as the climatological mean wind for that specific bin. The PV intrusion events reveal distinct seasonality and spatial reference points. In the NH, these events peak during the winter months and align with regions of intense westerly winds exceeding 10 m/s across the central-east Pacific and Atlantic. Interestingly, secondary peaks occur in the same regions during NH summer months (from May to August) but are not associated with the background westerly winds. Similarly, in the SH, peaks in PV intrusion events are observed during similar months, albeit with a slight shift in the seasonality. Primary peak is observed over the Pacific domain from September to December. During SH winter, these events coincide with the location and seasonality of the westerly wind maxima in NH winter. Additionally, secondary peaks are noted from January to April over the central Pacific and from December to April over the Atlantic. The consistency with previous climatological studies is reassuring (Fröhlich & Knippertz, 2008; Waugh & Polvani, 2000), highlighting the robustness of the observed patterns and the identified events. Nevertheless, the presence of PV intrusion events in the absence of westerly background winds raises intriguing questions and warrants deeper exploration.

Hovmoller plots of PV at 350 K as a function of time versus longitude for different northern latitudes : 20°N, 15°N, 12.5°N and 10°N in figure 2.3 and 2.4 are investigated to verify the time and space evolution of the identified PV intrusions. Figure 2.3 shows observation of frequent zonally propagating synoptic-scale PV intrusion events across different latitudes from January 1st 1979 to March 12th 1979. These events exhibit eastward propagation, with episodes propagating both meridionally and zonally and are primarily observed to occur over the east Pacific and Atlantic. As the events shift closer to the equator, their amplitudes and zonal scales

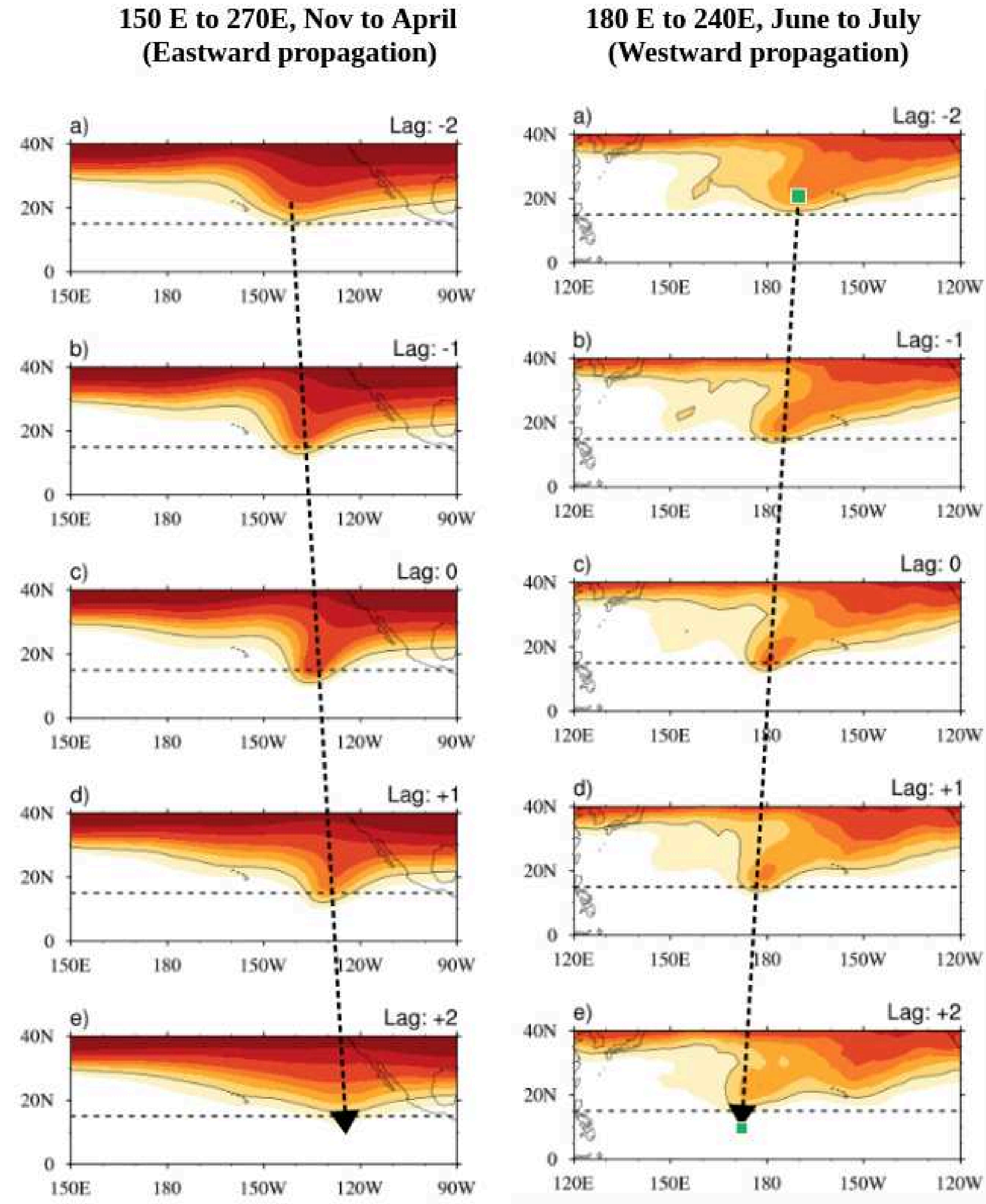

Figure 2.5. Lead-lag life cycle composite plot of northern hemispheric PV intrusion events for : left column a) to e) eastward propagating events that occur over 150°E to 270°E during November to April, right column a) to e) westward propagating events that occur over 180°E to 240°E during June to August. The PV intrusion events are longitudinally translated to 135°W for the eastward propagating events and to 180°E for the westward propagating events. The black solid line represents the 1.5 PVU contour. The black dashed line represents the 15°N latitude. Dashed arrows point towards the direction of zonal phase propagation.

diminish, with some failing to manifest at deeper tropical latitudes. Dissipative processes make the PV values latitude-sensitive, suggesting the use of lower cutoff thresholds for identifying the

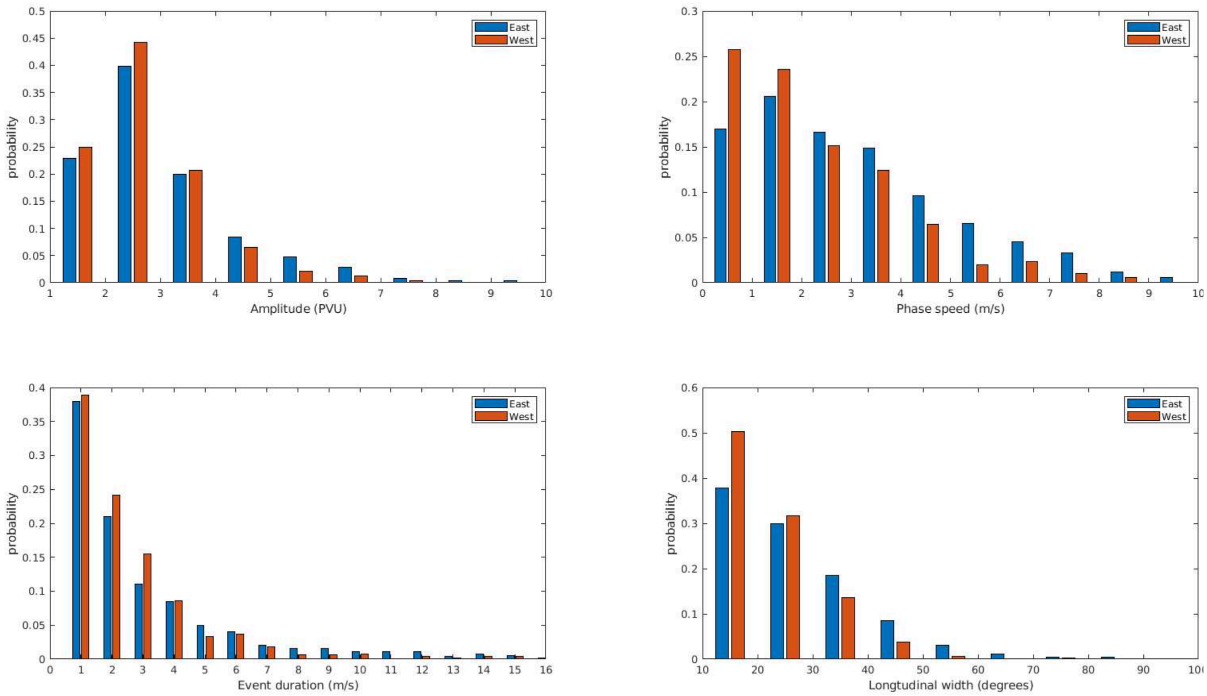

Figure 2.6. Frequency of occurrence (probability) of northern hemispheric PV intrusion events for different bins of a) Amplitude (PVU), b) Phase speed (m/s), c) event duration (days) and d) longitudinal width (degrees). The blue bars denote the eastward propagating events and the orange bars indicate westward propagating events.

PV intrusion events in deeper tropical latitudes. In contrast, examination of the time-longitude evolution of PV at 350 K during the NH summer months, when the strength of the westerlies over the western hemisphere are weak, from June 4th, 1979, to August 13th, 1979, also reveals frequent occurrences of extratropical air intrusion episodes (figure 2.4). Similar to previous observations, these events propagate in both meridional and zonal directions, but with a primary westward phase velocity. These events also show a significant reduction in their amplitude and zonal scale as they move equatorward. The PV intrusion events are observed over the west, central and east Pacific, as well as over the Atlantic. Similar PV intrusion events are observed even in the SH (figure not shown). These findings underscore the need for detailed analyses to comprehend the full spectrum of the extratropical PV intrusions.

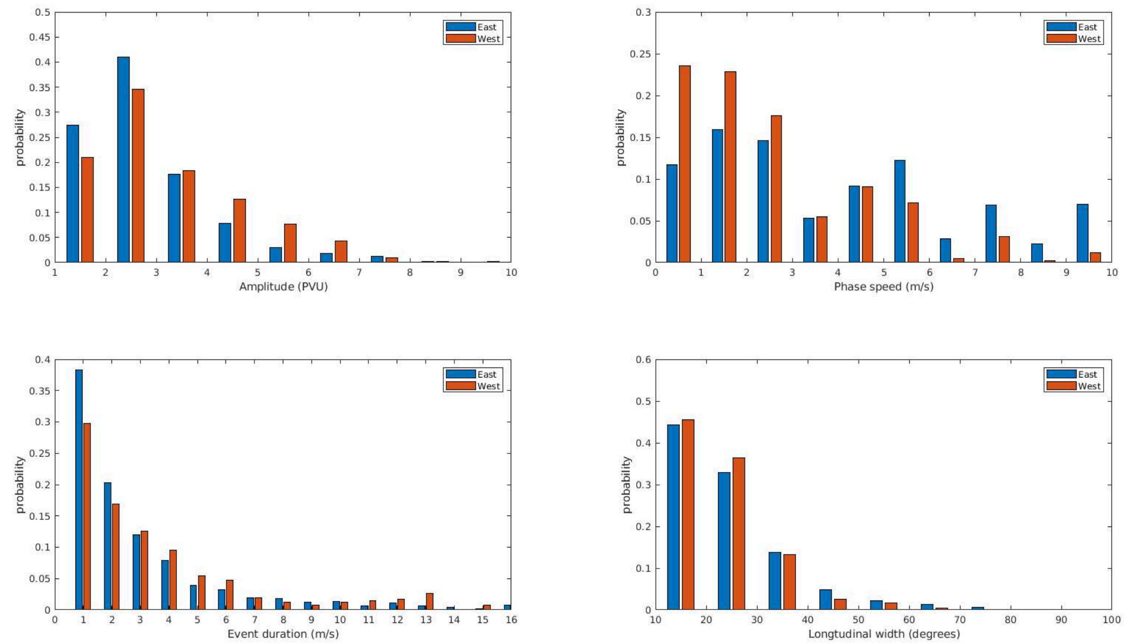

Figure 2.7. Frequency of occurrence (probability) of southern hemispheric PV intrusion events for different bins of a) Amplitude (PVU), b) Phase speed (m/s), c) event duration (days) and d) longitudinal width (degrees). The blue bars denote the eastward propagating events and the orange bars indicate westward propagating events.

Motivated by the observation of zonally eastward and westward propagating events from figure 2.3 and 2.4, the local zonal phase speed of the events are calculated for individual cases. Figure 2.2 b, 2.2 c, and 2.2 e, 2.2 f show the classification of frequency of occurrence of the events into eastward and westward propagating categories for the NH and SH, providing insights into the seasonality and domains of activity of the PV intrusion events. Eastward propagating events are collocated with ambient westerly flow for both the NH and SH cases. However, the eastward propagating events observed over the Atlantic in the SH during the November to April do not co-occur with westerly winds (figure 2.2 e). As can be observed in figure 2.2 c and 2.2 e, SH and NH westward events show a reverse seasonality with peak activity during SH summer and NH summer respectively. Clearly, all these events occur when the zonal mean circulation in the tropical - subtropical region are not strong westerlies. The number of the eastward propagating events (75% of the total PV intrusions events) are significantly larger than the westward propagating events (25% of the total PV intrusions events). Similar to the eastward events, the westward events also show a preference over the East Pacific and Atlantic, but interestingly, those occurring in the SH, peaking between May and August, also occur in the west and central Pacific regions. Several studies have pointed out a correlation between tropical synoptic-scale disturbances and extratropical wave influences during the summer months in both the hemispheres (Cheng et al., 2022; Sakaeda & Roundy, 2014; Suhas et al., 2020). Exploring the potential role of these events in triggering or amplifying tropical synoptic-scale disturbances would be interesting since these PV intrusion events are realized in the tropics even in the absence of strong westerly winds. Future detailed analysis is needed to understand what background conditions support the existence and westward movement of these disturbances.

To confirm the horizontal structures and the classification of the PV intrusion events into eastward and westward propagating events, life cycle composite maps are plotted. Figure 2.5 illustrates the distinctions between the eastward and the westward propagating events: the black dotted line represents the 15°N latitude, and the black continuous line marks the 1.5 PVU boundary. The composite maps were created by longitudinally translating the day 0 longitude location of the PV intrusion events to a reference value of 135°W for the Pacific and 30°W for the events that occur in the Atlantic ocean. Coloured contours depict PV values at 350 K for both eastward events over the Pacific Ocean in the left column, and westward events over the Atlantic Ocean in the right column. By analyzing the lead-lag composite maps, we can observe the PV intrusions featuring a zonal phase propagation; eastward for the eastward-propagating events, and westward for the westward-propagating ones. The scale of these events are found to be comparable with synoptic-scale motions, exhibiting an average lifespan ranging from 4 to 7 days. Additionally, the average composite zonal phase speed is noted to fall within 1 to 10 m/s. Upon comparison, significant differences between the eastward and westward propagating events are noted in terms of their amplitude and duration. Specifically, the eastward-propagating events demonstrate higher amplitudes and phase speeds in comparison to the westward-propagating events. Furthermore, the former category (eastward events) tends to have longer durations than the latter (westward events). The lead-lag composite maps produced for the SH events also verified the robustness of the classification of the PV intrusion events in eastward and westward propagating events (figure not shown).

Figures 2.6 and 2.7 illustrate key features of eastward and westward propagating PV intrusion events in the NH and SH, detailing aspects such as amplitude, phase speed, event duration, and longitudinal width. Notably, eastward propagating events in the NH are characterized by higher PV amplitudes than their westward counterparts, a trend that inversely applies to SH intrusion events. Furthermore, eastward propagating events exhibit faster zonal phase speeds in comparison to the slower phase speeds of westward events, occurring particularly in the NH. In terms of event duration, eastward propagating events tend to last longer in the NH, while in the SH, longer durations are observed for westward propagating events. Regarding longitudinal width, eastward propagating events extend wider than westward events in both hemispheres, with more marked differences in the NH. The distinct eastward and westward propagation of PV intrusion events observed during different seasons, coupled with variations in wave properties and associated background winds on which these disturbances are embedded, suggests that these events may play a crucial role in triggering different categories of tropical modes (Hoskins & Yang, 2016; G.-Y. Yang & Hoskins, 1996). Alternatively, there could be differences in the degree of association between tropical modes and the characteristics of the corresponding extratropical PV intrusions. The underlying mechanisms driving tropical synoptic-scale motions associated with eastward and westward PV intrusions could therefore be distinct. Westward propagating PV intrusions, typically observed during summer when background winds are easterly or weakly easterly, are likely to excite or amplify tropical modes predominantly through resonant forcing mechanisms. In contrast, eastward propagating events may favor direct forcing through interaction via the westerly wind ducts.

2.4 Summary and Conclusion

This study provides a comprehensive analysis of PV intrusion events using 44 years of ECMWF ERA5 reanalysis data from 1979 to 2022 at the 350 K isentropic surface, revealing significant insights into their global climatology. The analysis identifies 3584 PV intrusion events at 15°N and 15°S latitudes, with a notable predominance in the NH compared to the SH. Peak activity occurs during NH winter months, over the East Pacific and Atlantic Ocean domains, aligning with previous observations (Fröhlich & Knippertz, 2008; Postel & Hitchman, 1999; Waugh & Polvani, 2000; Wernli & Sprenger, 2007). These findings underscore the seasonal variability and geographical distribution of PV intrusions, highlighting their importance in the extratropical-tropical interaction when the background winds are westerlies over the WH.

The study highlights the observation of distinct zonal propagation patterns of PV intrusion events: eastward and westward (Yang and Hoskins 1996). Eastward propagating events are more prevalent during NH winter and the transitional months from NH summer to winter, while westward propagating events peak during NH and SH summer months identified at 15°N and 15°S, respectively. A particularly notable aspect is that events propagating westward tend to occur more frequently in regions where the background zonal flow lacks strong westerly winds, (Yang and Hoskins, 2016; Hoskins and Yang, 2016). The occurrence of westward propagating PV intrusion events throughout the year, particularly during NH and SH summer, respectively, suggests their role in influencing tropical synoptic-scale disturbances even in the absence of westerly wind ducts. Differences in characteristics between eastward and westward propagating PV intrusions are observed, with eastward events showing longer durations and faster phase speeds compared to westward events. These differences indicate the possibility of varying mechanisms of influence on tropical disturbances that may be associated with the eastward and westward propagating PV intrusion events. The study's findings prompt further investigation into whether specific types of eastward or westward propagating tropical disturbances, such as Kelvin waves or mixed Rossby-gravity (MRG) waves, are preferentially associated with either category of PV intrusion. Since, the eastward events are observed when the background winds are westerly winds, it is possible that they may be influencing tropical synoptic-scale motions through local forcing mechanism while the westward propagating events, which mostly are supported over weak westerly or easterly background winds could be associated with the remote resonant kind of forcing.

The identification of a considerable number of synoptic-scale PV intrusion events across both hemispheres (NH and SH) further stresses the potential these events have in influencing tropical synoptic-scale motions. This revelation brings to light the importance of delving deeper into the relationship between these PV intrusions and other significant tropical atmospheric phenomena, such as the Madden-Julian Oscillation (MJO) or Mixed Rossby Gravity (MRG) wave events. Understanding the nuances of this relationship could significantly advance our knowledge in predicting and modeling atmospheric phenomena, acknowledging the complexity of interactions that govern weather and climate patterns globally. Thus, the connection between MRG wave events and PV intrusion events presents a fertile area for research, potentially unraveling scope for new dimensions of tropical-extratropical interaction mechanisms.

Chapter III

MRG waves and their association with the intrusion of extratropical disturbances

3.1 Introduction

MRG waves are synoptic-scale westward-propagating disturbances observed in dynamic and convective fields over the equatorial region (Hendon & Liebmann, 1991; Kiladis et al., 2016; Takayabu, 1994b, 1994a, 1994a; Suhas et al., 2020; Takayabu & Nitta, 1993; Wheeler & Kiladis, 1999). Pronounced cross-equatorial meridional winds and vortices distributed symmetrically about the equator are the prominent features of MRG waves. MRG waves are more frequently observed over the Pacific domain during boreal summer and fall (Hendon & Liebmann, 1991; Kiladis et al., 2016; Magaña & Yanai, 1995; Suhas et al., 2020; Yasunaga, 2011). Several studies have shown that the MRG waves are sensitive to the dynamic and convective background fields in which they are embedded (Wang & Xie, 1996; Zhang & Webster, 1989, 1992). MRG waves are found to be more frequent during the La Niña phase of the El Niño Southern Oscillation (ENSO) and they are confined to the upper troposphere when there is westerly vertical shear or to the lower troposphere when there is easterly vertical shear (T. Feng et al., 2016; Kiladis et al., 2016; Takayabu & Nitta, 1993; Wang & Xie, 1996).

MRG waves play a pivotal role in dictating the variability and predictability of tropical weather. For example, MRG waves originating over the central or east Pacific often transition to tropical depressions and cyclones over the west Pacific (WP) (Aiyyer & Molinari, 2003; T. Feng et al., 2016; Takayabu & Nitta, 1993; Zhou & Wang, 2007). Recent studies indicate that MRG dynamics play a major role in initiating large-scale organized convection over the Indian Ocean (IO) (Takasuka et al., 2019; Takasuka & Satoh, 2020, 2021). Contribution of easterly momentum via vertically propagating MRG waves is vital for the quasi-biennial oscillation (QBO), a dominant mode of stratospheric circulation (Holton & Lindzen, 1972; Yanai et al., 1968). MRG waves were identified to be one of the factors that caused the disruption in QBO activity during

2015–2016 period (Lin et al., 2019). Recent theoretical and observational studies point out that dry dynamics is as important as moist dynamics in explaining the initiation, structure and propagation of the Madden–Julian Oscillations (MJO) and MRG wave is a core part of such theories (Pritchard & Yang, 2016; Takasuka et al., 2019; Takasuka & Satoh, 2020; D. Yang & Ingersoll, 2011). Since MRG waves bear the character of both Rossby and inertia–gravity waves, understanding the dynamics of MRG waves is crucial for improving the method of initialisation and thereby the skill in predicting tropical weather.

Since the advent of satellite observations, many studies have been conducted to understand the structure, propagation and excitation mechanisms of MRG waves (Hendon & Liebmann, 1991; Kiladis et al., 2016; Takayabu & Nitta, 1993; Yanai & Lu, 1983; Zangvil & Yanai, 1981; Zhang & Webster, 1992). Tropical convection, lateral forcing of extratropical disturbances, underlying sea surface temperature (SST) configuration, hydrodynamical instability and wave–wave interactions are suggested as possible mechanisms that can excite MRG waves (Hendon & Liebmann, 1991; Kiladis et al., 2009; Magaña & Yanai, 1995; Randel, 1992; Ripa, 1983). Many of the studies that tried to address the properties of MRG waves and their interactions with other modes of variability often focused on the convectively coupled MRG waves (Kiladis et al., 2016; Suhas et al., 2020; Wheeler et al., 2000; Wheeler & Kiladis, 1999). However, not all MRG wave activity may have a direct association with convection. For example, over the eastern Pacific and Atlantic domains, even while the synoptic-scale perturbation kinetic energy is high, the large-scale convection–circulation coupling strength is weak and hence a large fraction of MRG waves over these regions may not have a direct association with convection (Chen et al., 2016; G. Yang & Hoskins, 2016). Theoretical and observational studies recognise extratropical wave intrusions as one of the main sources of synoptic-scale variability over such regions where the probability of the occurrence of organized convection is less (Charney, 1963; Tomas & Webster, 1994; Webster & Holton, 1982). Linear wave theory identifies the presence of the upper-tropospheric westerly wind ducts as an important condition that would permit the intrusions of extratropical disturbances (Webster & Holton, 1982). Many observational studies show that extratropical intrusions through the upper-tropospheric westerly ducts can trigger tropical convection and equatorial waves (Kiladis, 1998; G. Yang & Hoskins, 2016). Wave energy accumulation and dispersion of energy from other locations can also induce synoptic-scale variability over regions where organized convective activity is less active (Hoskins & Yang, 2016; Webster & Chang, 1988; G. Yang & Hoskins, 2016). Hence a convection-based (e.g., using outgoing longwave radiation [OLR], precipitation, brightness temperature, etc.) identification of MRG wave activity would be an underestimate, as there might be several MRG wave events that might not have a strong signature in convective fields. Therefore, in order to have a comprehensive understanding of the MRG wave activity and their properties, it is important to use a method that is equally sensitive to all categories of MRG waves.

In this study we plan to conduct a climatological survey of MRG waves and characterize them over the whole tropics and separately over different geographical domains. Several past studies that brought out the characteristics of the MRG waves adopted a case study-based approach, which were mostly conducted over localized regions using data of limited sample size (Hendon & Liebmann, 1991; Liebmann & Hendon, 1990; Takayabu, 1994b; Takayabu & Nitta, 1993). Another set of studies extracted the climatological properties of MRG waves over a wider domain using a combination of wavenumber–frequency filtering and linear regression methods (Kiladis et al., 2009, 2016; Suhas et al., 2020; Wheeler et al., 2000). Since the observed MRG waves are localized in space and time, a Fourier-based wave isolation method might not be ideal for bringing out the local characteristics of the waves, as Fourier transform employs the assumption that the MRG waves are global in nature and are continuous. Alternatively, wavelet and windowed wavenumber–frequency spectral analysis are used to capture the localized equatorial wave events (Dias & Kiladis, 2014; Kikuchi, 2014). However, these approaches are also not very effective in capturing the episodic MRG events. In order to better capture the spatial and temporal inhomogeneous nature of MRG wave activity, we use an event-based MRG wave identification method proposed by(Au-Yeung & Tam, 2018).

Since the main objective of the study is to characterize the MRG waves of all kinds, we chose the 200 hPa meridional wind as the primary variable to identify the MRG wave events. The upper-tropospheric winds capture both convectively coupled MRG waves over the Pacific and IO domains and dry MRG waves over the central and east Pacific and Atlantic domains (Kiladis et al., 2016; Magaña & Yanai, 1995; Randel, 1992; Wheeler & Kiladis, 1999; Yanai & Lu, 1983; G.-Y. Yang et al., 2003). The MRG signal in the lower atmosphere is mainly contaminated by the tropical depressions (TD), as it is very difficult to separate out these disturbances (Au-Yeung & Tam, 2018; Takasuka & Satoh, 2020; Takayabu & Nitta, 1993). However, the MRG event identification method based on upper-tropospheric winds is less likely to be contaminated by TD, as the influence of TD is largely confined to the lower to middle troposphere (T. Feng et al., 2016). Recent studies bring out observational evidence for the role of upper-tropospheric MRG waves in triggering lower-level MRG waves and their subsequent transition to TD and tropical cyclones (Au-Yeung & Tam, 2018; Zhou & Wang, 2007). The intrusion of extratropical disturbances over certain tropical regions is also considered as a triggering mechanism for MRG waves (Kiladis et al., 2016; Magaña & Yanai, 1995; Mak, 1969b; G. Yang & Hoskins, 2016; Zhang & Webster, 1992). According to linear wave theory, extratropical disturbances are more likely to intrude over tropical regions where the background winds are westerly (Webster & Holton, 1982). There exists a direct link between the strength of the mean westerly winds and the intensity of energy carried by the extratropical disturbances. The observation of a stronger westerly wind duct in the upper troposphere over the central and east Pacific and Atlantic domains makes 200 hPa meridional wind an ideal parameter for quantifying MRG events associated with extratropical intrusions. Although many previous studies brought out observational evidence for the role of extratropical forcing in triggering MRG waves (Kiladis et al., 2016; Magaña & Yanai, 1995; Randel, 1992; G. Yang & Hoskins, 2016; Zangvil & Yanai, 1981), the relative contribution of such a forcing has not been quantified.

It is expected that a detailed climatology of the MRG events and their characterisation over different geographical domains will provide an observational basis for a complete assessment of MRG excitation mechanisms. It will also serve as a testbed for evaluating the skill of climate models in simulating the MRG waves. Since the MRG waves are unique to the tropics and they play an active role in tropical-scale interactions, realistic simulation of MRG waves is crucial for ensuring the reliability of models in simulating the weather and climate variability. It has been noted that extratropical disturbances could modulate the tropical synoptic-scale variability (Charney, 1963; Mak, 1969a). A recent study (Vishnupriya et al., 2022) showed that about 15% of the monsoon low-pressure systems are triggered by extratropical air intrusions over the Pacific. A set of recent studies revealed that equatorward-propagating extratropical Rossby waves from the NH and SH and their association with MRG waves contribute nearly half of the wave forcing that caused disruption in the westerly phase of the QBO (Kang et al., 2020; Kang & Chun, 2021; Lin et al., 2019). These results demonstrate the close association between tropical and extratropical dynamics and highlight the importance of quantifying the contribution of extratropical disturbances in modulating the MRG waves. Since QBO is considered a source of predictability on the seasonal time-scales, a comprehensive understanding on the relative role of extratropical disturbances in modulating the MRG wave events is also crucial for improving the prediction skill of extratropical seasonal forecasts (Gray et al., 2018). We believe that analysis of MRG events using 40 years of reanalysis data will help address the long-standing issue of the degree of involvement of extratropical disturbances in determining the MRG waves in the tropics.

3.2 Data and Methodology

European Centre for Medium-Range Weather Forecasts Re-Analysis (ERA-Interim) six-hourly 0.5 ∘ × 0.5 ∘ horizontal-resolution zonal and meridional components of the winds at 200 hPa and daily 2.5 ∘ × 2.5 ∘ horizontal-resolution PV on the 350-K isentropic surface from 1 January 1979 to 31 August 2019 are the primary data used in this study (Dee et al., 2011).

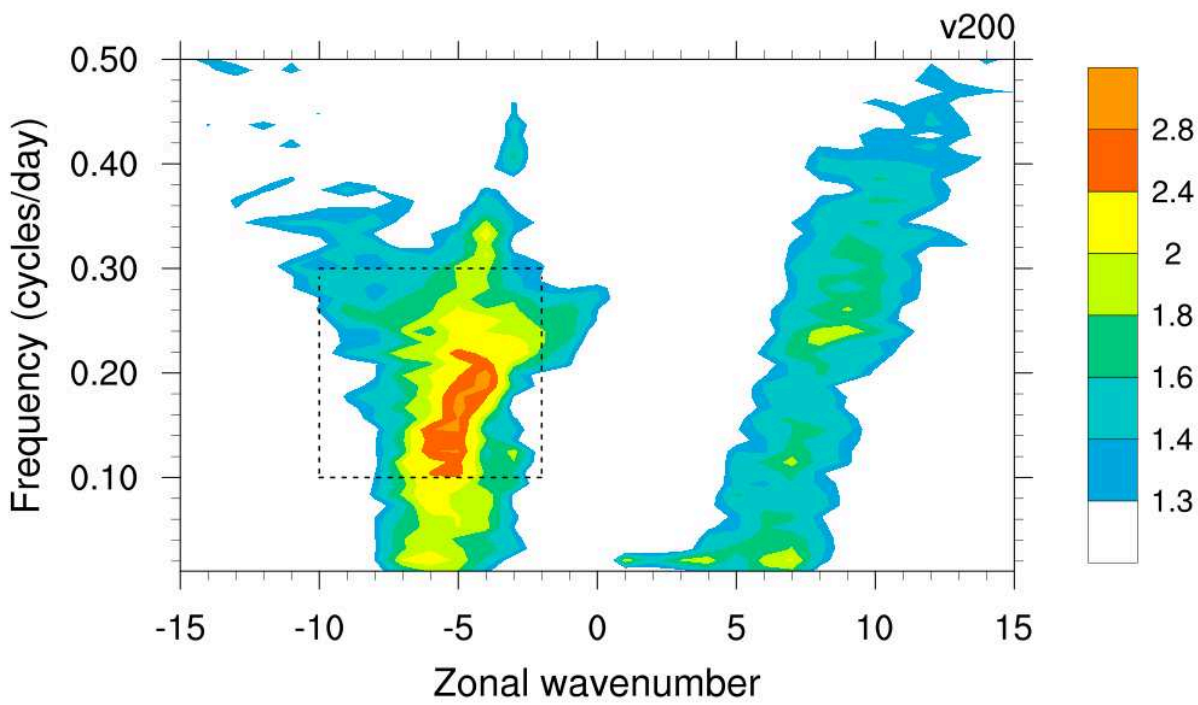

Figure 3.1. Wavenumber-frequency power spectra of the symmetric component of meridional wind at 200 hPa (v200) normalized by red background spectra. The black dotted box represents the wavenumbers and frequencies corresponding to peak mixed Rossby-gravity wave activity. The spectral peaks greater than 1.3 units are statistically significant at 99% confidence level.

Figure 3.1 shows the symmetric wavenumber–frequency power spectra of 200 hPa meridional wind in the tropics (15 ∘ S–15 ∘ N) normalized by the red background (Wheeler & Kiladis, 1999). MRG wave power is prominently distributed in westward-propagating wavenumbers −10 to −2 in the 3–10-day period. It is interesting to note the presence of significant spectral peaks in the eastward wavenumbers as well. Some part of the eastward spectral power might be a result of Doppler shifting of n = 2 equatorial Rossby (ER) and MRG waves by the zonal flow (G. Yang et al., 2023; G. Yang & Hoskins, 2016) and some fraction of the eastward spectral power might be contributed by the intrusion of extratropical disturbances (Kiladis, 1998). Even though the spectral power associated with eastward-propagating MRG waves is less than that associated with westward-propagating MRG waves, it contributes to a large fraction of the eastward-propagating synoptic-scale variability in the western hemisphere (G. Yang & Hoskins, 2016). However a proper investigation of eastward-propagating MRG waves demands a separate study and in this study, we focus on westward-propagating MRG waves. In the following sections westward-propagating MRG waves are referred to simply as MRG waves.

MRG wave events at the 200 hPa level are identified by following the methodology of (Au-Yeung & Tam, 2018). The method is ideal for capturing the episodic behavior of the MRG wave events. Westward-propagating strong equatorial meridional winds are the typical signature of the MRG waves and the MRG wave event identification methodology was designed by exploiting this property. The method estimates the instantaneous properties of the MRG waves such as the amplitude, trapping scale, frequency, wavelength and phase speed during the entire duration of an event. The crux of the methodology is based on the imposition of the theoretical meridional structure of MRG waves onto the meridional wind anomalies (Matsuno, 1966). The meridional wind anomalies are estimated by filtering meridional winds in the westward wavenumbers 2–10 and 3–10-day periodicity. Since the meridional winds associated with MRG waves are symmetrically distributed about the equator, only the symmetric meridional wind anomalies are imposed onto the theoretical meridional structure. The MRG event identification methodology involves multiple steps. At first, the longitudes marking the centers of the MRG wave events are located by identifying the local maxima and minima of the meridional wind anomaly at the equator for each instant. Only the longitudes where the meridional wind anomalies exceed a value equal to 20% of the maximum, meridional wind amplitudes are recorded to avoid very weak MRG wave events. Secondly, the meridional structure of the MRG waves is estimated at all those longitude locations by fitting the meridional wind anomalies at the equator onto the theoretical meridional structure of MRG waves using the equation given below.

$$v_{fitted}(x, y, t) = v_{data}(x, y = 0°, t)D_0(y), \quad (3.1)$$

$$D_0(y) = e^{-\left(\frac{y}{2y_0}\right)^2}, \quad (3.2)$$

where v_{fitted} is the meridional wind of MRG waves and v_{data} is the meridional wind anomaly, x, y, t represent the longitude, latitude and time points, respectively, $D_0(y)$ is the n = 0 parabolic cylindrical function which describes the meridional structure of the n = 0 equatorial wave mode (Yang et al., 2003) and y 0 represents the trapping scale or idealized representation of meridional extent of the MRG wave. y_0 is a free parameter and MRG meridional winds are estimated for y_0 ranging from 0.5° to 20°.

The error associated with the estimation of MRG meridional winds is quantified as follows:

$$E(x, t) = \frac{\sqrt{\frac{1}{n}\sum_{y=0^o}^{y=20^o}\left(v_{data}(x,y,t) - v_{fitted}(x,y,t)\right)^2}}{|v_{data}(x,y = 0^o,t)|} \quad (3.3)$$

where E represents the error as a function of longitude and time and n represents the number of latitude points between 0° and 20° .

Finally, the observed maximum (minimum) of meridional wind anomaly at a longitude and time step is considered as a part of an MRG event only if it is linked to the next time step in a way that the maximum (minimum) of meridional wind anomaly should be observed within 20° west of the previous longitude point. A cluster of longitude and time points that satisfy the above criteria for a duration ranging from two to eight days with at least one point exhibiting an error value less than or equal to 5% is classified as an MRG wave event. To avoid double counting, we have identified the MRG wave events by considering only the positive phase of the meridional wind anomaly.

Even though the wave-fitting method employed in the study is derived from the wave projection methodology of Yang et al. (2003), there are significant differences between the two

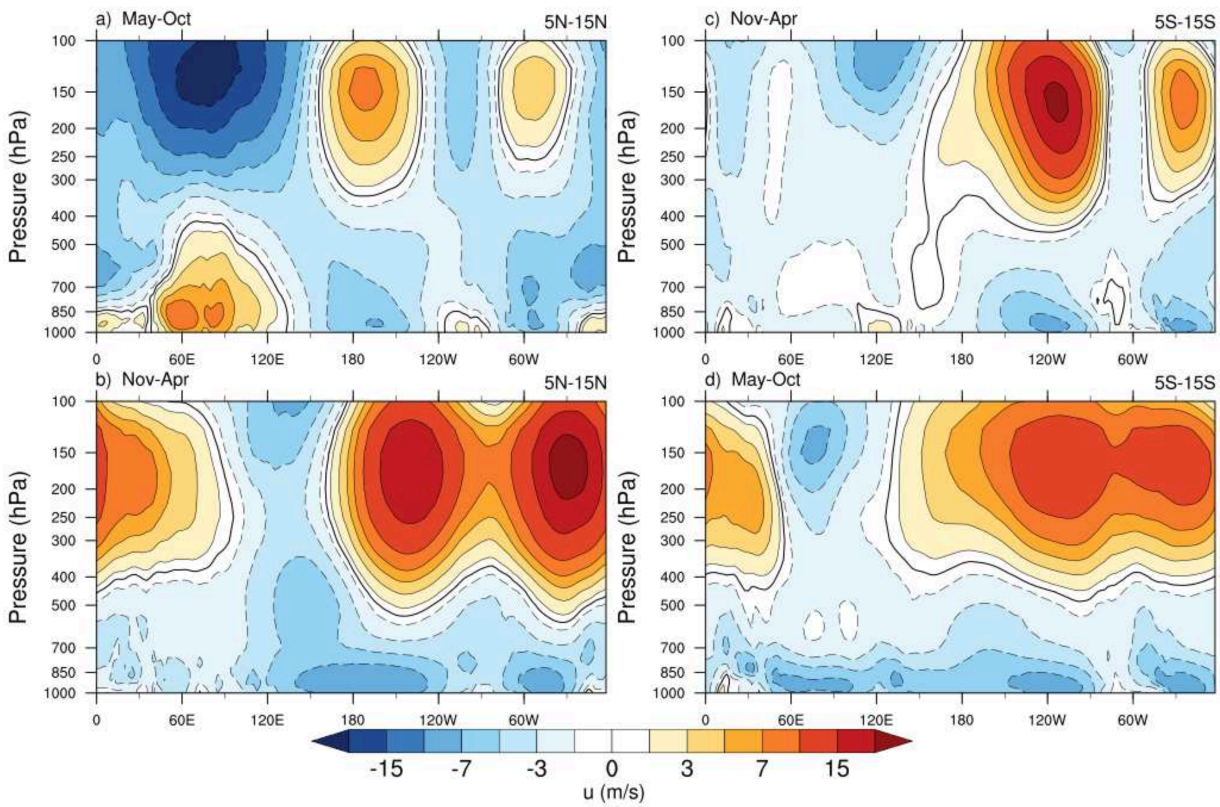

Figure 3.2. Seasonal longitude-pressure distribution of time mean zonal wind anomalies averaged over latitudes a) 5 N to 15N for May to October, b) 5 N to 15 N for November to April, c) 5 S to 15 S for November to April and d) 5 S to 15 S for May to October.

approaches. In the wave projection method parabolic cylindrical functions are used as the basis function and since the parabolic cylindrical functions are orthogonal, the projection of dynamical fields onto the theoretical structure of equatorial waves does not permit the mixing of different equatorial waves, whereas in the wave-fitting method, the imposition of meridional wind anomalies 1 onto the meridional structure of MRG waves, while capturing the equatorially trapped and equatorially symmetric character of MRG waves, also allows for the mixing of MRG waves with the other equatorial waves of similar characteristics (e.g., n = 2 equatorial Rossby waves). However, it is expected that the limited wavenumber and frequency filtering range (2–10 westward wavenumbers and 3–10-day periodicity) used for extracting the meridional wind anomalies would minimize the possibility of mixing MRG waves with the n = 2 and higher even-number meridional modes of ER waves that exhibit a low-frequency character. It has been recognised that the presence of background circulation can modulate the restoring force of equatorial waves, which in turn can cause variability in the trapping scale of equatorial

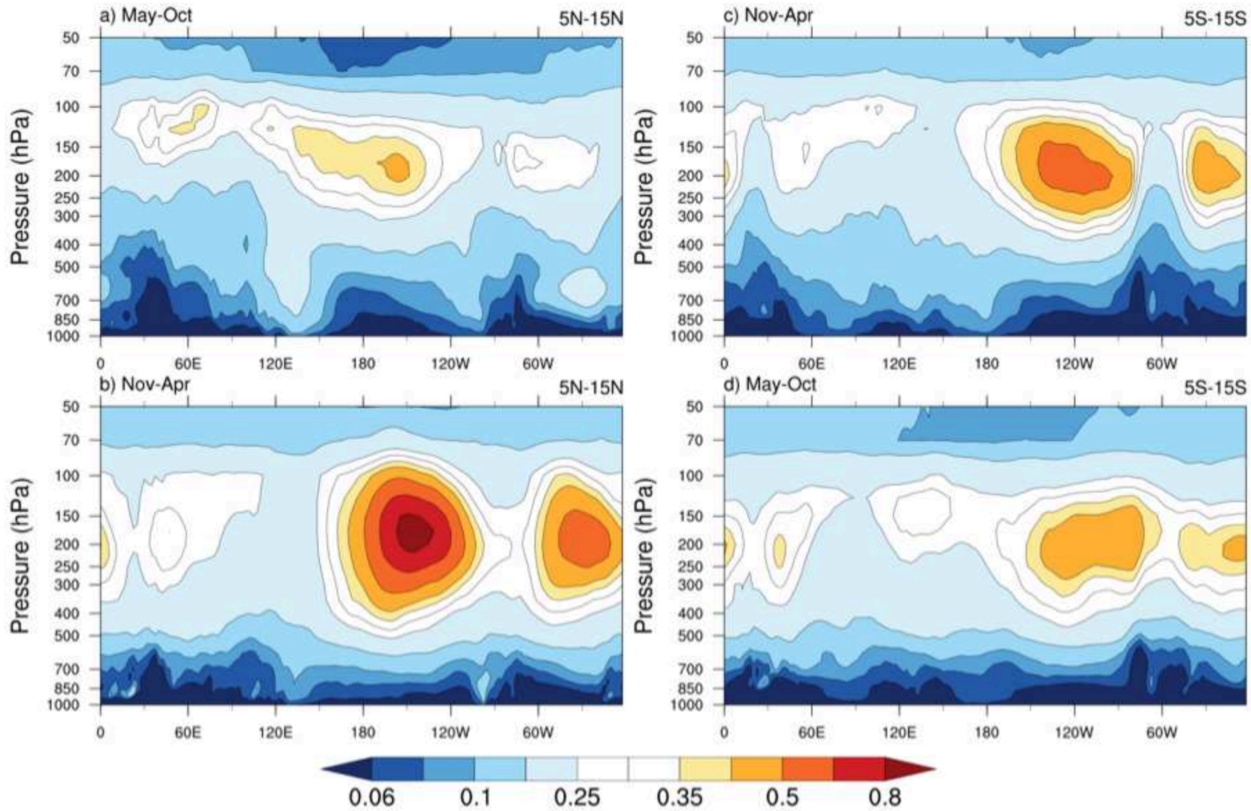

Figure 3.3. Longitude–pressure distribution of 3–10-day power spectra in zonal winds (m^2s^{-2}) averaged over : (a) 5°N–15°N latitudes for northern hemispheric summer seasons (May–October); (b) 5°N–15°N latitudes for northern hemispheric winter seasons (November–April); (c) 5°S–15°S latitudes for southern hemispheric winter seasons (May–October); and (d) 5°S–15°S latitudes for southern hemispheric summer seasons (November–April).

waves (Zhang & Webster, 1989). Since easterly and westerly winds are observed in the tropical upper troposphere, we do expect notable differences in the trapping scales of MRG wave events. Unlike the wave projection method, the wave-fitting method treats the trapping scale as a variable parameter and it enables estimating the instantaneous value of the trapping scale (Au-Yeung & Tam, 2018). There is a possibility that the intrusion of extratropical disturbances over the westerly ducts might lead to an overestimation of the trapping scale and in turn impact the identification of MRG wave events. However, the close similarity between the MRG wave events identified using wave-fitting and wave projection methods (figure not shown), gives more confidence in the wave-fitting-based approach used in the study. A recent study (Knippertz et al., 2022) provides a comprehensive review on the subject of equatorial wave identification techniques.

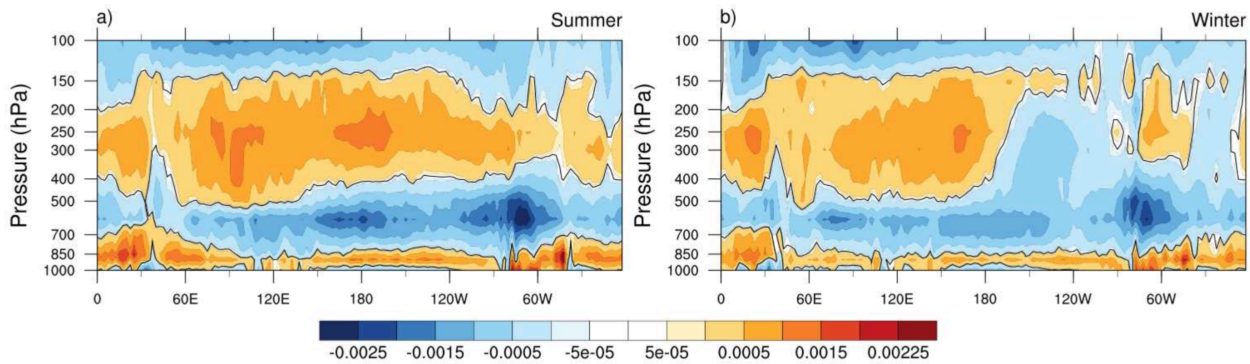

Figure 3.4. Longitude–pressure distribution of 3–10-day co-spectra of temperature and vertical pressure velocity averaged over the tropics (15 ◦ S–15 ◦ N) for (a) northern hemispheric summer seasons (May–October); and (b) northern hemispheric winter seasons (November–April). Temperature and vertical pressure velocity anomalies are normalized with respect to their respective standard deviation before estimating the cross-spectra.

We have identified 2390 MRG wave events at 200 hPa for the 1979–2019 period. Important dynamical properties of the MRG waves during different time instances of an MRG wave event are estimated as follows. The maximum of meridional wind anomaly at the equator is taken as the amplitude of the MRG wave. The trapping scale is estimated from the y 0 values which show minimum error. The instantaneous wavenumber of an MRG wave event is estimated by applying Fourier transform in space. Instantaneous phase speed of an MRG wave event is estimated using the fourth-order Runge–Kutta finite difference method. Statistical significance of the differences in wave properties of the MRG wave events are tested by conducting Student's t and F tests.

The presence of extratropical disturbances over the subtropical and tropical region during MRG wave events is identified by following the methodology of (Waugh & Polvani, 2000). Waugh & Polvani, 2000 traced the intrusion of extratropical air into the tropical region by exploiting the PV conservation in the absence of diabatic processes. By following a similar strategy, PV on the 350-K isentropic surface is used as a tracer to identify the extra- tropical wave intrusions during MRG wave events. Since the 350-K isentropic surface lies in the lower stratosphere in the extratropics and in the upper troposphere in the tropics (close to 200 hPa), the observation of higher PV on the 350-K isentropic surface over the tropical region suggests the presence of extratropical air in the tropics. An MRG wave event is grouped as the one associated with extratropical wave intrusions only when the criteria involving amplitude and duration of the PV at 350 K over a region where the MRG waves are active, are satisfied. It is noted that the ext-

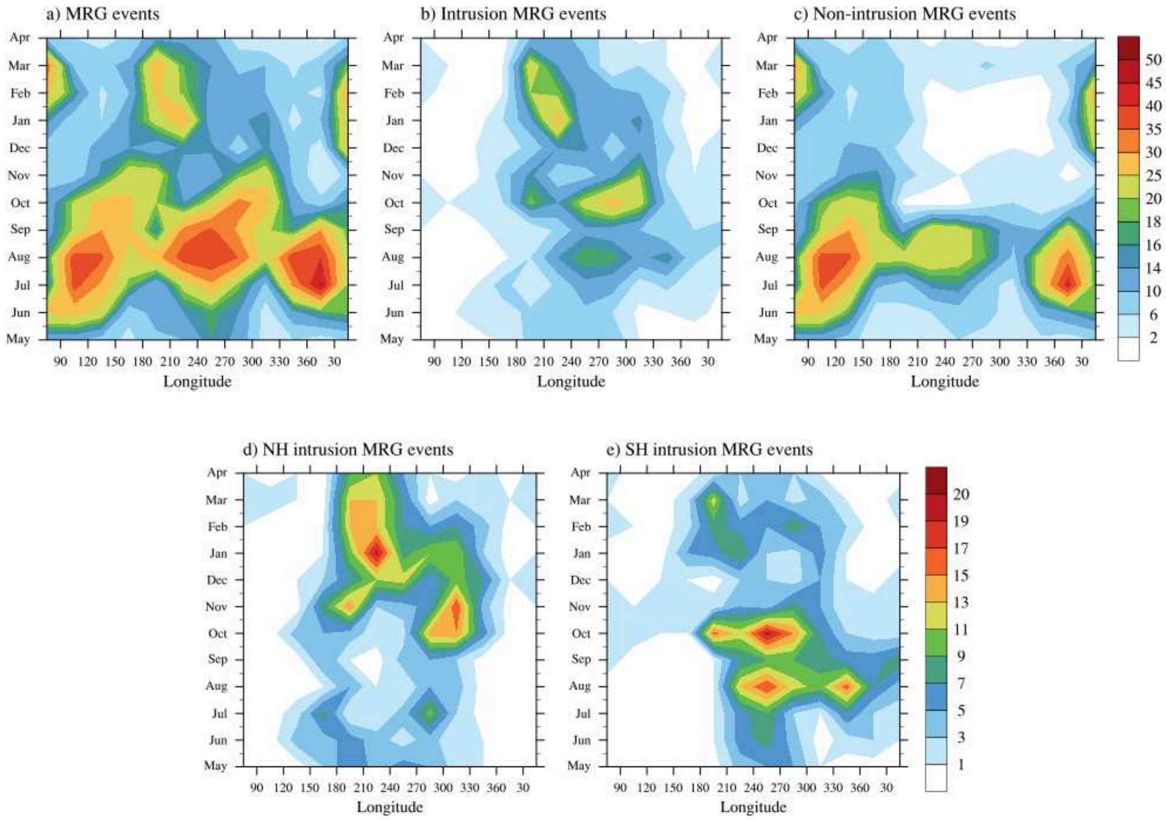

Figure 3.5. Month–longitude distribution of number of occurrences of mixed Rossby–Gravity (MRG) wave events at 200 hPa observed for the period 1979–2019. (a) Total number of occurrences of MRG wave events; (b) number of occurrences of MRG wave events that are associated with the intrusions of extratropical disturbances; (c) number of occurrences of MRG wave events that are not associated with the intrusions of extratropical disturbances, number of occurrences of MRG wave events that are associated with the intrusions of extratropical wave disturbances via (d) the northern hemisphere and (e) the southern hemisphere.

ratropical disturbances can intrude into the tropics by taking NH and SH pathways. First, the amplitude of the PV at 350 K must be greater than 1 PVU at 15°N or 15°S within 40° east or west of the longitude at which the meridional wind of MRG waves exhibits a maximum. Second, the above condition must be satisfied for at least two days before the peak MRG wave activity and the high PV amplitude should be persistent over a longitudinal extent of 10°. If an MRG event satisfies these two criteria, such an MRG event is classified as an intrusion MRG event.

3.3 Results and Discussions

The equatorial wave characteristics, including that of MRG waves, are known to be sensitive to the mean zonal winds (Hoskins & Yang, 2016; Wang & Xie, 1996; G. Yang & Hoskins, 2016; Zhang & Webster, 1989, 1992). In addition to Doppler shifting of the intrinsic frequency, mean

MRG event category	**Indian Ocean (50°E-110°E)**	**West Pacific Ocean (110°E-180°E)**	**East Pacific Ocean (180°E-90°W)**	**Atlantic Ocean (180°E-90°W)**	**Total MRG events**
Intrusion MRG events	29	77	480	314	900 (37%)
Non-intrusion MRG events	361	387	276	466	1490 (63%)
Total MRG events	390 (16%)	464 (19%)	756 (32%)	780 (33%)	2390

Table 3.1. Number of occurrence of intrusion mixed Rossby–Gravity (MRG) events, non-intrusion mixed Rossby–Gravity (MRG) events and total MRG events observed over the Indian Ocean, West Pacific Ocean, central–east Pacific Ocean and Atlantic Ocean domains for the period 1979–2019.

zonal winds can modulate the dynamics of MRG waves and restrict MRG wave activity either to the upper or the lower troposphere (Wang & Xie, 1996; Zhou & Wang, 2007). Figure 3.2 shows the longitude–pressure distribution of mean zonal winds averaged over the NH (5 ◦ N–15 ◦ N) and SH (5 ◦ S–15 ◦ S) tropical regions, during NH summer and winter seasons. Westerly ducts are known to support extratropical–tropical interactions which might result in the excitation of MRG waves (Magaña & Yanai, 1995; Randel, 1992; Webster & Holton, 1982). Several previous studies have brought out observational evidence for the NH and SH pathways of extratropical intrusions and the subsequent interactions with MRG waves (Kiladis et al., 2016; Magaña & Yanai, 1995; G. Yang & Hoskins, 2016; G.-Y. Yang et al., 2007a, 2007b). Well-developed westerly wind ducts are observed in the upper troposphere over the central–east Pacific and Atlantic domains in the winter hemispheres (Figure 3.2 b,d), while the westerly wind ducts are weak and mostly confined to a smaller region in the summer hemisphere (Figure 3.2 a,c). It implies the higher likelihood of upper-tropospheric intrusions of extratropical disturbances during winter seasons. On the other hand, in the lower troposphere, westerly winds are observed only during NH summer; its amplitude is weak and is limited to the NH IO domain. The dominance of easterly zonal wind regime in the lower troposphere indicates that the lower troposphere is less conducive for the extratropical intrusions and the upper-tropospheric wind fields are chosen for quantifying the MRG–extratropical interactions.

Since MRG waves belong to the class of synoptic-scale variability, the synoptic-scale (3 -

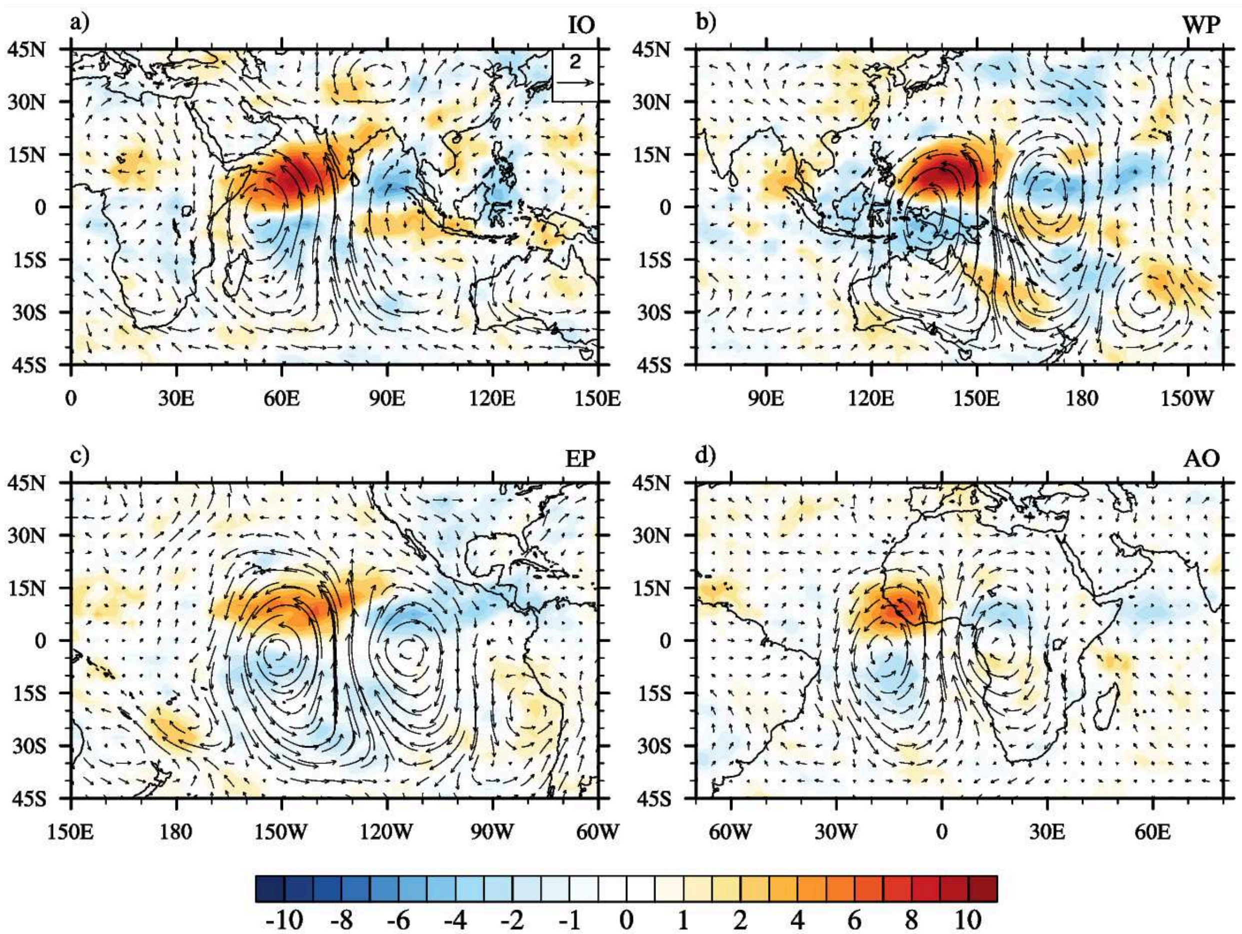

Figure 3.6. Composites Composites of mixed Rossby–Gravity (MRG) wave events constructed using 3–15-day bandpass-filtered 200 hPa wind (ms^{-1}) and outgoing longwave radiation (OLR; Wm^{-2}) anomalies over: (a) the Indian Ocean (IO); (b) West Pacific Ocean (WP); (c) central–east Pacific Ocean (EP); and (d) Atlantic Ocean (AO) domains. While compositing the wind and OLR anomalies are longitudinally translated to a reference longitude corresponding to maximum occurrence of MRG wave events for each domain.

10 days) spectral variance of zonal winds is examined for the NH (5°N–15°N) and SH (5°S–15°S) tropical regions during summer and winter seasons. Synoptic-scale spectral variance is estimated by computing the power spectra for multiple 90-day segments and averaging it for 3–10-day periodicity. The longitude–pressure distribution of synoptic-scale variance of zonal winds exhibits similar seasonal and geographical preferences as the zonal mean winds (Figure 3.3). Strong synoptic-scale variance is observed in the mid to upper troposphere mostly in the

western hemisphere, and the synoptic-scale disturbances are more prominent over the winter hemisphere (Figure 3.3 b,c). The longitude–pressure distribution of synoptic-scale variance of meridional winds is similar to that of the zonal winds (figure not shown). The regions of strong synoptic-scale wind variance represent the regions of maximum perturbation kinetic energy (PKE). The observed colocation of westerly wind ducts and the PKE maxima corroborates the findings of many previous studies (Arkin & Webster, 1985; Chen et al., 2016; Webster & Chang, 1988; Webster & Holton, 1982). The available potential energy (APE) to PKE conversions is examined by calculating the co-spectra between pressure vertical velocity and temperature for NH summer and winter seasons (Figure 3.4). A positive co-spectral power is an indicator of APE to PKE conversions and it can be used as a measure of convection-wave coupling strength (Chen et al., 2016; Yanai et al., 2000). From the longitude– pressure distribution of synoptic-scale (3 – 10 day) co-spectral power (Figure 3.4a), it is evident that the generation of synoptic-scale motions through convection is predominant in the entire tropical upper troposphere during the summer season, while the upper-tropospheric APE to PKE conversion is weak in the western hemisphere during the winter season and it is noticeably absent over the central and east Pacific (EP) and Atlantic Ocean (AO) (Figure 3.4 b). While the westerly wind ducts are collocated with the synoptic-scale PKE maxima, the conspicuous absence of APE to PKE conversions over the westerly wind duct locations implies that the synoptic-scale motions over such regions are likely to be caused by dynamical processes or extratropical forcing (Charney, 1963; Holton, 2004). Recent studies based on the one-dimensional wave propagation theory rule out the variation of zonal flow and wave energy accumulation as the source of synoptic-scale PKE maxima in the western hemisphere (Hoskins & Yang, 2016; Yang & Hoskins, 2016).

In a nutshell, analysis of the mean zonal winds, synoptic-scale variance and conversion of APE to PKE implies that the excitation mechanisms of upper-tropospheric MRG waves can differ regionally and can have seasonal preferences. Examining the number of occurrences of MRG wave events as a function of longi- tude and months would help in understanding whether the MRG wave events exhibit any spatial and temporal clustering. Using the methodology of Au-Yeung and Tam, 2018; the spatial–temporal distribution of MRG events is analyzed by calculating the monthly frequency of occurrence of MRG wave events in 30° longitude bins. Figure 3.5 a shows the climatological distribution of 200 hPa MRG wave events during the months of January to December for the period 1979 to 2019. The analysis shows that MRG wave events occur over all the major ocean basins and exhibit a clear seasonality. More than 60% of the total MRG wave events are observed during NH summer season. A major fraction of MRG wave events over the Indian, Pacific and Atlantic Ocean domains occur during NH summer and secondary maxima of MRG wave events are observed during the NH winter season over the central–east Pacific and IO domains.

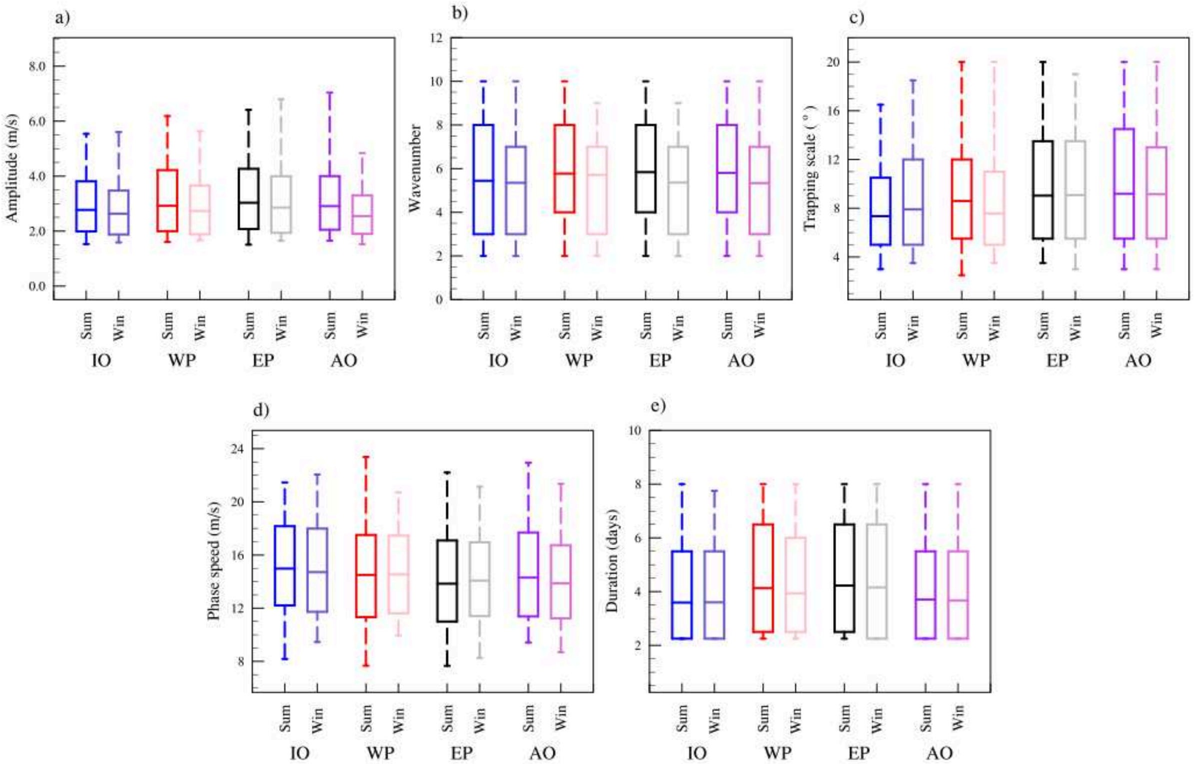

Figure 3.7. Range (maxima, minima), 90th percentile, mean, and 10th percentile of (a) amplitude (ms^{-1}); (b) wavenumber; (c) trapping scale (°); (d) phase speed (ms^{-1}); and (e) duration (days) of MRG wave events observed over Indian Ocean (IO, blue), West Pacific (WP, red), central–east Pacific (EP, black) and Atlantic Ocean (AO, purple) domains during northern hemispheric summer (Sum, dark color) and northern hemispheric winter (Win, light color).

Based on the spatial distribution of MRG wave events, we have identified four preferred domains of MRG activity – IO (covers 50°E to 109.5°E), WP (covers 110°E to 179.5°E), EP (covers 180°E to 89.5°W) and AO (covers 90°W to 49.5°E) domains. The statistics of MRG wave events over different domains are summarized in Table 3.1. As indicated by many previous studies, about 65% of the MRG wave events are observed over the EP and AO domains (Kiladis et al., 2016; Randel, 1992; Suhas et al., 2020; Yang & Hoskins, 2016). It is interesting to note that about two-thirds of the total MRG wave events are equally distributed over the EP and AO domains. The robustness of the method of identification of MRG wave events is confirmed by examining the MRG wave event composites of dynamical fields over the four domains. Figure 3.6 shows the MRG wave event composites of 3–15 day filtered 200 hPa wind and stream function anomalies over the IO, WP, EP and AO domains. The composites are constructed with respect to the reference longitudes around which the largest number of MRG wave events is observed in each domain. The selected reference longitude for the IO, WP, EP and AO domains are 70°E, 120°E, 135°W and 40°W, respectively. Although the horizontal structure of the MRG waves appears to be similar over all the domains, some differences in their properties are observed over the different domains. For example, the amplitude, wavelength and meridional extent of the MRG waves are larger over the EP domain (Figure 3.6 c). It is also evident that the convection–circulation coupling strength of MRG wave events varies over different domains. The observation of stronger convection–circulation coupling over the IO and WP domains the prevalence of moist dynamics.

MRG event category	**Indian Ocean (50°E to 110°E)**			**West Pacific Ocean (110°E to 180°E)**			**Central-east Pacific Ocean (180°E to 90°W)**			**Atlantic Ocean (90W° to 50°E)**			**Total**
	NH intrusion	SH intrusion	NH & SH intrusion	NH intrusion	SH intrusion	NH & SH intrusion	NH intrusion	SH intrusion	NH & SH intrusion	NH intrusion	SH intrusion	NH & SH intrusion	
Intrusion: NH summer	0	8	0	36	3	0	68	154	6	50	113	10	448 (19%)
Intrusion: NH winter	10	10	1	22	12	4	162	73	17	85	44	12	452 (19%)
Non-intrusion: NH summer	209			266			220			333			1028 (43%)
Non-intrusion: NH winter	152			121			56			133			462 (19%)
Total	390 (16%)			464 (19%)			756 (32%)			780 (33%)			2390

Table 3.2. Number of occurrences of NH intrusion MRG events, SH intrusion events, cooccurrence of NH and SH intrusion MRG events and non-intrusion MRG events observed during NH summer and winter for 1979-2019.

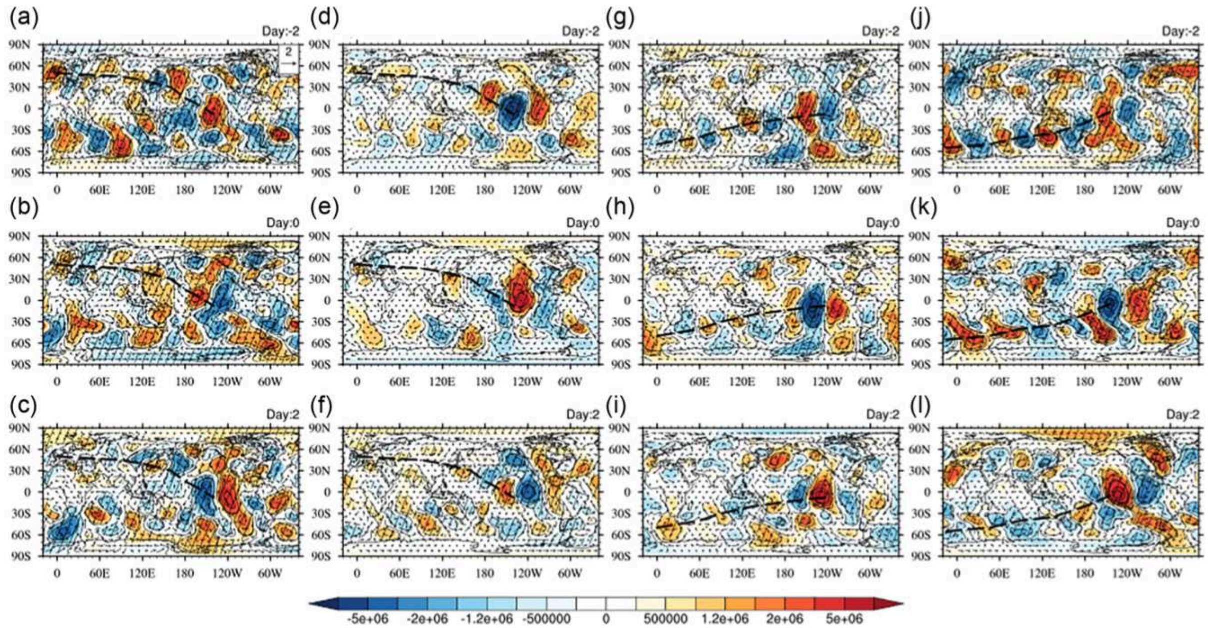

Figure 3.8. Lead–lag composites of intrusion MRG wave events over the central-east Pacific Ocean domain, constructed using 3–15-day bandpass-filtered 200 hPa wind (ms^{-1}) and stream function (m^2s^{-1}) anomalies. Positive (negative) lag represents the number of days after (before) the maximum mixed Rossby–Gravity (MRG) wave amplitude. (a–c) NH intrusion MRG wave events during NH summer; (d–f) NH intrusion MRG wave events during NH winter; (g–i) SH intrusion MRG wave events during NH summer; and (j–l) SH intrusion MRG wave events during NH winter. Black dashed curves highlight the intrusions of extratropical disturbances. Stippled regions are statistically significant at the 95% confidence level.

The differences in important wave properties such as the amplitude, wavenumber, trapping scale, phase speed and duration of the individual MRG wave events over all the four domains are further evaluated. Figure 3.7 shows the range, mean and 90th- and 10th-percentile values of the MRG wave properties over the different domains during summer and winter seasons. Clear seasonality in the major MRG wave properties is observed across all domains. The amplitude of MRG waves is higher during NH summer and the largest- and smallest-amplitude MRG wave events are observed over the EP and AO domain, respectively (Figure 3.7 a). It is noted that the difference in the distribution of amplitude of the MRG waves during summer and winter over the WP and AO domains are statistically significant at the 95% confidence level. In other words, compared to the other domains, the amplitudes of the MRG wave events over the IO and EP domain exhibit less seasonal variability. Summer–winter differences in the distribution of wavenumbers over the EP and AO domains are statistically significant at the 90% confidence level. The MRG wave events exhibit a shorter wavelength (larger wavenumber) during the NH summer season (Figure 3.7 b). The MRG convection–circulation coupling strength is stronger during the NH summer (Suhas et al., 2020) and studies (Aiyyer & Molinari, 2003; Zhou & Wang, 2007) indicate that the MRG scale selection is strongly tied to the active feedback between frictional convergence and convective processes. The shorter wavelength observed during NH summer might be related to a stronger feedback between frictional convergence and convection (Zhou & Wang, 2007). The relatively smaller trapping scale of MRG wave events over the IO and WP domains (Figure 3.7 c) suggests that convection probably plays a dominant role in triggering the MRG waves over these domains (Figure 3.6 a,b). Tropical organized convection makes the atmosphere less stable and decreases the effective equivalent depth which in turn reduces the trapping scale of wave disturbances (Kiladis et al., 2009). A relatively larger trapping scale is observed over the less convectively active EP and AO domains (Figure 3.7 c). Zonal mean winds and extratropical forcing also play a role in determining the trapping scale of MRG waves (Zhang & Webster, 1989; 1992). The larger trapping scale might be indicative of the role of wave–mean flow interactions and intrusions of extratropical disturbances in triggering MRG wave events over these domains. The MRG wave phase speeds range from 12 to 17 $m \cdot s^{-1}$ and in contrast to the other parameters, they do not show much seasonality and variations across the different domains (Figure 3.7 d). The duration of MRG wave events is also not very sensitive to the season. However, longer-duration MRG wave events are observed over the Pacific domain (Figure 3.7 e). The possible link between MRG wave events and intrusions of extratropical disturbances are investigated by examining the PV on the 350-K isentropic surface. Using the intrusion identification methodology described above, we find that about 37% of the MRG wave events are associated with intrusions of extratropical disturbances and the majority (54%) of such MRG wave events occur during NH winter (Table 3.2). The longitudinal distribution of monthly frequency of occurrence of MRG wave events associated with and without intrusions of extratropical disturbances is shown in Figure 3.5 b,c. It is indicated in Table 3.1 that significant intrusion MRG wave events are further classified as NH (SH) intrusion MRG wave events in the case when extratropical air intrusions occur in the NH (SH), respectively. In rare cases, when intrusions are observed in both hemispheres, the event is classified based on the fraction of intrusion MRG wave events (88%) occurs over the EP and AO domains, and about half of the

MRG wave events over these domains are associated with intrusions of extratropical disturbances. On the other hand, a large fraction of the MRG wave events (86%) over the IO and

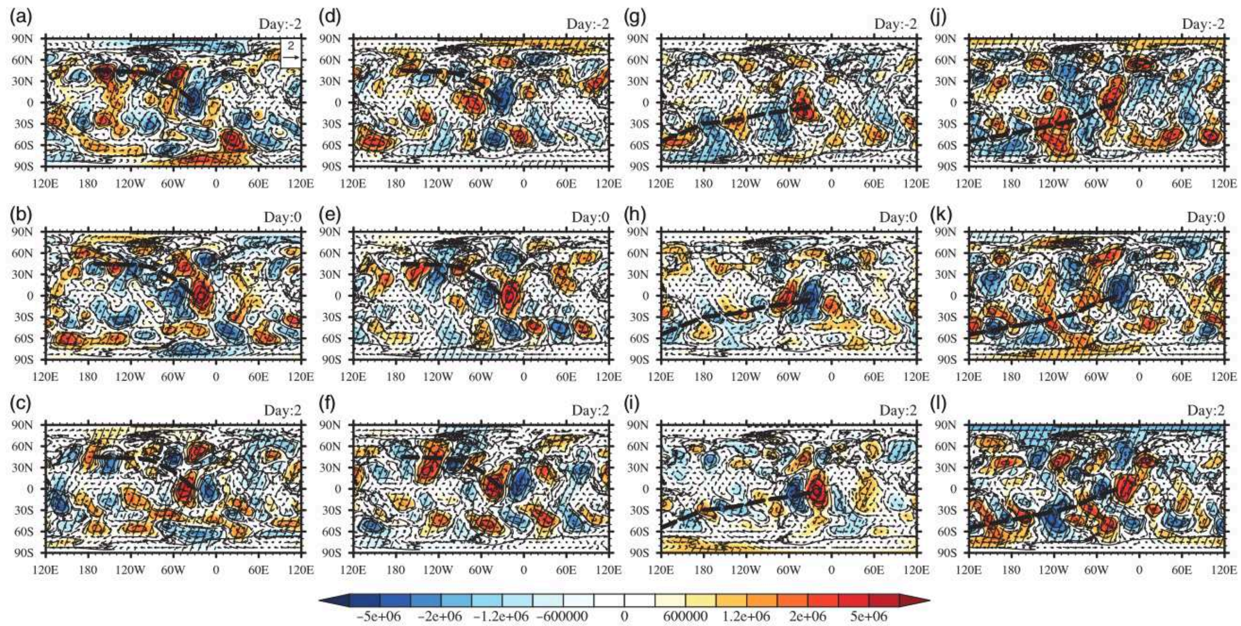

Figure 3.9. Same as figure 3.8 but for the Atlantic domain.

WP domains is not associated with intrusions of extratropical disturbances, consistent with the existence of an upper-level easterly basic state that would preclude the propagation of Rossby wave energy into those regions.

Intrusion MRG wave events are further classified as NH (SH) intrusion MRG wave events in the case when extratropical air intrusions occur in the NH (SH), respectively. In rare cases, when intrusions are observed in both hemispheres, the event is classified based on the strength of the PV. The statistics and seasonality of the NH and SH intrusion MRG events and non-intrusion MRG events over the four domains are summarized in Table 3.2. The longitudinal distribution of monthly frequency of occurrence of NH and SH intrusion MRG wave events is shown in Figure 3.5 d,e. The analysis reveals that intrusion of extratropical disturbances from both the NH and the SH is equally important in the genesis of MRG wave events. Except Yang & Hoskins, 2016 ; Kiladis et al., 2016, all other past studies only reported the association between the intrusion of extratropical disturbances via SH and MRG wave events (e.g., Magaña & Yanai, 1995; Suhas et al., 2020). The NH intrusion MRG wave events exhibit a maxima over the EP during December–January and over the AO during October–November. Likewise, a large number of SH intrusion MRG wave events is observed during SH winter. Consistent with the inferences made from the distribution of mean zonal winds, the winter hemisphere with the westerly wind ducts seem to provide a favorable environment for the occurrence of intrusion

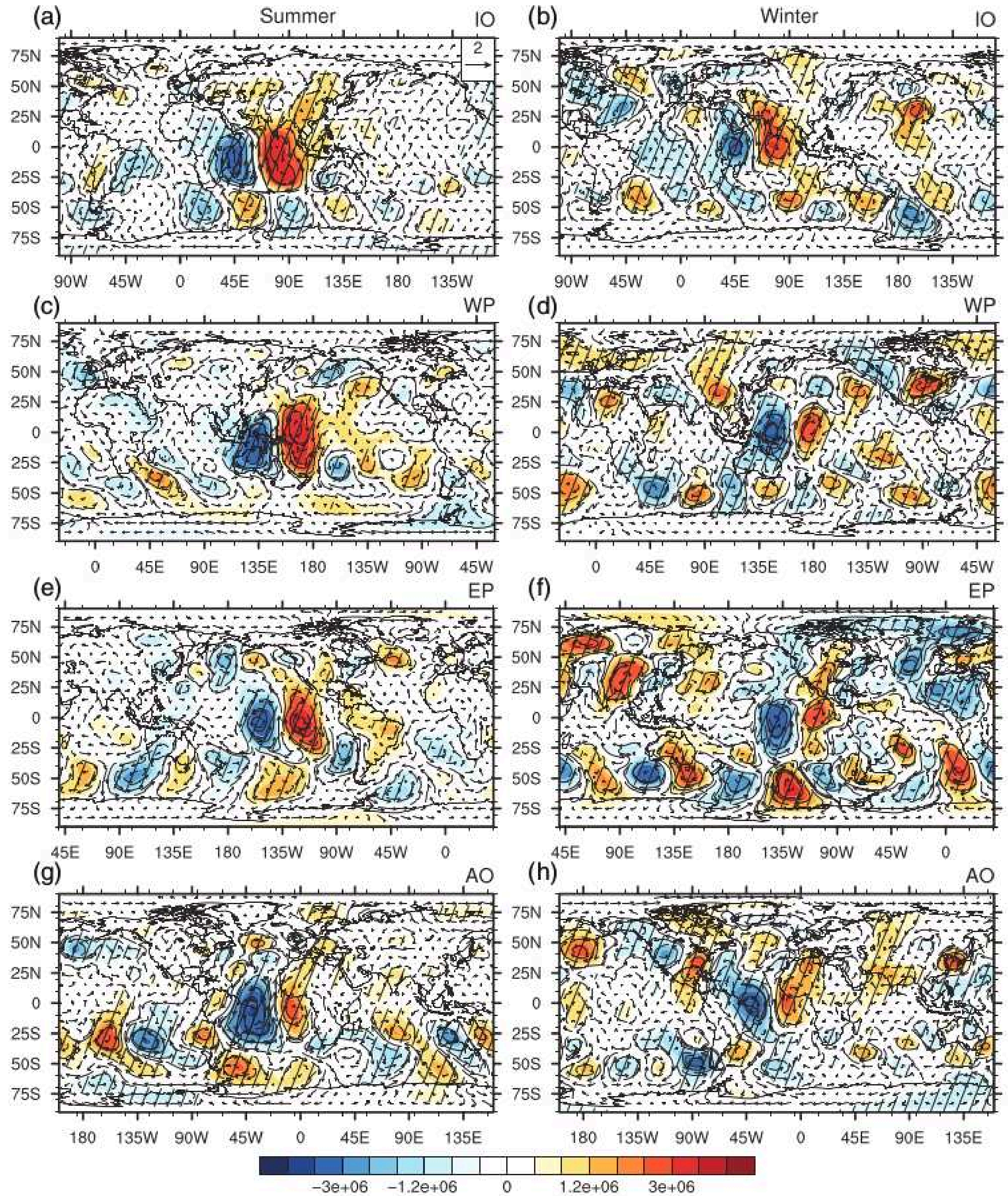

Figure 3.10.Composite non-intrusion mixed Rossby–Gravity (MRG) wave events constructed using 3–15-day bandpass - filtered 200 hPa wind (ms^{-1}) and stream function (m^2s^{-1}) anomalies over the composites of 3–15-day

bandpass- filtered 200 hPa wind (ms^{-1}) and stream function (m^2s^{-1}) anomalies of non-intrusion MRG events occurring over: (a,b) the Indian Ocean; (c,d) West Pacific; (e,f) central–east Pacific; and (g,h) Atlantic Ocean domains during NH summer (left column) and winter (right column). Stippled regions are statistically significant at 95% confidence level.

MRG wave events (Figure 3.2 b,d). About 70% of the intrusion MRG wave events over the EP and AO domains are observed in the winter hemisphere.

Spatial–temporal evolution of the upper-tropospheric tropical and extratropical dynamical fields during MRG wave events is examined for further validating the intrusion and non-intrusion MRG wave event classification. Lead–lag composites of dynamical fields associated with MRG wave events are constructed by identifying the day and longitudinal location of the amplitude maxima corresponding to each MRG wave event and translating the longitudinal locations to a reference longitudinal location and separately averaging the dynamical fields two days before, two days after and on the day of the MRG amplitude maxima. Figure 3.8 shows the lead–lag composites of 3–15-day filtered wind and stream function anomalies at 200 hPa associated with the intrusion MRG wave events over the EP domain. Statistical significance of the composites of MRG wave events are tested by conducting t-tests. Northwest–southeast-oriented stream function anomalies propagating from the NH extratropical to tropical region are found in the composites of NH intrusion MRG wave events during summer and winter (Figure 3.8 a–f). At the same time, southwest–northeast-oriented eastward-propagating wave trains composed of alternate cyclonic and anticyclonic wind anomalies arching towards the equator are found in the SH in the composites of SH intrusion MRG wave events during summer and winter (Figure 3.8 g–l). The observation of differences in the amplitude of the intruding extratropical disturbances two days before (stronger) and two days after (weaker) the MRG wave event amplitude maxima indicates the role of extratropical disturbances in triggering the MRG wave events. Weakening of the intruding extratropical disturbances a few days after the MRG amplitude maxima could be explained based on the PV–convection relationship. Past studies showed the occurrence of convection downstream of the intruding extratropical disturbances over the EP (Kiladis, 1998). Diabatic heating associated with convection can induce anticyclonic anomalies in the upper level which in turn can weaken the pre-existing cyclonic anomalies through destructive interference and thereby weaken the wave trains. Similar to life cycle composites of the intrusion MRG wave events over the EP domain, northwest–southeast oriented and southwest–northeast oriented equatorward and eastward propagating extratropical disturbances are observed over the AO domain during summer and winter (Figure 3.9). It seems that the inter-hemispheric propagation of extratropical disturbances is more likely over the AO domain (Figure 3.9 a–f). It can be deduced from the lead–lag composites that the intruding extratropical disturbances exhibit wavenumbers in the range of 4–7 (Figures 3.8, 3.9).

Figure 3.10 represents the composites of 3–15-day filtered 200 hPa wind and stream function anomalies of non-intrusion MRG wave events over the IO, WP, EP and AO domains during summer and winter. The composites are created for the day of the maximum MRG amplitude of non-intrusion MRG wave events. As expected, the composites of MRG non-intrusion wave events show that extratropical disturbances are either absent or weak and do not intrude into the tropics during NH summer and winter over all the domains (Figure 3.10). The results of the composite analyses for intrusion and non-intrusion MRG wave events validate the robustness of the method employed in classifying the MRG wave events.

Some previous studies based on idealized modeling experiments argued that lateral forcing and different configurations of mean winds can induce differences in the properties of MRG waves (Mak, 1969; Wang & Xie, 1996; Zhang & Webster, 1992). To explore whether the intrusion and non-intrusion MRG wave events exhibit notable differences in their properties, the statistical modes of the amplitude, wavenumber, trapping scale, phase speed and duration of the two groups of MRG wave events are examined during summer and winter (Figure 3.11). The analysis is restricted to the EP and AO domains since approx. 88% of the intrusion MRG wave events are observed over these domains. The non-intrusion MRG wave events exhibit a larger amplitude during the summer season compared to winter over both domains (Figure 3.11 a,f), consistent with the larger MRG amplitude observed during summer (Figure 3.7 a). Over the EP domain, where the largest-amplitude MRG wave events are observed, during the winter season, intrusion MRG wave events exhibit a larger amplitude than the non-intrusion MRG wave events and during the summer season, the amplitude of non-intrusion MRG wave events exceeds that of intrusion MRG wave events. This explains the low seasonal variability in MRG amplitude over the EP domain. Zhang & Webster, 1992; hypothesized that the MRG waves would exhibit stronger amplitudes in the regions of westerly mean zonal winds, under the influence of lateral intrusions. As seen in Figure 3.2, the upper-tropospheric westerly wind ducts are well developed over the EP and AO domains only during the winter season. Consistent with this, the amplitude of intrusion MRG wave events is higher than that of the non-intrusion MRG wave events over the EP domain during the winter season (statistically significant at the 95% confidence level) (Figure 3.11 a). Over the AO domain, where the smallest-amplitude MRG wave events are observed, the summer intrusion MRG wave events exhibit a larger amplitude compared to their winter counterparts (Figure 3.11 f). Even though the MRG wave events prefer to have higher wavenumbers during NH summer over the EP and AO domains, the wavenumbers of intrusion and non-intrusion MRG wave events do not exhibit a clear separation except over the EP domain during NH winter (Figure 3.11 b,g). Unlike the distribution of amplitudes and wavenumbers, statistical modes of trapping scales of intrusion and non-intrusion MRG wave events exhibit a clear separation over the EP and AO domains and it is evident from Figure 3.11 c,h that the intrusion MRG events are less trapped to the equator (statistically significant at the 90% confidence level). However, the phase speeds and duration of the intrusion and non-intrusion MRG wave events do not show a noticeable difference in their distributions over the EP and AO domains (Figure 3.11 d,e,i,j).

The whisker plots provide some insights on the role of extratropical disturbances in the genesis of MRG waves over the EP. According to linear wave theory, lateral forcing by eastward-moving extratropical disturbances cannot cause resonance in westward-propagating MRG waves (Yang & Hoskins, 2016). However, contrasting differences in the wave properties of intrusion and non-intrusion MRG wave events over the EP during NH winter indicate the possibility of resonant interactions. For example, the intrusion MRG wave events have a stronger amplitude and a larger meridional extent compared to non-intrusion MRG wave events (statistically significant at the 90% confidence level) (Figure 3.11 a,c). The intrusion MRG wave events also exhibit a spatial scale similar to that of the extratropical disturbances (wavenumber 4–7) implying that resonant interactions may be a primary mechanism for the genesis of MRG wave events during NH winter. During NH summer, on the other hand, extratropical disturbances seemingly act as a catalytic factor in intensifying the MRG wave events. Past studies have shown observational evidence for the decisive role of intrusion of extratropical disturbances in determining the strength of the MRG waves during NH summer (Magaña & Yanai, 1995; Suhas

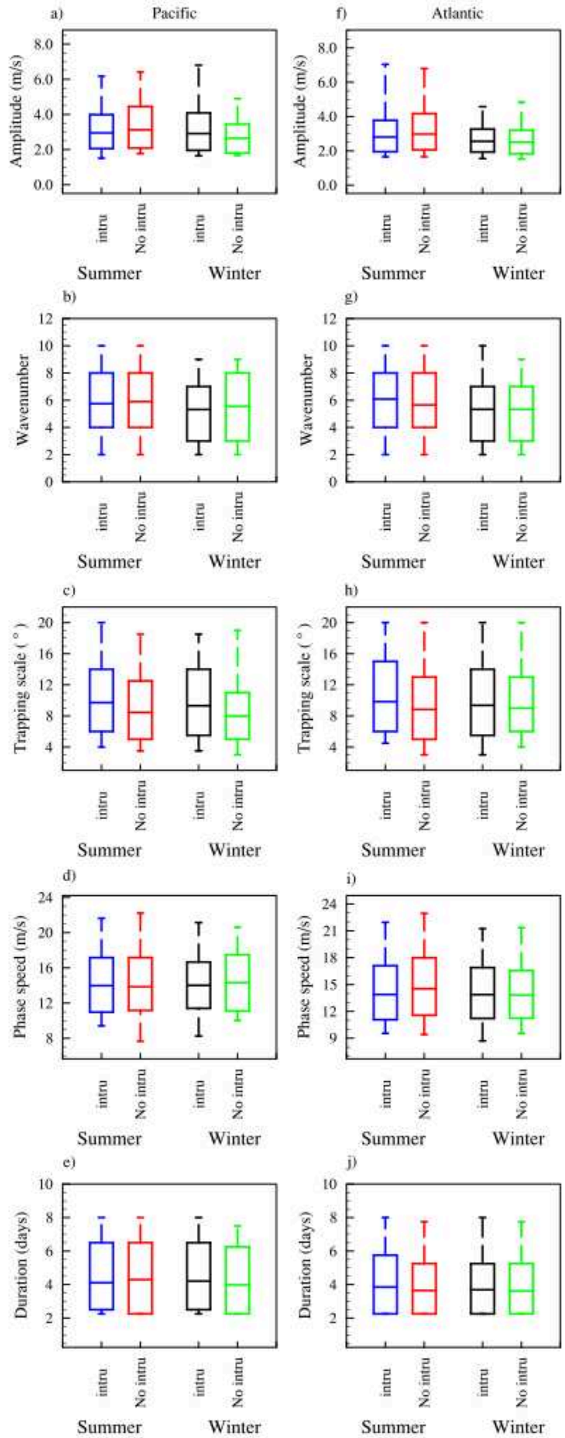

Figure 3.11. Range (maxima, minima), 90th percentile,mean, and 10th percentile of: (a,f) amplitude ($m \cdot s^{-1}$); (b,g) wavenumber; (c,h) trapping scale (◦); (d,i) phase speed ($m \cdot s^{-1}$); and(e,j) duration (days) of intrusion and non-intrusion mixed Rossby–Gravity (MRG) wave events occurring over the central–east Pacific (left column) and Atlantic Ocean (right column) domains during NH summer and winter. Blue and black boxes represent intrusion, red and green boxes represent non-intrusion MRG wave events, respectively for NH summers and NH winters.

et al., 2020). It can be deduced from the shorter wavelengths, smaller trapping scales (Figure 3.11 b,c), and stronger convection–circulation coupling strength (Suhas et al., 2020) exhibited by the MRG wave events during NH summer that they could be primarily triggered by convective processes. However, the observed weakening of the strength of MRG waves in the absence of intrusion of extratropical disturbances via the SH suggests that lateral forcing may be instrumental in amplifying their amplitude.

3.4 Summary and Conclusions

In this study we have conducted a survey of westward propagating MRG wave events at 200 hPa and quantified their association with the intrusions of extratropical disturbances using ERA-I reanalysis data for the period 1979–2019. MRG wave events are identified by imposing the theoretical meridional structure of MRG waves onto the equatorial meridional wind anomalies (Au-Yeung & Tam, 2018). The method is ideal for capturing the episodic nature of MRG waves and it also provides the instantaneous values of its amplitude, phase speed, wavenumber and trapping scale. We have identified 2390 MRG wave events in the upper troposphere and the majority (61%) of them occurred during the months of May–October (Figure 3.5). As pointed out by many previous studies, MRG wave events over the EP and AO domains account for a major chunk (65%) of the total MRG wave events (Table 1). Statistical modes of wave properties of the MRG wave events over the IO, western Pacific, EP and AO reveal that not only the frequency of occurrence but also the amplitude, wavenumber and trapping scale of the MRG wave events exhibit a clear seasonality (Figure 3.7). MRG wave events exhibit higher amplitudes and shorter wavelengths during the NH summer. MRG wave events observed over the IO domain are more closely trapped to the equator during NH summer. The MRG wave events observed in the western hemisphere are less trapped to the equator and it is also noted that the trapping scales do not exhibit significant seasonal variability. The phase speeds of the MRG wave events do not exhibit significant variability.

MRG wave events are classified as intrusion MRG wave events if the PV on the 350-K isentropic surface at 15 ◦ N/S latitude in the spatial–temporal neighborhood of the MRG wave events is greater than 1 PVU. Such events are further classified as NH intrusion or SH intrusion MRG wave events based on the hemisphere where the intrusions of extratropical disturbances are observed. We find that 37% of the MRG wave events are associated with intrusions of extratropical disturbances and a large majority (88%) of such events occur over the EP and AO domains. Larger numbers of NH (SH) intrusion MRG wave events are found to occur during the NH (SH) winter. Although the intrusions of extratropical disturbances occur in both hemispheres over the EP and AO domains, it is interesting to note that nearly 70% of the intrusions of extratropical disturbances associated with the MRG wave events occur in the winter hemisphere. The predominant preference of the winter hemispheric route of intruding extratropical disturbances corroborates the extratropical–tropical interaction theory of Webster & Holton, 1982. Detailed analysis reveals that the amplitude, wavenumber and trapping scale of intrusion and non-intrusion MRG wave events are distinctly different only over the EP during NH winter (Figure 3.11). The intrusion MRG wave events exhibit higher amplitudes, lower wavenumbers, and larger trapping scales compared to the non-intrusion MRG wave events. Coherent evolution of extratropical and tropical disturbances is evident in the intrusion MRG wave events life cycle composites (Figures 3.8, 3.9) validating the classification of MRG wave events into intrusion and non-intrusion categories. Equatorward-propagating extratropical disturbances show northwest–southeast and southwest–northeast tilt in the NH and the SH, respectively. It is inferred from the life cycle composites that extratropical disturbances associated with the MRG wave events have wavenumbers in the range of 4–7. Stronger extratropical disturbances a few days before the MRG amplitude maxima and weakening of extratropical disturbances a few days after the MRG amplitude maxima indicate the possibility that such MRG wave events might be forced by the extratropical disturbances.

The study reveals that 37% of the MRG wave events are associated with intrusions of extratropical disturbances. It implies that external forcing of MRG waves is as important as their in-situ genesis mechanisms. Even though the diagnostic analyses may be insufficient to clearly establish the impact of lateral forcing via extratropical disturbances in exciting MRG wave events, probable scenarios can be deduced from the analyses. The observation of stronger amplitudes and larger trapping scales exhibited by intrusion MRG wave events and the similarity in spatial scales of the MRG wave events and extratropical disturbances suggest the role of resonant interactions between these two modes over the EP during NH winter. Past studies showed that the intrusions of extratropical disturbances is a crucial factor governing the strength of MRG waves during NH summer and fall (Magaña & Yanai, 1995; Suhas et al., 2020).

However, the absence of a clear difference in the amplitudes of intrusion and non-intrusion MRG wave events over the EP and AO domains during NH summer rules out the possibility of resonant interactions. It could be possible that the MRG waves are excited by random convective perturbations over the EP and Atlantic domains which in turn might be amplified by the intruding extratropical disturbances (Garcia & Salby, 1987). Without such amplification by intrusions of extratropical disturbances, the growth of the MRG perturbations induced by convective processes may be limited.

Chapter IV

Doppler shifted eastward propagating MRG waves

4.1 Introduction

MRG waves are a fundamental mode of tropical synoptic-scale motions, characterized by an intrinsic westward phase propagation (Hendon & Liebmann, 1991; Matsuno, 1966; Wheeler & Kiladis, 1999; Yanai & Maruyama, 1966). They are derived as special solutions of the shallow water model on an equatorial beta plane under the assumption of zero background flow (Matsuno, 1966). MRG waves represent equatorially trapped modes that exhibit mixed characteristics of low-frequency Rossby waves (rotational) and high-frequency inertio-gravity waves (divergent). The theoretical framework of westward propagating MRG (MRG) waves reveals a predominant rotational component centered at the equator, coupled with an anti-symmetric quadrupole structure in wind convergence-divergence (convection) and geopotential height fields (Kiladis et al., 2009, 2016; Wheeler et al., 2000; G.-Y. Yang et al., 2003). The background mean zonal flow plays a crucial role in modulating MRG wave propagation characteristics and dispersion properties through Doppler shifting effects (Dias & Kiladis, 2014; G.-Y. Yang et al., 2003, 2007b, 2007a; Zhang & Webster, 1989). A strong westerly flow can reverse the intrinsic westward propagation of WMRG waves, resulting in eastward propagating E-MRG waves while preserving their dynamic and thermodynamic horizontal structures (G. Yang & Hoskins, 2016; G.-Y. Yang et al., 2003, 2007a, 2007b). While the signature of MRG waves is observed throughout the tropical atmosphere, maximum perturbation kinetic energy for synoptic-scales are occurs in the upper troposphere, particularly during the NH winter over the Pacific and Atlantic ocean basins (Arkin & Webster, 1985; Hoskins & Yang, 2016; G. Yang & Hoskins, 2016; G.-Y. Yang et al., 2003). The enhanced activity is attributed to the development of strong westerly ducts in the upper troposphere over the tropics during these seasons, acting as active hubs for both MRG waves and their Doppler-shifted eastward propagating counterparts (E-MRG waves).

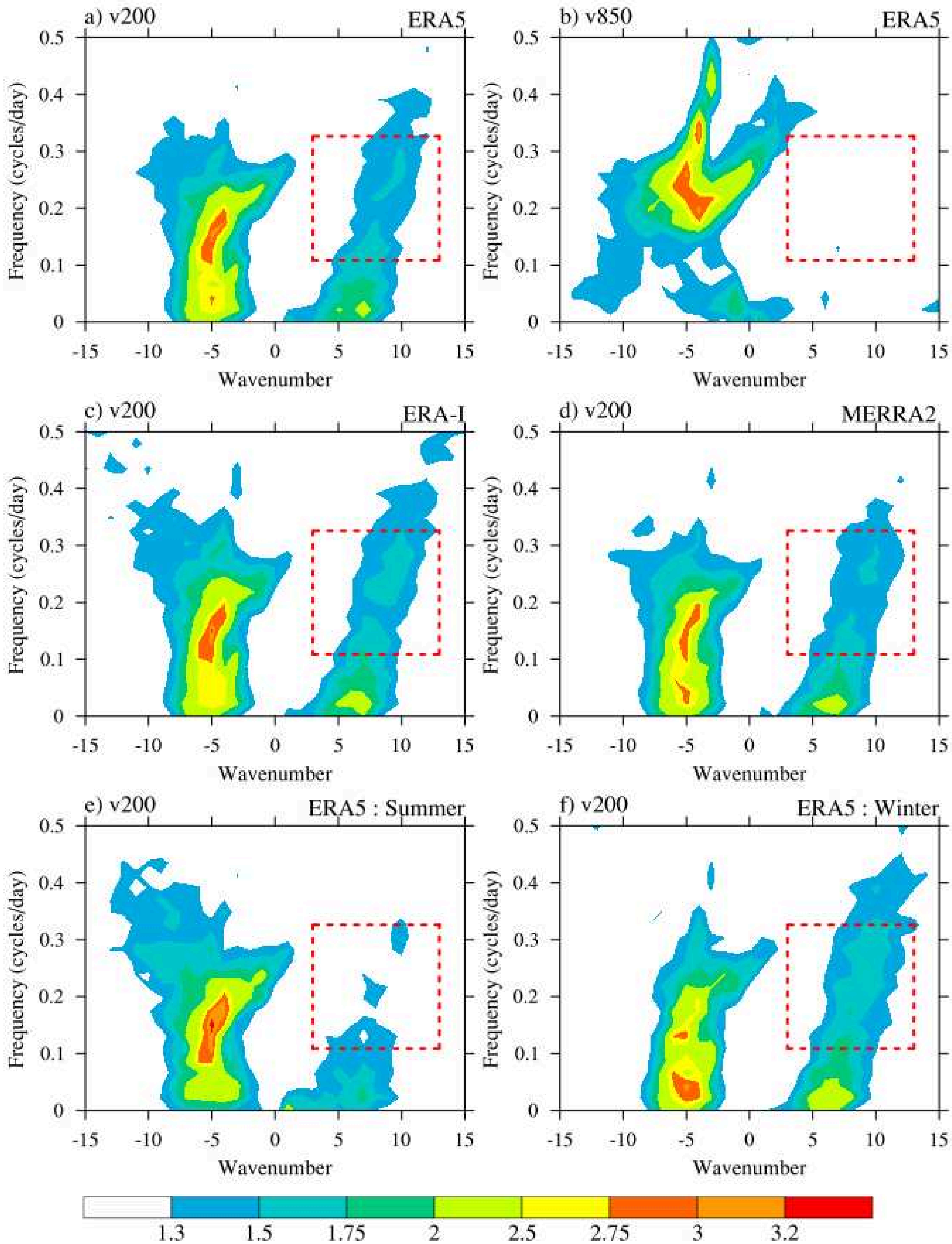

Figure 4.1. Wavenumber-frequency power spectra for the symmetric component of meridional wind representing the total power normalized by the red background spectra for the tropics (10°S-10°N) at a) 200hPa and b) 850hpa using ERA5 data for the period of 1979 to 2022, c) 200 hPa using ERA-I data from 1979 to August 2019, d) 200 hPa using MERRA2 data for 1980 to 2022, e) 200 hPa for summer (May to October) and f) 200 hPa for winter (November to April) using ERA5. The spectral peaks are statistically significant at 99% confidence level.

The motivation for this work stems from the observation of significant power in the eastward wavenumbers of the normalized wavenumber and frequency power spectra of the symmetric component of the meridional wind at 200 hPa. While the power in the westward synoptic-scale wavenumbers of the symmetric meridional wind is well documented and corresponds to the westward propagating MRG waves, the sources contributing to the eastward power are not as clear (Shreya & Suhas, 2024). The lower frequency component in the eastward wavenumbers could be attributed to the Doppler shifting of higher order even Rossby modes (n=2), which however requires separate attention and the current study will solely focus on the power in synoptic-scales. One possible contributing factor to the eastward power in synoptic-scale is the convectively coupled Kelvin waves (CCKWs). However, CCKWs activity is expected to be relatively low during boreal winter over the east Pacific when the eastward variance peaks. Conditions over the east Pacific during DJF are unfavorable for convection as well as for SH intrusions (Roundy & Frank, 2004; Wheeler et al., 2000). Another potential source are the eastward propagating synoptic-scale disturbances (EPSDs) observed in cloudiness signals to the north of the ITCZ convective belt during DJF that are associated with extratropical high potential vorticity trains into the tropics from the NH extratropics (Huaman et al., 2020; Kiladis, 1998; Kiladis & Weickmann, 1992c). Although the EPSDs are documented well (Huaman et al., 2020), they are associated primarily to storm tracks propagating from the NH extratropics into the tropics through westerly wind ducts. A significant factor that could contribute to the synoptic-scale eastward variance is the presence of E-MRG waves in the deep tropics (Yang and Hoskins, 2016).

Modeling studies in the past have highlighted the crucial role of the background mean flow in modulating mixed Rossby-gravity (MRG) waves through Doppler shifting effects. Zhang & Webster, 1989 reported that in the presence of a sheared basic westerly flow, westward propagating equatorial waves like MRG waves become considerably less trapped equatorially, increasing their susceptibility to latitudinal interaction with extratropical disturbances. A series of subsequent studies, (Zhang & Webster, 1992 ; Zhang, 1993) discovered that MRG waves are strongly influenced by both Doppler and non-Doppler effects of the background mean flow, especially when combined with lateral forcing from extratropical sources, whether stationary or mobile. Larger amplitude MRG waves tend to occur in mean westerly background flows compared to easterly flows, highlighting further the significance of the background flow in modulating the amplitude and propagation characteristics of MRG waves. Perhaps most importantly, Zhang & Webster, 1992 and Zhang, 1993 found that the Doppler effects of a westerly background mean flow could modulate MRG waves, resulting in an eastward propagating equatorial E-MRG wave response in the presence of a transient extratropical forcing. (Wang & Xie, 1996; G.-Y. Yang et al., 2003) showed that under strong westerly background flows exceeding 10 m/s, shorter zonal scale mixed Rossby-gravity (MRG) waves were more susceptible to eastward advection compared to larger waves. As a result, short MRG waves in the upper troposphere over the eastern Pacific and Atlantic ocean basins exhibited loosely coupled vertical structures with waves in the lower troposphere due to the Doppler shifting effects of the westerly flow. Thus the background flow and its interactions with external forcing is crucial in accurately representing total upper tropospheric MRG wave dynamics.

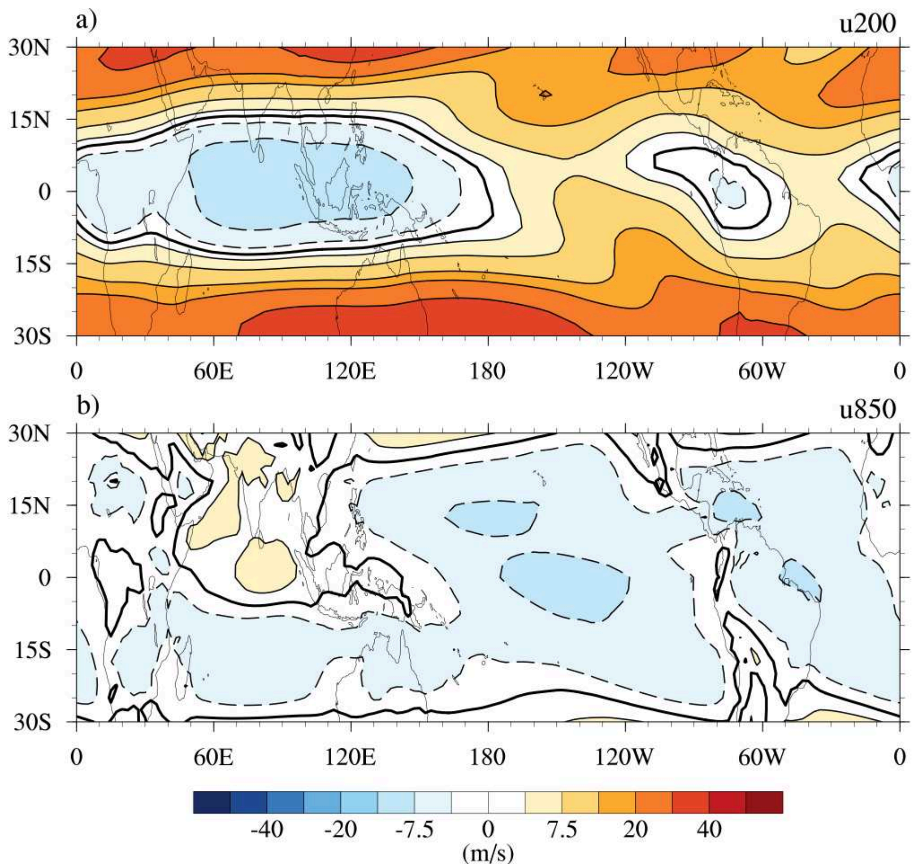

Figure 4.2. Climatology of zonal wind (m/s) for 44 years from 1979 to 2022 at a) 200 hPa and b) 850 hPa. Seasonal climatology of zonal wind (m/s) at 200 hPa calculated for c) NH winter (November to April) and d) NH summer (May to October). Thick solid contour marks the zero zonal wind at 200 hPa, the thin contour marks the regions of westerly winds and the dotted lines represent the regions of easterly winds.

G.-Y. Yang et al. (2003, 2007a, 2007b), reported a classic case study of an upper-tropospheric Doppler-shifted E-MRG wave structure coupled with off-equatorial convection around 13-15 July 1992 over the east Pacific-Atlantic region. Utilizing wave projection techniques, they found that the ambient westerly flow Doppler-shifted the WMRG wave, resulting in an E-MRG wave exhibiting an eastward phase speed in the range of 10-13 m/s and a shorter wavelength (global wavenumber 6) compared to the coexisting MRG wave. Dias & Kiladis (2014), demonstrated a consistent shift in the dispersion properties of convectively coupled MRG waves towards higher wavenumbers, supporting the dominant role of Doppler shifting by the ambient zonal flow over the tropics. However, this overlap alone is insufficient to conclusively attribute the observed shifts solely to Doppler effects, as non-Doppler effects of the zonal flow could also modify the wave dynamics. G. Yang & Hoskins (2016), suggested that Doppler-shifted E-MRG and eastward propagating n = 1 Rossby waves explain approximately 40% of the upper-tropospheric eastward meridional wind variance. They documented the ENSO-related variation of extratropical-forced E-MRG waves, exhibiting stronger activity during La Niña over the Eastern Pacific and El Niño over the Atlantic when westerly ducts are well-developed, corroborating the modeling studies of Zhang & Webster (1992). The E-MRG filtered variance was highly localized in space and time, with most contributions from the Western Hemisphere during winters and a strong interannual variability favoring La Niña years or stronger westerlies. Despite the identification of Doppler-shifted E-MRG waves over the past four decades, a formal survey of these events and their relative contribution to the total upper-tropospheric variance compared to MRG waves is lacking in the literature.

The analyses conducted in past studies underscore the importance of conducting focused studies to verify whether a significant fraction of equatorial wave modes are modified by the Doppler shifting of the ambient zonal flow. Since the E-MRG wave events are spatially and temporally in-homogeneous, an event based analysis method is necessary to quantify their relative contribution. Thus fourier based methods that assume the waves modes to be cyclic in space and time (Wheeler & Kiladis, 1999) may not be of help. Also, event identification methods that are based on Fouier decomposition in wavenumber space into eastward and westward propagating modes may result in misidentification of standing oscillations as propagating wave modes (Au-Yeung & Tam, 2018; G.-Y. Yang et al., 2003). Since these events are highly sensitive to the zonal mean flow and occur when the background winds are strong westerlies, these disturbances may not conform to the exact theoretical structure of linear shallow water waves for a resting atmosphere. An event-based analysis that is less constrained by assumptions from linear theory should be implemented. The multidimensional Empirical Mode Decomposition (EMD) technique which does not involve any Fourier decompositions or does not impose any constraints from linear wave theory will be employed to identify wave events using the meridional wind at 200 hPa. Previous studies have primarily focused on the existence and characteristics of E-MRG waves rather than their significance in the overall tropical variability. Therefore, exploring the relative contribution of E-MRG waves to the eastward synoptic-scale variance in the upper tropospheric symmetric meridional wind spectra would enhance our understanding of their significance in modulating tropical variability.

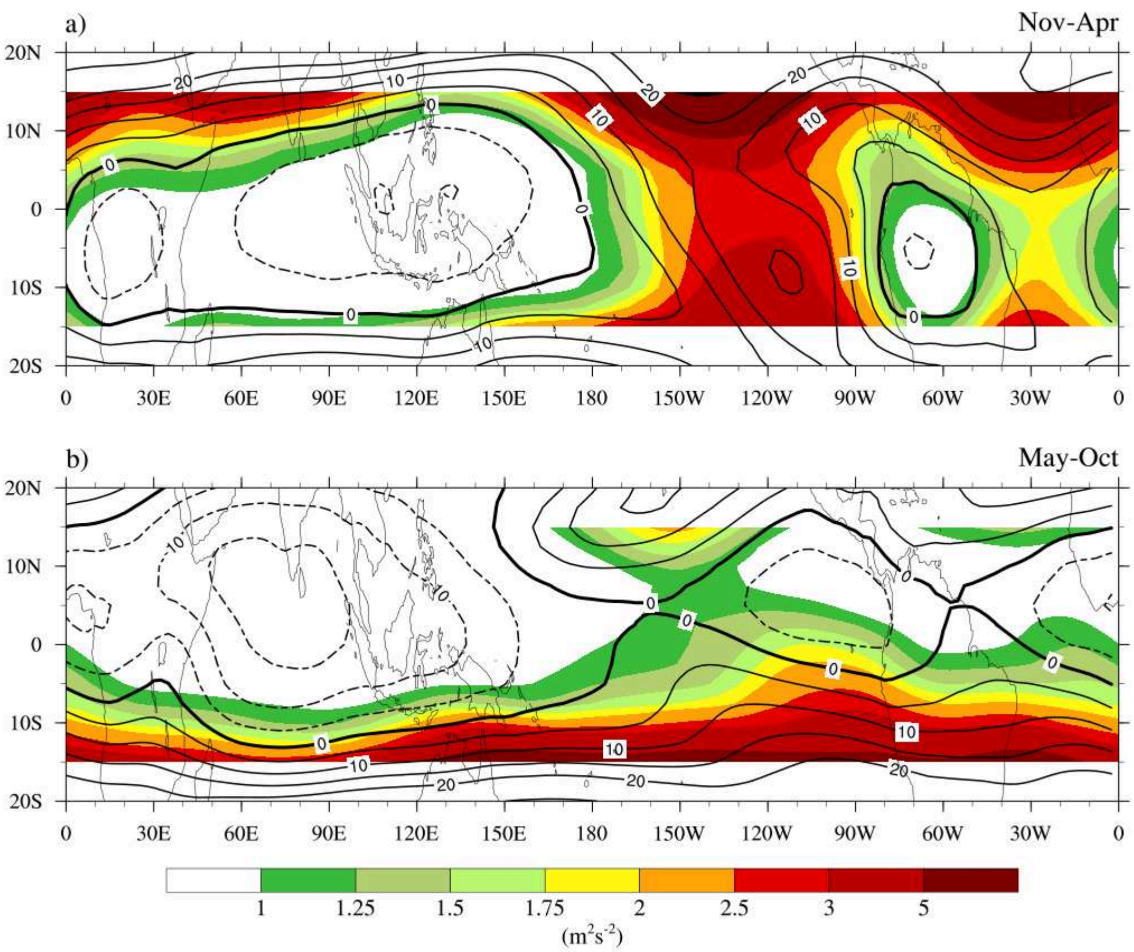

Figure 4.3. Colour contours represent the variance of meridional wind at 200 hPa (m^2s^{-2}) for filtered v200 for eastward wavenumbers in the range of 2 to 15 and frequencies corresponding to 3 to 15 days plotted for 15°S to 15°N and the overlaid line contours represent the seasonal time mean zonal winds at 200 hPa for a) NH summer (May to October) and b) NH winter (November to April) from 1979 to 2022.

4.2 Data and Methodology

The study utilizes wind and geopotential data from three prominent reanalysis datasets : ECMWF ERA5 from 1979 to 2022, ERA-Interim from 1979 to August 2019, and MERRA-2 from 1979 to 2018. The wind at 200 hPa and 850 hPa levels are used. The temporal and spatial resolutions of the datasets are daily and 2.5°X2.5°, respectively. By comparing data from these sources, the study aims to demonstrate that observed peaks in eastward wavenumbers of normalized symmetric meridional wind at 200 hPa in the tropics are consistent and not solely artifacts of any single dataset. Meridional wind anomalies symmetric at the equator are particularly indicative of MRG wave activity for synoptic-scales (3 to 12 days) (figure 4.1). The wavenumber and frequency normalized power spectra is computed using 46-day time segments, focusing on the symmetric component of meridional wind between latitudes 10°S and 10°N. To calculate the normalized power spectra, the methodology outlined by (Wheeler & Kiladis, 1999) is followed. To address the dominance of red noise in the tropical atmosphere, the spectra are normalized against a red background spectra, emphasizing on significant spectral peaks associated with equatorial waves. Seasonal variations are analyzed by computing power spectra separately for NH summer (May to October) and winter (November to April), with each season comprising an ensemble average over 44 years. Regional power spectra for the eastern and western hemispheres are evaluated by selecting longitudes from 50°E to 180°E and 180°E to 50°E, respectively, with padding applied to cover the entire longitudinal range (Dias & Kiladis, 2014).

The lead-lag correlation analysis between wind and geopotential fields is conducted by employing an eastward wave index. This index is derived by area averaging meridional wind at 200 hPa, filtering for eastward wavenumbers ranging from 2 to 15 and frequencies spanning 3 to 15 days. The study region encompasses the eastern Pacific tropical zone, bounded by latitudes 2.5°S to 2.5°N and longitudes 232.5°E to 237.5°E. This geographic domain is chosen due to its significant amplitude variability in eastward synoptic-scales, particularly during the NH winter. The composite horizontal structures are constructed using 3 to 15 days filtered wind and geopotential anomalies by applying a weighted Lanczos filter.

The method employs three-dimensional Empirical Mode Decomposition (3D-EMD) method to discern equatorial E-MRG wave events using 3rd Intrinsic Mode function (IMF3)

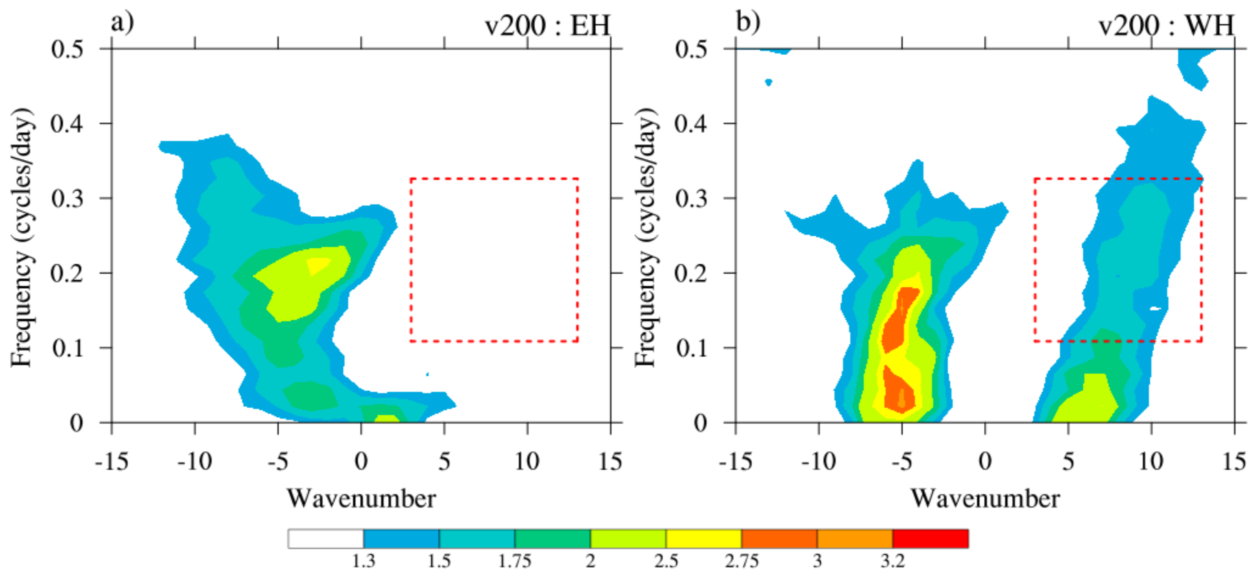

Figure 4.4. Regional wavenumber-frequency power spectra of the symmetric component of meridional wind at 200hPa calculated by normalizing the total power by red background spectra for the tropics (10°S - 10°N) for the a) eastern hemisphere (EH, 50°E to 180°E) and b) western hemisphere (WH, 180°E to 50°E).

(Sun and Wu 2020). This technique is particularly adept at handling non-linear and non-stationary signals. In this process, the original signal (equatorial meridional wind at 200 hPa), presumed to exhibit a wavy form, undergoes decomposition into upper and lower envelopes, along with a mean function. It qualifies as an IMF if it meets certain criteria, including having only one extremum between successive zero crossings and possessing a mean value of zero. The decomposition continues iteratively until the residue represents either a monotonic trend or contains at most one interior extremum across the entire temporal domain. The IMF3 specifically corresponds to disturbances within the frequency range of 3 to 12 days, serving as the reference meridional wind component for E-MRG event identification. These events are characterized by zonally eastward-propagating disturbances with cross-equatorial maxima (minimas) in meridional wind and propagation speeds ranging from 2 m/s to 25 m/s. The algorithm records the first longitudinal location of maxima in IMF3 values within specific latitudinal bounds of 5°N to 5°S for each time step and tracks the evolution of these events as they propagate both temporally and zonally with an eastward phase speed. To prevent double counting of events, the evolution of only the maxima is tracked, (similar events are identified using the minima) ensuring that each event is uniquely characterized without redundancy. The duration of each event is determined by the span of days exhibiting eastward-propagating wave activity within the equatorial region. The amplitude of the E-MRG wave event is defined by the highest recorded value of IMF3 during this period. The spatial and temporal coordinates corresponding to this peak amplitude are designated as the day 0 values for each event.

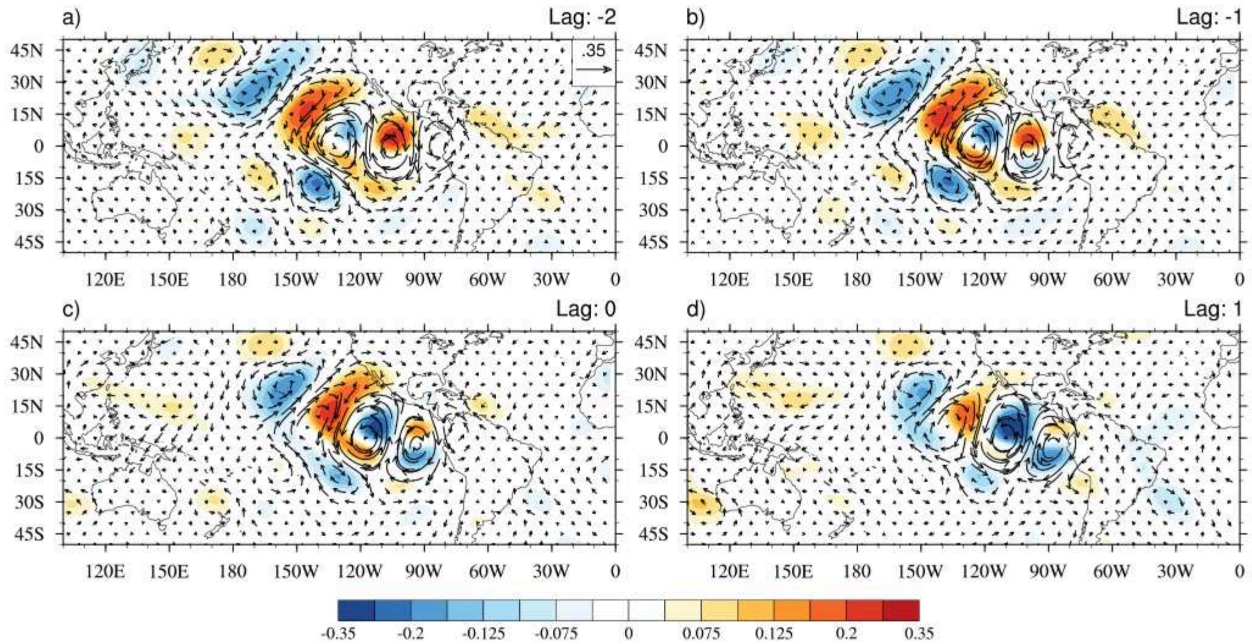

Figure 4.5. Lead-lag spatial correlation of 3 to 15 days filtered wind (vectors) and geopotential anomalies at 200 hPa with eastward synoptic-scale wave index created by spatially averaging wavenumber-frequency filtered v200 for eastward wavenumber 2 to 15 and periods from 3 to 15 days over the domain 5°N to 5°S and 252. °E to 257.5°E for a)-d) November to January for the duration of 1979 to 2022.

The EMD technique diverges from traditional methods by incorporating local frequency and spatial components instead of relying on fixed basis functions like cyclic sines and cosines (Wheeler & Kiladis, 1999; Kiladis et al., 2016; Dais et al., 2014). Conventional wave identification methods heavily lean on linearity assumptions, presuming that the tropical atmosphere adheres strictly to linear theory. This approach facilitates the decomposition of the original signal into various modes corresponding to component wavenumbers and frequencies. Unlike Fourier-based filtering techniques, EMD automatically segregates high frequency and high wavenumber red noise components into the lowest IMF components, eliminating the incorporation of red noise into wave identification. Multiple studies have highlighted significant effects of Doppler and non-Doppler components of the zonal mean background on rotationally dominant wave modes like MRG and Rossby waves (Dias & Kiladis, 2014; G. Yang & Hoskins, 2016; Zhang & Webster, 1989, 1992). Consequently, using a method minimizing linearity assumptions from equatorial wave theory becomes more prudent. Additionally, EMD does not assume that the total intraseasonal variability in wavenumber filtered anomaly fields can be linearly decomposed into contributions from various equatorial wave modes (Wheeler & Kiladis, 1999; G.-Y. Yang et al., 2003). This feature makes EMD ideal for studying scale interactions between modes of different scales and wave-wave nonlinear interactions. Furthermore, Fourier-based decomposition techniques for separating eastward and westward propagating signals may misinterpret standing oscillations as equal powers in both directions. The EMD technique captures the spatial and temporal inhomogeneous nature of the MRG waves while minimizing the impact of inherent assumptions associated with linear theory and Fourier based filtering on the analysis.

Empirical orthogonal function (EOF) analysis method is used to account for the Kelvin wave activity. Kelvin wave activity shows peaks during the boreal spring months of March to June over the central-east Pacific domain. The zonal wind at 200 hPa is filtered for eastward wavenumbers in the range of 2 to 15 and frequencies corresponding to 3 to 20 days. The zonal background is calculated using a 21 day running mean. The first two EOF modes are found to occur in pairs depicting the eastward propagating Kelvin waves modes. They account for a total 30% of the Kelvin wave variability during March to June months over the east Pacific. The phase composite of the Kelvin waves are constructed using the principal components corresponding to EOF1 and EOF2.

4.3 Results and discussions

The symmetric wavenumber–frequency power spectra of meridional wind (figure 4.1) normalized by the red background (Wheeler & Kiladis, 1999) is calculated by averaging the symmetric component of meridional wind for 48 days time segments and over 10 S to 10 N latitudes. Significant power spectral peaks for synoptic-scales (the red dotted box denotes the domain of interest) are observed in the eastward as well as westward wavenumbers at the 200 hPa (figure 4.1a). Although the westward wavenumbers power is stronger, the power in the eastward wavenumbers is also significant and is comparable to the westward counterpart. The power in the westward synoptic-scale wavenumbers in the meridional wind is documented well and corresponds to the westward propagating MRG waves (will be abbreviated as MRG waves throughout this paper) (Kiladis et al., 2016; Takayabu, 1994a, 1994b; Shreya & Suhas, 2024; Wheeler & Kiladis, 1999). The signature for the MRG waves can be found throughout the depth of the troposphere as well as the lower stratosphere (Kiladis et al., 2009, 2016; G.-Y. Yang et al., 2003). However, the power in the eastward wavenumbers can only be observed in the upper troposphere at the 200 hPa level with no signature in the lower troposphere at the 850 hPa (figure 4.1 a,b). The power in the eastward wavenumbers for the symmetric v200 is consistent across multiple reanalysis products such as ERA-Interim from 1979 to 2019 and MERRA2 data from 1980 to 2018 (figure 4.1c, d) and is therefore not an artifact of the ERA5 dataset. Tropical synoptic-scale disturbances, including MRG waves, are sensitive to the variations of the background flow over which they are embedded (Dias & Kiladis, 2014; Suhas et al., 2020; Wang & Xie, 1996; G. Yang & Hoskins, 2016; Zhang, 1993; Zhang & Webster, 1989; 1992). Figure 4.2 depicts the time mean background zonal winds in the upper and lower troposphere at the 200 hPa and 850 hPa respectively. It can be observed that the regions over the western hemisphere i.e. the east Pacific and Atlantic ocean domain in the upper troposphere which also correspond to regions of maximum synoptic-scale perturbation kinetic energy (Arkin & Webster, 1985; Shreya & Suhas, 2024) are dominated by the westerly winds ducts, while in the lower troposphere the mean flow throughout the tropics is easterly.

Figures 4.1e and 4.1f depict the seasonal power spectra of symmetric meridional wind at 200 hPa, during the NH summer and NH winter as per (Dias & Kiladis, 2014; Wheeler & Kiladis, 1999). Notably, the eastward spectral peaks at synoptic-scales exhibit high sensitivity to seasonal variations, with NH winter months with maximum activity. Conversely, stronger peaks in westward wavenumbers are observed during NH summer, attributed to MRG waves, potentially triggered by convection, along with a shift towards larger wavenumbers. This shift may be indicative of the dominant role of Doppler shifting by the ambient zonal flow over the tropics (Dias & Kiladis, 2014; G.-Y. Yang et al., 2003). To quantify the amplitude variability of the eastward synoptic-scale motions, spatial variance is calculated for v200 filtered for eastward wavenumbers 2 to 15 and frequencies 3 to 15 days, which is represented as coloured contours in figure 4.3. Since the primary interest is in exploring the variability in the tropical region, the eastward variance values beyond 15 N and 15 S are masked. NH winter shows a clear preference for eastward variance over the western hemisphere, as depicted in Figure 4.3a. Overlaying the

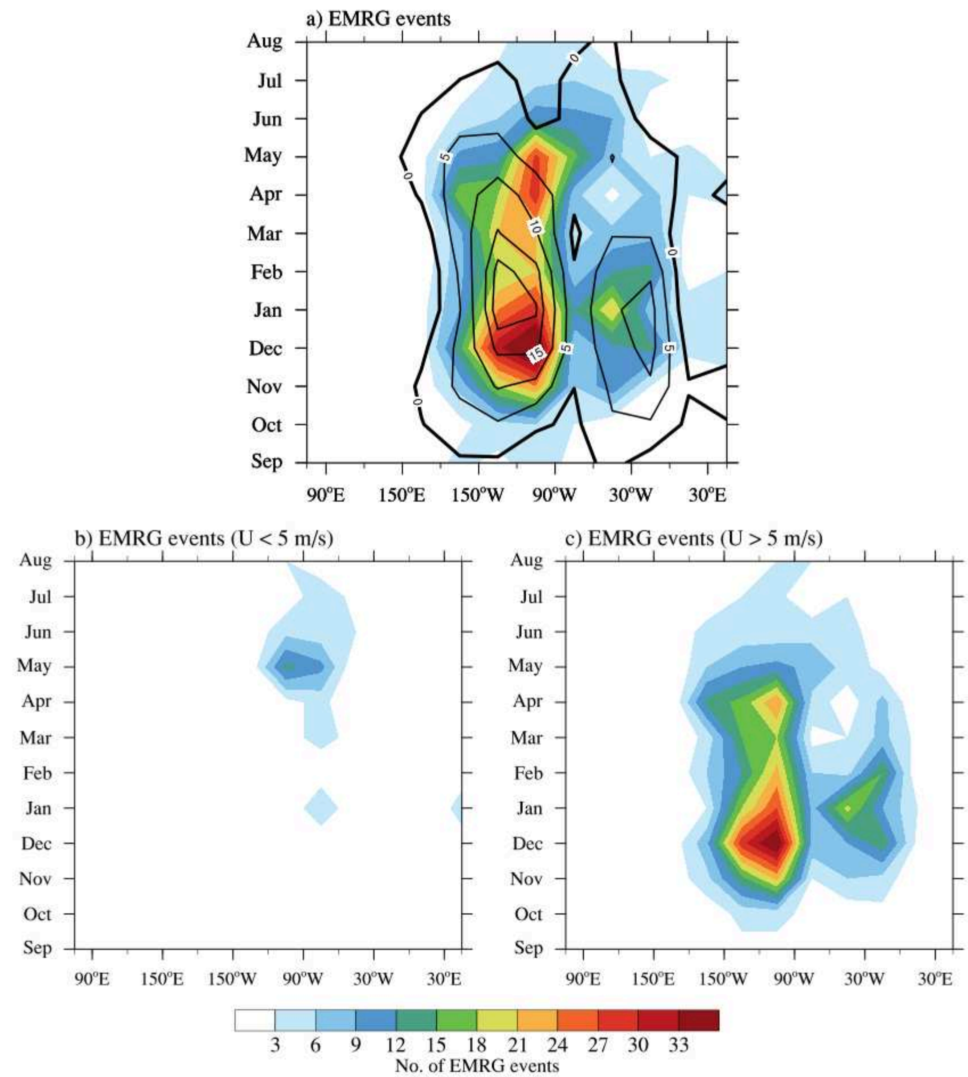

Figure 4.6. Monthly-longitude distribution of the number of occurrence of a) total E-MRG wave events, b) E-MRG wave events associated with local mean zonal wind $\bar{U}$ less than 5 m/s (easterly or weak westerly regime) and c) $\bar{U}$ greater than 5 m/s (strong westerly regime) for the period of 1979 to 2022, identified using Empirical Mode Decomposition (EMD) technique. Thin line contours indicate the 50th percentile value of 21- day running mean climatological westerly zonal wind at 200hPa (m/s) for 30° longitude and monthly bins and the thick black contour line marks the zero zonal mean at the 200 hPa.

seasonal background zonal wind fields as line contours in figure 4.3 highlights a direct correlation between the strength and variability of eastward synoptic-scale variance and the ambient flow configuration. The regional power spectra for the eastern hemisphere and western hemisphere (figure 4.4) corroborate the findings from the distribution of eastward variance and seasonal power spectra. Notably, only the western hemisphere (180°E to 50°E) contributes to the total eastward power in synoptic-scale eastward wavenumbers and frequencies, with no contribution from the EH. This observation underscores the seasonal and geographical preference for the eastward synoptic-scale variability associated with v200, suggesting that westerly wind ducts and extratropical forcing over the central-east Pacific and Atlantic Ocean domains may play a critical role in maintaining upper-level eastward variability over the tropics (Yang and Hoskins, 2016).

To estimate the horizontal structure of dominant disturbances contributing to eastward variance in v200 over the Western Hemisphere during NH winter, a reference eastward time index is computed over the East Pacific domain for December to February. The index is derived by area averaging filtered v200 for 3 to 15 days and eastward wavenumbers 2 to 15 over a 5° x 5° degrees box corresponding to the maximum eastward amplitude box during DJF over the equatorial east Pacific (2.5°S to 2.5°N, 232.5°E to 237.5°E). The regressed horizontal structures in 3 to 15 days filtered dynamical fields closely conforms to the theoretical structure of MRG waves with strong meridional wind and rotation component exhibiting equatorial symmetry (figure 4.5). The entire MRG wave moves eastward at about 8 m/s, indicating the presence of Doppler-shifted E-MRG waves. Strong eastward-moving extratropical wave trains from the NH are linked with tropical E-MRG wave activity. The E-MRG wave displays a zonal wavelength corresponding to global wavenumbers 6 to 8, suggesting that shorter zonal scale MRG waves are more likely to be influenced by Doppler shifting due to the westerly flow. Consequently, MRG waves in the upper troposphere may have weak vertically coupled structures with lower tropospheric MRG waves over the Western Hemisphere during NH winter extratropical Rossby waves (figure not shown), confirming the presence of these waves throughout NH winter months. The polarization relationship between geopotential and wind fields serves as a clear distinction between extratropical Rossby waves and tropical E-MRG waves. For eastward MRG waves, the geopotential distribution exhibits an antisymmetric quadrupole structure relative to the equator. In contrast, for extratropical Rossby waves, the geopotential maxima coincides with vorticity/rotation maxima. This observation dismisses the notion that these disturbances are merely extratropical storm tracks propagating into the tropics through the NH westerly wind ducts (Kiladis & Weickmann 1992; 1997; Huaman, 2020). Hence, despite limited documentation, aside from a few studies noting their existence, E-MRG waves warrant further investigation.

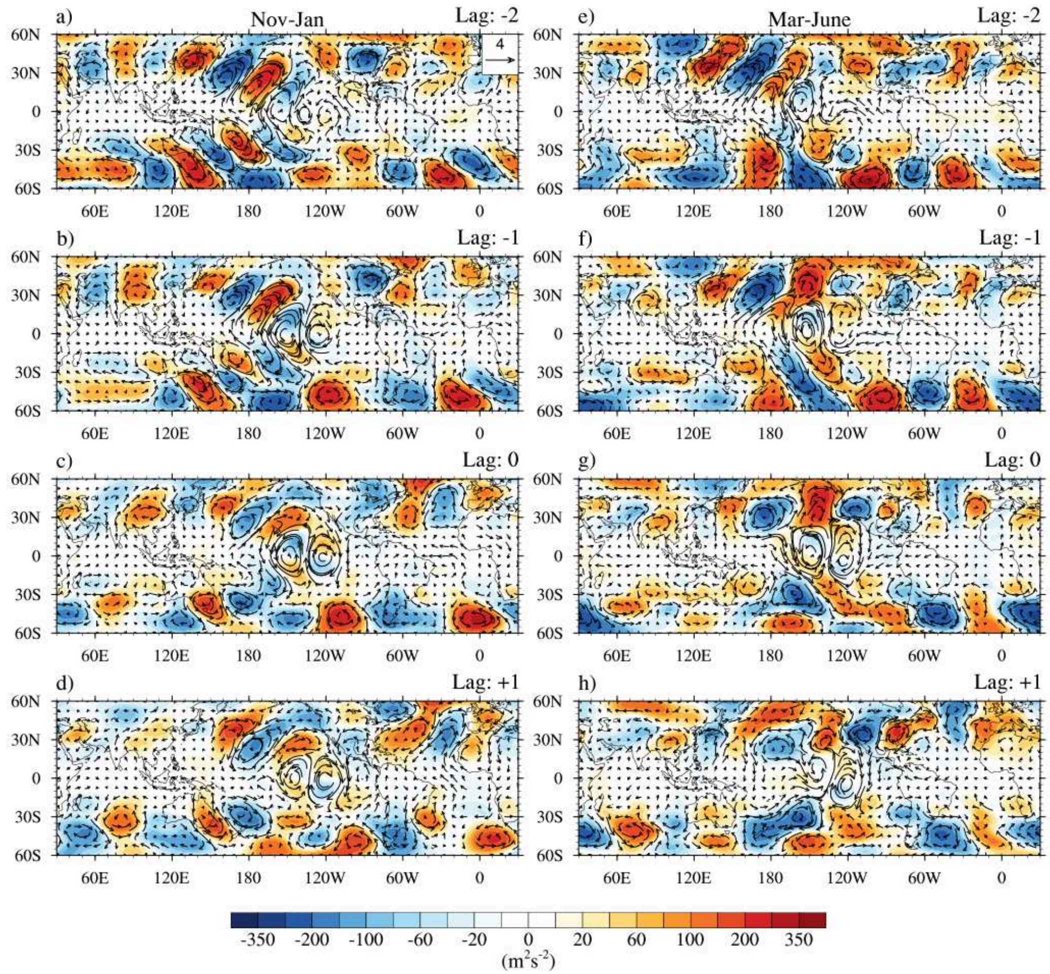

Figure 4.7. Lead-lag life cycle composites of 3-15 day filtered wind (vectors, m/s) and geopotential (contours, $m^2 s^{-2}$) anomalies of E-MRG events at 200hPa that are associated with a local westerly wind regime ($\bar{U}$ greater than 5m/s) occurring during a) to c) November to January (left column) and d) to e) March to June (right column) over the Pacific domain (210°E to 270°E) for 1979 to 2022. Wind and geopotential anomalies are translated longitudinally to the location of maximum occurrence of E-MRG activity over the Pacific domain (225°W).

Using the multidimensional EMD method by (Sun & Wu, 2020), episodes of E-MRG waves are identified using v200. The IMF3 component reported a total of 730 E-MRG waves events in the upper troposphere from 1979 to 2022. Figure 4.6 a) illustrates the month versus distribution of the frequency of occurrence of these E-MRG wave events, depicted as colored contours. The analysis reveals a strong regional preference, with the maximum number of events occurring over the east Pacific and Atlantic ocean domains. Seasonally, peak E-MRG activity over the Atlantic ocean is observed during the Boreal winter months of November to February. In contrast, E-MRG wave events over the east Pacific exhibit a bimodal distribution, with a pri-

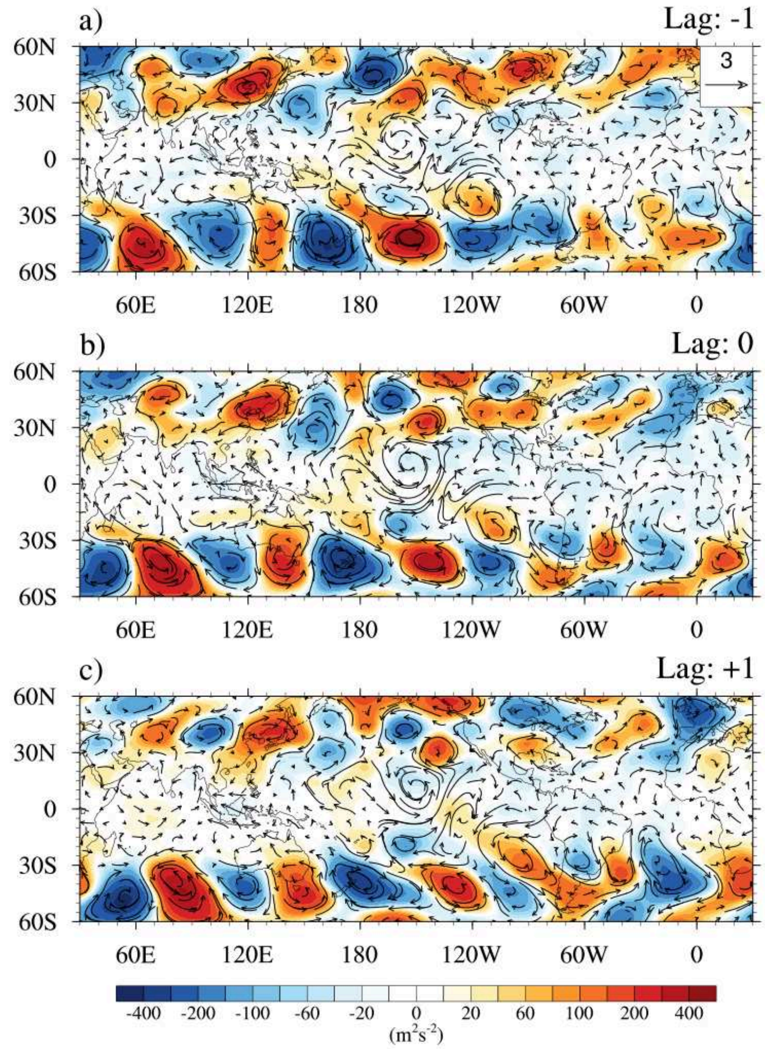

Figure 4.8. Lead-lag life cycle composites of 3-15 day filtered wind (vectors, m/s) and geopotential (contours, $m^2 s^{-2}$) anomalies of E-MRG events at 200hPa that are associated with a local westerly wind regime ($\bar{U}$ less than 5m/s) occurring during a) to c) March to June (right column) over the Pacific domain (210°E to 300°E) for 1979 to 2022. Wind and geopotential anomalies are translated longitudinally to the location of maximum occurrence of E-MRG activity over the Pacific domain (225°W).

mary peak during Boreal winter (November to January) and a secondary peak during Boreal spring to early summer (March to May). In Figure 4.6 a, the line contours illustrate the monthly and longitudinal distribution of climatological zonal winds in the upper troposphere (200 hPa). Regions that exhibit a preference for E-MRG wave activity in the east Pacific and Atlantic domains during NH winter months align with areas characterized by strong westerly background winds. Notably, the secondary peak in E-MRG wave event occurrences over the east Pacific from March to June correspond to periods of climatologically weak westerly winds, typically less than 5 m/s. The spatial and temporal characteristics of E-MRG wave events allow for the calculation

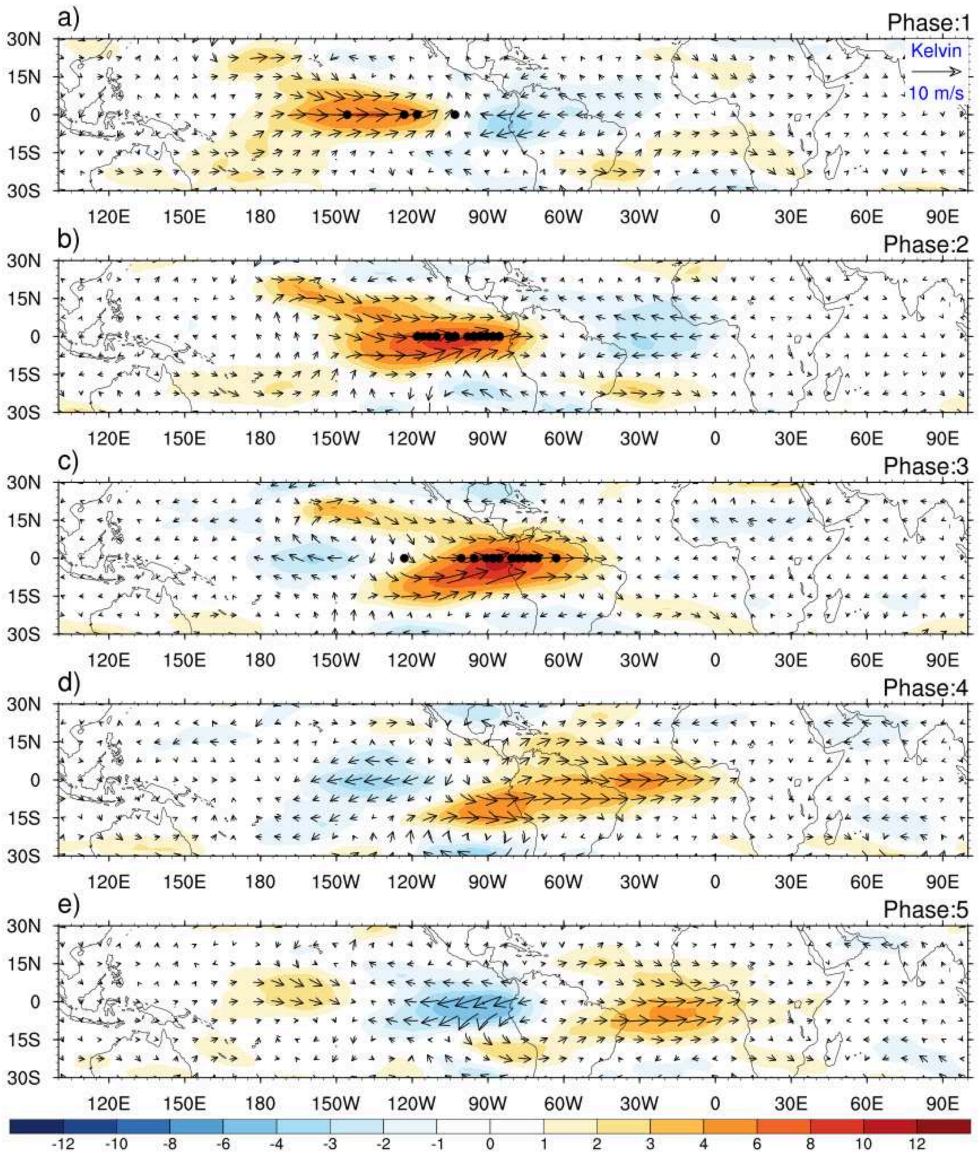

Figure 4.9. Kelvin wave phase composite generated from the leading two EOF modes for zonal wind anomalies at 200 hPa filtered for wavenumbers and frequencies corresponding to Kelvin wave over the Pacific domain (180°E to 300°E) from March to June for 1979 to 2022. The solid black dots represent the longitudinal location of occurrence of E-MRG wave events associated with a local mean easterly/weak westerly regime ($\bar{U}$ less than 5m/s).

of local background winds associated with each event. By averaging zonal winds over a longitudinal range of ±15° and a time range of ±5 days centered around the event location, the local mean zonal wind for each E-MRG event is determined. E-MRG events are then categorized based on the background state into westerly ($\bar{U}$ greater than 5 m/s) and easterly or weak easterly ($\bar{U}$ less than 5 m/s) conditions. Approximately 75% of upper tropospheric E-MRG wave events are linked to a local strong westerly background exceeding 5 m/s, while the remaining 25% are associated with easterly or weak westerly backgrounds below 5 m/s. The monthly and longitudinal distribution of E-MRG wave event occurrences for the two categories (Figure 4.6 b, c) reveals that the secondary peak in activity over the East Pacific during March to June, coincides with local $\bar{U}$ less than 5 m/s conditions, observed in Figure 4.6 a. Moreover, primary peaks in E-MRG wave event occurrences are directly tied to Doppler shifting by strong westerly background winds during NH winter (Yang & Hoskins, 2016), particularly when prevailing strong westerlies are evident in the upper troposphere (as illustrated in Figure 4.2 a and 4.3 a). These analyses confirm the reliability of calculating local means associated with each E-MRG event and offer insights into the dynamics influencing their activity.

To verify if the identified E-MRG wave events associated with $\bar{U}$ less than 5 m/s are truly representative of MRG waves structures and not random equatorial meridional wind signatures, horizontal lead-lag composite structures of the identified events are analyzed. In Figure 4.7 and Figure 4.8, composites for $\bar{U}$ greater than 5 m/s and $\bar{U}$ less than 5 m/s conditions, respectively, over the East Pacific domain are presented. These composites are constructed by longitudinally translating the day 0 location of E-MRG wave events to a reference point at 135°W, utilizing wind and geopotential anomalies at 200 hPa filtered for 3 to 15 days. For events associated with $\bar{U}$ greater than 5 m/s during November to January and March to June, the horizontal structures exhibit defined features resembling the theoretical MRG structure, showcasing eastward phase propagation akin to the regressed horizontal structures observed in Figure 4.5. These structures demonstrate symmetry with respect to the equator, with meridional wind and rotation patterns in congruence. Similar structures are observed over the Atlantic Ocean domain for $\bar{U}$ greater than 5 m/s (figure not shown). Interestingly, the lead-lag composites reveal a connection between tropical E-MRG wave activity and extratropical Rossby wave trains intruding from both the NH and SH. Notably, the amplitude of NH and SH extratropical Rossby wave trains diminishes after the peak E-MRG wave activity, suggesting a potential resonant forcing effect amplifying E-MRG wave activity. The observations highlight a reduced amplitude of E-MRG waves during March to June compared to November to April. In contrast, the lead-lag composites for E-MRG wave events associated with Ū less than 5 m/s during March to June over the East Pacific exhibit less distinct and symmetric features compared to those for Ū greater than 5 m/s. While the centers of meridional winds may be slightly shifted northward from the equator, the fundamental characteristics of MRG waves, such as cross-equatorial meridional wind components and cyclonic and anticyclonic rotations, remain evident with a clear eastward phase propagation.

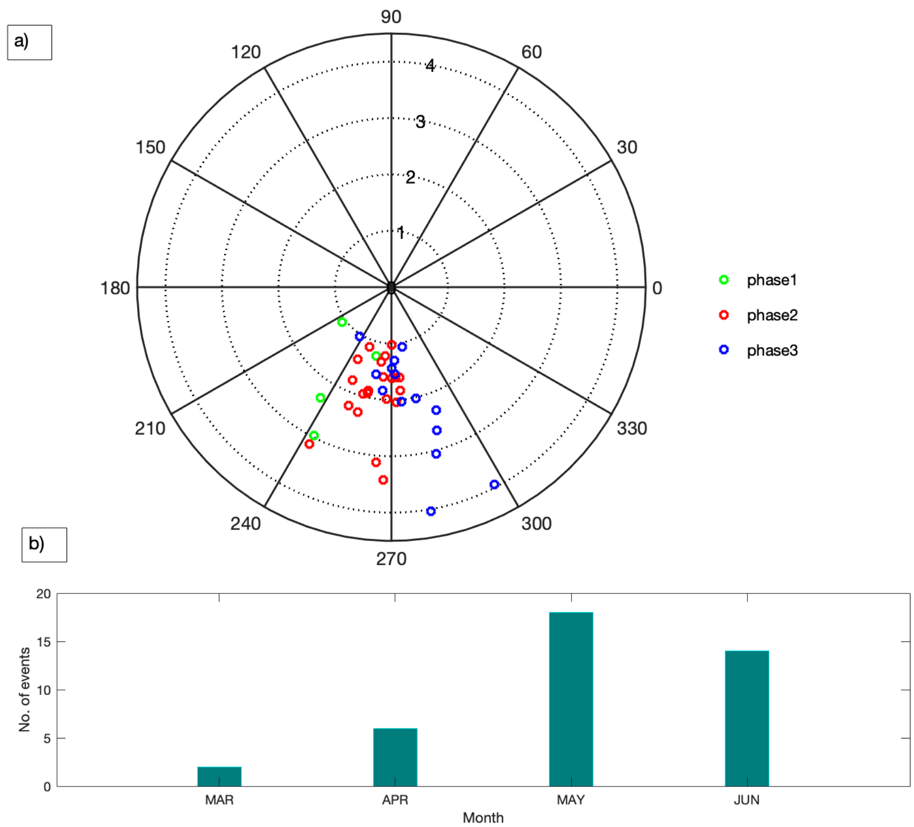

Figure 4.10. a) A Kelvin wave phase diagram, derived using the two leading EOF modes for zonal wind anomalies at 200 hPa, filtered for Kelvin wave wavenumbers and frequencies across the Pacific region (180°E to 300°E) during the months of March to June from 1979 to 2022. Each colored circle on the diagram represents an E-MRG wave instance that coincides with phases 1 to 3 of the westerly phase of Kelvin wave activity. The position of each circle signifies the longitudinal location of E-MRG wave event activity, with the distance from the center indicating the associated amplitude of Kelvin wave activity. b) A bar chart showing the number of E-MRG wave events that co-occur with the westerly phase of Kelvin waves during the months of March to June over the east Pacific.

During March to June, E-MRG wave events with meridional winds Ū less than 5 m/s exhibit a pronounced seasonal preference over the East Pacific. Concurrently, Kelvin wave activity in the region is notably strong during this period (Roundy & Frank, 2004; Straub & Kiladis, 2003; Takayabu et al., 2016; Wheeler et al., 2000; Wheeler & Kiladis, 1999). The Kelvin wave activity is associated with intruding wave trains from the SH during the March to

May (Kiladis, 1998; Kiladis & Weickmann, 1997; Roundy & Frank, 2004; Straub & Kiladis, 2003). Studies suggest that convectively coupled Kelvin waves originating in the west Pacific propagate eastward and reach the east Pacific (Roundy & Frank, 2004), where during Boreal springtime extratropical Rossby waves intruding from the NH amplify their amplitude, by inducing downstream convection in the tropics at synoptic-scales (Huaman et al., 2020). It seems plausible to explore the connection between the Kelvin waves and E-MRG waves with $\bar{U}$ less than 5 m/s over the East Pacific during MAMJ. EOF analysis was conducted over the central and east Pacific domain spanning from 180°E to 300°E, with Kelvin wave wavenumber and frequency filtered data (specifically filtered within the range of 3 to 20 days and eastward wavenumbers 2 to 15). The leading two EOF modes, EOF1 and EOF2, collectively explain 30% of the total variance. Combining EOF1 and EOF2, a phase composite for Kelvin wave activity over the East Pacific was derived. Concurrently, E-MRG wave events associated with mean zonal wind speeds ($\bar{U}$) less than 5 m/s over the same domain during the months of March to June were recorded. Given the known longitude coordinates of day 0 of the E-MRG wave events, occurrences matching the time when Kelvin wave activity peaks were identified. Figure 4.9 illustrates the composite horizontal structure of Kelvin waves for the initial 5 phases, represented in wind vectors and zonal wind contours. The location of E-MRG wave events, where $\bar{U}$ less than 5m/s, coinciding with Kelvin wave activity, is denoted by black dots. Out of 57 E-MRG wave events with zonal wind speeds $\bar{U}$ less than 5m/s during March to June over the east Pacific, 40 events were found to coincide with the westerly phase of large-scale Kelvin waves corresponding to global wavenumbers 2 to 3 (as depicted in Figure 4.9a to 4.9c). Approximately 70% of the Doppler-shifted MRG events occurring when $\bar{U}$ less than 5m/s over the east Pacific during March to June were facilitated by the westerly phase of the Kelvin waves. Notably, the easterly phase of the Kelvin waves during this period were suppressed.

The findings suggest the potential significance of the westerly phase of large-scale Kelvin waves as a transient background for facilitating the Doppler shifting of E-MRG wave events, which are associated with an easterly or weak westerly background. To substantiate this argument, two key factors must be examined:

1. The amplitude of the zonal winds associated with the westerly phase of the Kelvin waves should be sufficiently strong to facilitate the eastward translation of MRG waves.

2. The zonal scale of the E-MRG wave event must be small enough to fit within the half-wavelength scale of the Kelvin wave activity.

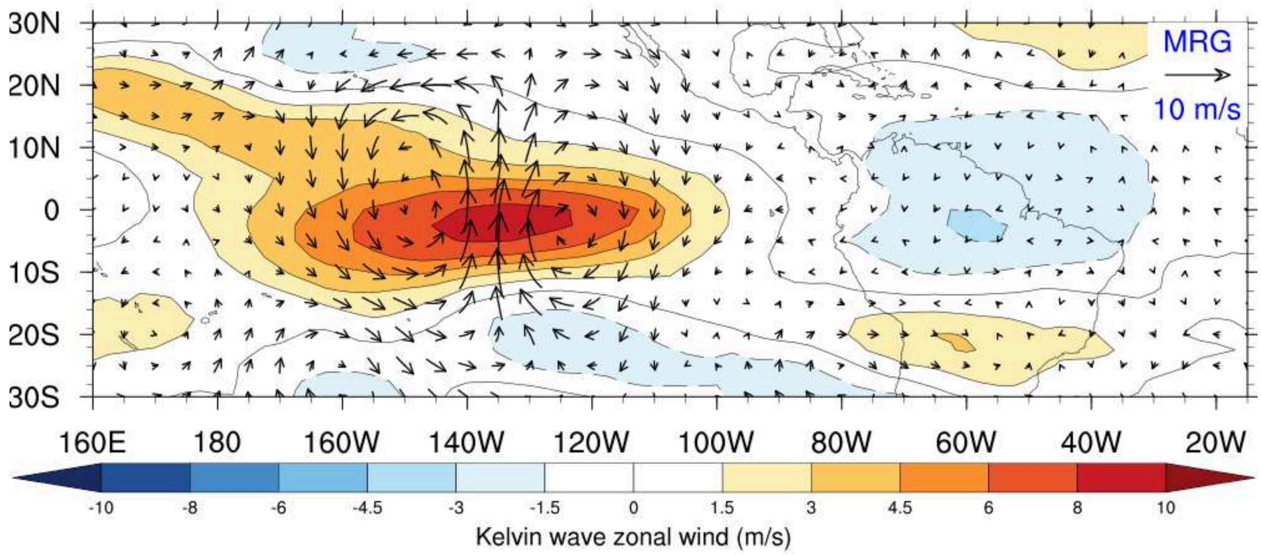

Figure 4.11. Horizontal wind composite (vectors, m/s) at 200 hPa for E-MRG wave events that co-occur within the westerly phase of large-scale Kelvin waves over east Pacific (180°E to 300°E) and during the months of March to June. The coloured contours represent the Kelvin wave zonal wind composite at 200 hPa over the east Pacific and during the months of March to June from 1979 to 2022. Wind anomalies are translated longitudinally to the location of maximum occurrence of E-MRG activity over the Pacific domain (225°W).

Firstly, the amplitude of Kelvin wave activity during instances of E-MRG wave events can be evaluated. A phase diagram for Kelvin waves (Figure 4.10 a) displays green, red, and blue hollow circles representing the amplitude of Kelvin wave activity during co-occurrence with E-MRG wave events. Notably, all E-MRG wave events coincide with the westerly phase of Kelvin waves exceeding amplitudes greater than one standard deviation. Additionally, Figures 4.9 a to 4.9 c depict the averaged amplitude of zonal winds associated with the westerly phase of Kelvin waves, reaching maximum values as high as 10 m/s. Given that this is an averaged value, individual event amplitudes can be expected to be likely higher or close to this value, thus sufficiently capable of inducing Doppler shifting of E-MRG wave events. Secondly, the zonal scale compatibility is assessed by overlaying the longitudinally translated composite horizontal structure onto the wind field of identified E-MRG wave events over the westerly phase of the Kelvin composite in zonal winds. In Figure 4.11, colored contours represent the Kelvin wave phase composite, while wind vectors illustrate the horizontal composite structure in wind at 200 hPa. Remarkably, one full E-MRG wavelength, typically exhibiting global wavenumbers 6–7, fits entirely within the westerly phase of large-scale Kelvin waves. Moreover, the amplitude of the westerly phase of Kelvin waves exceeds 10 m/s, while the composite easterly phase during this period is significantly subdued. These observations support the hypothesis of possible Doppler shifting of E-MRG wave events by transient local Kelvin wave eddies when background winds are less than 5m/s, unsupportive for Doppler shifting by the ambient flow.

4.4 Summary and Conclusions

The current study formally documents the structure, frequency of occurrence and propagation characteristics of eastward propagating Doppler shifted E-MRG wave events at 200 hPa using ERA5 reanalysis data for the period 1979–2022. E-MRG wave events are identified by using the multi-dimensional EMD technique for the equatorial meridional wind anomalies (Sun & Wu, 2020). This approach enables event-based identification of E-MRG waves, capturing their evolution in time and zonal direction without imposing stringent assumptions inherent in linear theory or Fourier-based equatorial wave identification methods. A total of 730 E-MRG wave events in the upper troposphere were identified, all confined to the central-East Pacific and Atlantic Ocean domain, characterized by the development of westerly winds over the tropics during NH winter (see Figure 4.5). Notably, nearly 30% of the total MRG wave variability over the Western Hemisphere during Boreal winter and spring stems from Doppler-shifted E-MRG wave events (Shreya & Suhas, 2024). Consequently, the relative contribution of E-MRG waves to overall MRG wave activity, and by extension, to the broader spectrum of eastward synoptic-scale variability over the western hemisphere seems crucial. The observation that a substantial portion of MRG wave events over the western hemisphere manifest as Doppler-shifted eastward-propagating E-MRG waves, while retaining their theoretical horizontal structure, suggests that a significant segment of the tropical atmosphere adheres to linear dynamics in regions characterized by strong westerly winds during NH winter, when wave-convection coupling is weak and the upper tropospheric western hemisphere lacks organized deep convection. The upper level western hemisphere thus emerges as a potential focal point for sustaining synoptic-scale activity in the tropical atmosphere (Shreya & Suhas, 2024; Yang & Hoskins, 2016).

E-MRG wave events arise directly from the linear interaction between the westerly background mean flow and synoptic-scale activity. These events are categorized into two groups based on the associated local mean flow: strong westerly ($\bar{U}$ greater than 5m/s) and weak westerly or easterly ($\bar{U}$ less than 5m/s). The observation that 75% of E-MRG wave events occur with $\bar{U}$ greater than 5m/s over the East Pacific and Atlantic during boreal winter months validates the definition and identification of E-MRG wave events (figure 4.6 b). However, the remaining 25% of E-MRG wave events associated with $\bar{U}$ less than 5m/s are exclusively observed over the East Pacific domain and exhibit peak activity during boreal spring (figure 4.6 c). In the horizontal composite structures of E-MRG wave events, associations with wave trains originating from both the NH and SH are evident (figure 4.7). This suggests the potential involvement of eastward-propagating extratropical Rossby wave dynamics in amplifying E-MRG wave activity through resonant interactions (Hoskins & Yang, 2016).

To the best of our knowledge, this study represents the first objective classification of E-MRG wave events based on associated local mean background winds. The westerly wind ducts prevailing over the western hemisphere during NH winters primarily drive the Doppler shifting of the majority of E-MRG wave events. Conversely, E-MRG wave events linked with weak westerly or easterly zonal means over the East Pacific during March to June coincide with the westerly phase of large-scale and high amplitude Kelvin wave eddies (figure 4.9, 4.10, and 4.11). The preferred scale of E-MRG wave events falls within the shorter range of 5000 km to 6000 km (figure 4.5, 4.7, 4.8). Consequently, the westerly phase of robust, planetary scale Kelvin waves (with wavenumbers 2 to 3), exhibiting subdued easterly components, can acts as a transient background capable of fully submerging one full wavelength of an MRG wave event, and reversing its phase propagation to eastward. The principal finding of this study underscores the significant contribution of the westerly phase of robust Kelvin waves in facilitating the Doppler shifting of E-MRG wave events, particularly when the background zonal mean flow is not conducive to Doppler shifting the MRG waves.

Chapter V

Summary and Conclusions

Mixed Rossby-Gravity (MRG) waves are equatorially trapped synoptic-scale disturbances that exhibit the properties of both slowly evolving Rossby and quickly evolving gravity waves. MRG waves play a critical role in cyclogenesis and initiates many important modes of variability. For example, tropical depression, easterly waves, and the Madden-Julian Oscillation (MJO) (Kiladis et al., 2009; Takasuka & Satoh, 2021; Zhou & Wang, 2007). Therefore, understanding the factors that initiate and maintain the MRG waves is crucial. Motivated by compelling results from many modeling studies that provide evidence for the extratropical forcing of MRG waves (Hoskins & Yang, 2000; Mak, 1969a; Wilson & Mak, 1984; Zhang, 1993) the primary objective of the thesis is set to quantify the association between the laterally propagating extratropical disturbances and MRG waves using long record of reanalysis data. This objective is met by identifying individual episodes of MRG waves and intruding extratropical disturbances.

In the first chapter of the thesis, we document all episodes of lateral intrusion of extratropical disturbances into the tropics, occurring in both the NH and SH, using ERA5 reanalysis for the period 1979-2022. The identification of intruding extratropical disturbance is performed using potential vorticity (PV) on 350-K surface by leveraging the principle that PV is conserved along an isentropic surface during an adiabatic process. We assume that PV can act as a tracer for tracking the movement of air parcels from the extratropical to the tropical region. Thus, laterally propagating extratropical disturbances can be traced by following the trajectory of the air parcels with high PV value from the extratropical to tropical region. Using PV at the 350-K isentropic surface, which is nearly parallel to 200 hPa pressure level, a total of 3,678 PV intrusion events were recorded. It was found that the frequency of PV intrusion events exhibit strong seasonal and regional preference. Majority of the PV intrusions occurred in the central-east Pacific and the Atlantic Ocean domains during the boreal winter season when the westerly wind ducts are well developed. The majority (75%) of PV intrusion events propagate eastward while the remaining set of events propagate westward. The westward propagating PV intrusions are observed in both the Hemispheres in their respective summer season. The identification of a considerable number of PV intrusion events within the tropical atmosphere lays the groundwork for quantifying the association between the intrusion of extratropical disturbances and MRG waves.

In the second chapter, observational evidence is presented, revealing that a significant portion (37%) of MRG wave events in the upper troposphere is linked to the intrusion of extratropical wave disturbances particularly over the western hemisphere during the NH winter, in regions characterized by westerly wind ducts. The MRG wave events are identified by using the characteristic signature of the theoretical structure of MRG waves, which is a strong and symmetric component in the meridional wind at 200 hPa, using the ERA-Interim reanalysis dataset for 40 years from 1979 to 2019. A wave fitting method (Au-Yeung & Tam, 2018) is used to identify episodes of MRG waves, totaling 2,390 events globally. The MRG waves events are further classified as MRG with intrusion using a metric-based on association with PV at 350 K at the 15°N or 15°S latitude exceeding a threshold of 1 PVU units, realized four days before the maximum in the MRG wave activity is observed in the tropics. Notably, nearly 70% of the intrusion MRG events occurred in the Western Hemisphere, where the westerly wind ducts are well-developed and during the winter season. The intrusion MRG wave events that occur during NH winter months over the central-east Pacific have larger amplitude and more extensive meridional extent compared to non-intrusion MRG wave events. These observations coupled with the observation that these MRG waves have a similar spatial scale as the extratropical disturbances imply that resonant interactions may be a primary mechanism for the genesis of MRG wave events during the winter. In contrast, during summer, the observation of higher amplitude of intrusion MRG wave events along with larger trapping scales point towards the fact that these events might be primarily triggered by convection, with extratropical forcing playing a secondary role in amplifying these disturbances.

The upper tropospheric western hemisphere during boreal winter acts as a hub for observing MRG waves that exhibit both eastward and westward propagation. Detailed diagnostic analyses reveal that the eastward events can be categorized as Doppler-shifted MRG (E-MRG) wave events (G. Yang et al., 2023; G. Yang & Hoskins, 2016; G.-Y. Yang et al., 2003). Doppler shifted MRG wave events result from the modification of the restoring force of MRG waves due to linear interaction with a strong westerly background wind, leading to a zonal phase reversal of the intrinsic phase speed of the MRG wave from westward to eastward. Using the Empirical Mode Decomposition (EMD) method 730 E-MRG wave events are identified using ERA5 equatorial meridional wind data at 200 hPa from 1979 to 2022. All of the E-MRG wave events prefer the regions of the East Pacific and Atlantic Ocean, primarily during boreal winter months. 75% of these events are found to be associated with strong large-scale westerly winds, while, on contrary 25% events show associated with large-scale easterly winds. However, the E-MRG wave events with large-scale easterly winds show a seasonal preference for boreal spring and early summer and are found to occur over the East Pacific. Detailed analysis shows that the westerly phase of Kelvin waves play an important role in creating a conducive environment for the Doppler shifting of E-MRG wave events when the large-scale winds are easterly. These findings also provide evidence for linear wave-wave interaction between large and small-scale tropical waves. Life cycle composites of the E-MRG wave events also show a strong association with eastward propagating extratropical disturbances, indicating the possible role of resonant amplification due to extratropical forcing.

While numerous past studies (Takayabu, 1994a, 1994b; Wheeler & Kiladis, 1999; G.-Y. Yang et al., 2003), have illustrated that the observed equatorial waves largely conform to spatial-temporal scales and horizontal structures predicted by the linear wave dynamics, they fall short in quantifying their frequency of occurrences. Additionally, assessing whether the observed alignment between observed equatorial waves and linear theory is merely coincidental or indicative of a significant degree of agreement. The present study tries to bridge this gap by employing event-based analysis methods, enabling a more definitive statement regarding MRG waves. Specifically, it has been found that in conditions where organized deep convection over the Western Hemisphere during NH winter is absent (figure 3.4 b), yet westerly winds are present in the tropical upper troposphere (figure 3.3), results obtained from the scale analysis for large-scale tropical motions remain valid (Charney 1963, Holton 2004). Notably, almost 50% of MRG wave activity over the western hemisphere during winter is associated with the intrusion of extratropical disturbances. This association occurs during a period when the primary trigger of equatorial waves, namely latent heat release through convection, is markedly weak. Hence, this thesis underlines the fact that extratropical forcing of MRG waves may be crucial as the in-situ forcing mechanism.

References

Aiyyer, A. R., & Molinari, J. (2003). Evolution of Mixed Rossby–Gravity Waves in Idealized MJO Environments. *Journal of the Atmospheric Sciences*, *60*(23), 2837–2855. https://doi.org/10.1175/1520-0469(2003)060<2837:EOMRWI>2.0.CO;2

Albers, J. R., Kiladis, G. N., Birner, T., & Dias, J. (2016). Tropical Upper-Tropospheric Potential Vorticity Intrusions during Sudden Stratospheric Warmings. *Journal of the Atmospheric Sciences*, *73*(6), 2361–2384. https://doi.org/10.1175/JAS-D-15-0238.1

Arkin, P. A., & Webster, P. J. (1985). Annual and Interannual Variability of Tropical-Extratropical Interaction: An Empirical Study. *Monthly Weather Review*, *113*(9), 1510–1523. https://doi.org/10.1175/1520-0493(1985)113<1510:AAIVOT>2.0.CO;2

Au-Yeung, A. Y. M., & Tam, C.-Y. (2018). Dispersion Characteristics and Circulation Associated with Boreal Summer Westward-Traveling Mixed Rossby–Gravity Wave–Like Disturbances. *Journal of the Atmospheric Sciences*, *75*(2), 513–533. https://doi.org/10.1175/JAS-D-16-0245.1

Barnes, E. A., & Hartmann, D. L. (2012). Detection of Rossby wave breaking and its response to shifts of the midlatitude jet with climate change. *Journal of Geophysical Research: Atmospheres*, *117*(D9), 2012JD017469. https://doi.org/10.1029/2012JD017469

Bennett, J. R., & Young, J. A. (1971). THE INFLUENCE OF LATITUDINAL WIND SHEAR UPON LARGE-SCALE WAVE PROPAGATION INTO THE TROPICS. *Monthly Weather Review*, *99*(3), 202–214. https://doi.org/10.1175/1520-0493(1971)099<0202:TIOLWS>2.3.CO;2

Berrisford, P., Hoskins, B. J., & Tyrlis, E. (2007). Blocking and Rossby Wave Breaking on the Dynamical Tropopause in the Southern Hemisphere. *Journal of the Atmospheric*

Sciences, *64*(8), 2881–2898. https://doi.org/10.1175/JAS3984.1

Charney, J. G. (1963). A Note on Large-Scale Motions in the Tropics. *Journal of the Atmospheric Sciences*, *20*(6), 607–609. https://doi.org/10.1175/1520-0469(1963)020<0607:ANOLSM>2.0.CO;2

Charney, J. G. (1969). A Further Note on Large-Scale Motions in the Tropics. *Journal of the Atmospheric Sciences*, *26*(1), 182–185. https://doi.org/10.1175/1520-0469(1969)026<0182:AFNOLS>2.0.CO;2

Chen, B., Tung, W., & Yanai, M. (2016). Multiscale Temporal Mean Features of Perturbation Kinetic Energy and Its Budget in the Tropics: Review and Computation. *Meteorological Monographs*, *56*, 8.1-8.23. https://doi.org/10.1175/AMSMONOGRAPHS-D-15-0017.1

Cheng, Y.-M., Tulich, S., Kiladis, G. N., & Dias, J. (2022). Two Extratropical Pathways to Forcing Tropical Convective Disturbances. *Journal of Climate*, *35*(20), 2987–3009. https://doi.org/10.1175/JCLI-D-22-0171.1

Dee, D. P., Uppala, S. M., Simmons, A. J., Berrisford, P., Poli, P., Kobayashi, S., Andrae, U., Balmaseda, M. A., Balsamo, G., Bauer, P., Bechtold, P., Beljaars, A. C. M., Van De Berg, L., Bidlot, J., Bormann, N., Delsol, C., Dragani, R., Fuentes, M., Geer, A. J., … Vitart, F. (2011). The ERA‐Interim reanalysis: Configuration and performance of the data assimilation system. *Quarterly Journal of the Royal Meteorological Society*, *137*(656), 553–597. https://doi.org/10.1002/qj.828

Dias, J., & Kiladis, G. N. (2014). Influence of the basic state zonal flow on convectively coupled equatorial waves. *Geophysical Research Letters*, *41*(19), 6904–6913. https://doi.org/10.1002/2014GL061476

Dominguez, C., Done, J. M., & Bruyère, C. L. (2020). Easterly wave contributions to seasonal rainfall over the tropical Americas in observations and a regional climate model. *Climate Dynamics*, *54*(1–2), 191–209. https://doi.org/10.1007/s00382-019-04996-7

Feng, T., Yang, X.-Q., Zhou, W., Huang, R., Wu, L., & Yang, D. (2016). Synoptic-Scale Waves in Sheared Background Flow over the Western North Pacific. *Journal of the Atmospheric Sciences*, *73*(11), 4583–4603. https://doi.org/10.1175/JAS-D-16-0064.1

Feng, X., Yang, G.-Y., Hodges, K. I., & Methven, J. (2023). Equatorial waves as useful precursors to tropical cyclone occurrence and intensification. *Nature Communications*, *14*(1), 511. https://doi.org/10.1038/s41467-023-36055-5

Fröhlich, L., & Knippertz, P. (2008). Identification and global climatology of upper-level troughs at low latitudes. *Meteorologische Zeitschrift*, *17*(5), 565–573. https://doi.org/10.1127/0941-2948/2008/0320

Funatsu, B. M., & Waugh, D. W. (2008). Connections between Potential Vorticity Intrusions and Convection in the Eastern Tropical Pacific. *Journal of the Atmospheric Sciences*, *65*(3), 987–1002. https://doi.org/10.1175/2007JAS2248.1

Garcia, R. R., & Salby, M. L. (1987). Transient Response to Localized Episodic Heating in the Tropics. Part II: Far-Field Behavior. *Journal of the Atmospheric Sciences*, *44*(2), 499–532. https://doi.org/10.1175/1520-0469(1987)044<0499:TRTLEH>2.0.CO;2

Gray, L. J., Anstey, J. A., Kawatani, Y., Lu, H., Osprey, S., & Schenzinger, V. (2018). Surface impacts of the Quasi Biennial Oscillation. *Atmospheric Chemistry and Physics*, *18*(11), 8227–8247. https://doi.org/10.5194/acp-18-8227-2018

Hayashi, Y. (1970). A Theory of Large-Scale Equatorial Waves Generated by Condensation Heat and Accelerating. *Journal of the Meteorological Society of Japan. Ser. II*, *48*(2), 140–160. https://doi.org/10.2151/jmsj1965.48.2_140

Hayashi, Y. (1976). Non-Singular Resonance of Equatorial Waves Under the Radiation Condition. *Journal of the Atmospheric Sciences*, *33*(2), 183–201. https://doi.org/10.1175/1520-0469(1976)033<0183:NSROEW>2.0.CO;2

Held, I. M., & Hoskins, B. J. (1985). Large-Scale Eddies and the General Circulation of the Troposphere. In *Advances in Geophysics* (Vol. 28, pp. 3–31). Elsevier. https://doi.org/10.1016/S0065-2687(08)60218-6

Hendon, H. H., & Liebmann, B. (1991). The Structure and Annual Variation of Antisymmetric Fluctuations of Tropical Convection and Their Association with Rossby–Gravity Waves. *Journal of the Atmospheric Sciences*, *48*(19), 2127–2140. https://doi.org/10.1175/1520-0469(1991)048<2127:TSAAVO>2.0.CO;2

Holton, J.R.. (2004). Introduction to dynamic meteorology, 4th edition. Amsterdam: *Elsevier Academic Press*, p. 535.

Holton, J. R., & Lindzen, R. S. (1972). An Updated Theory for the Quasi-Biennial Cycle of the Tropical Stratosphere. *Journal of the Atmospheric Sciences*, *29*(6), 1076–1080. https://doi.org/10.1175/1520-0469(1972)029<1076:AUTFTQ>2.0.CO;2

Hoskins, B. J., & Ambrizzi, T. (1993). Rossby Wave Propagation on a Realistic Longitudinally Varying Flow. *Journal of the Atmospheric Sciences*, *50*(12), 1661–1671. https://doi.org/10.1175/1520-0469(1993)050<1661:RWPOAR>2.0.CO;2

Hoskins, B. J., & Karoly, D. J. (1981). The Steady Linear Response of a Spherical Atmosphere to Thermal and Orographic Forcing. *Journal of the Atmospheric Sciences*, *38*(6), 1179–1196. https://doi.org/10.1175/1520-0469(1981)038<1179:TSLROA>2.0.CO;2

Hoskins, B. J., McIntyre, M. E., & Robertson, A. W. (1985). On the use and significance of isentropic potential vorticity maps. *Quarterly Journal of the Royal Meteorological*

Society, *111*(470), 877–946. https://doi.org/10.1002/qj.49711147002

Hoskins, B. J., & Yang, G.-Y. (2000). The Equatorial Response to Higher-Latitude Forcing. *Journal of the Atmospheric Sciences*, *57*(9), 1197–1213. https://doi.org/10.1175/1520-0469(2000)057<1197:TERTHL>2.0.CO;2

Hoskins, B. J., & Yang, G.-Y. (2016). The Longitudinal Variation of Equatorial Waves due to Propagation on a Varying Zonal Flow. *Journal of the Atmospheric Sciences*, *73*(2), 605–620. https://doi.org/10.1175/JAS-D-15-0167.1

Huaman, L., Schumacher, C., & Kiladis, G. N. (2020). Eastward-Propagating Disturbances in the Tropical Pacific. *Monthly Weather Review*, *148*(9), 3713–3728. https://doi.org/10.1175/MWR-D-20-0029.1

Itoh, H. (1978). Forced Equatorial waves under the Marginally Stable State with Respect to wave-CISK Mechanism. *Journal of the Meteorological Society of Japan. Ser. II*, *56*(3), 145–158. https://doi.org/10.2151/jmsj1965.56.3_145

Itoh, H., & Ghil, M. (1988). The Generation Mechanism of Mixed Rossby-Gravity Waves in the Equatorial Troposphere. *Journal of the Atmospheric Sciences*, *45*(4), 585–604. https://doi.org/10.1175/1520-0469(1988)045<0585:TGMOMR>2.0.CO;2

Kang, M.-J., & Chun, H.-Y. (2021). *Contributions of equatorial planetary waves and small-scale convective gravity waves to the 2019/20 QBO disruption*. https://doi.org/10.5194/acp-2021-85

Kang, M.-J., Chun, H.-Y., & Garcia, R. R. (2020). Role of equatorial waves and convective gravity waves in the 2015/16 quasi-biennial oscillation disruption. *Atmospheric Chemistry and Physics*, *20*(23), 14669–14693. https://doi.org/10.5194/acp-20-14669-2020

Kikuchi, K. (2014). An introduction to combined Fourier–wavelet transform and its application to convectively coupled equatorial waves. *Climate Dynamics*, *43*(5–6), 1339–1356. https://doi.org/10.1007/s00382-013-1949-8

Kiladis, G. N. (1998). Observations of Rossby Waves Linked to Convection over the Eastern Tropical Pacific. *Journal of the Atmospheric Sciences*, *55*(3), 321–339. https://doi.org/10.1175/1520-0469(1998)055<0321:OORWLT>2.0.CO;2

Kiladis, G. N., Dias, J., & Gehne, M. (2016). The Relationship between Equatorial Mixed Rossby–Gravity and Eastward Inertio-Gravity Waves. Part I. *Journal of the Atmospheric Sciences*, *73*(5), 2123–2145. https://doi.org/10.1175/JAS-D-15-0230.1

Kiladis, G. N., & Weickmann, K. M. (1992a). Circulation Anomalies Associated with Tropical Convection during Northern Winter. *Monthly Weather Review*, *120*(9), 1900–1923. https://doi.org/10.1175/1520-0493(1992)120<1900:CAAWTC>2.0.CO;2

Kiladis, G. N., & Weickmann, K. M. (1992b). Circulation Anomalies Associated with Tropical Convection during Northern Winter. *Monthly Weather Review*, *120*(9), 1900–1923. https://doi.org/10.1175/1520-0493(1992)120<1900:CAAWTC>2.0.CO;2

Kiladis, G. N., & Weickmann, K. M. (1992c). Extratropical Forcing of Tropical Pacific Convection during Northern Winter. *Monthly Weather Review*, *120*(9), 1924–1939. https://doi.org/10.1175/1520-0493(1992)120<1924:EFOTPC>2.0.CO;2

Kiladis, G. N., & Weickmann, K. M. (1997). Horizontal Structure and Seasonality of Large-Scale Circulations Associated with Submonthly Tropical Convection. *Monthly Weather Review*, *125*(9), 1997–2013. https://doi.org/10.1175/1520-0493(1997)125<1997:HSASOL>2.0.CO;2

Kiladis, G. N., Wheeler, M. C., Haertel, P. T., Straub, K. H., & Roundy, P. E. (2009).

Convectively coupled equatorial waves. *Reviews of Geophysics*, *47*(2), 2008RG000266. https://doi.org/10.1029/2008RG000266

Knippertz, P., Gehne, M., Kiladis, G. N., Kikuchi, K., Rasheeda Satheesh, A., Roundy, P. E., Yang, G., Žagar, N., Dias, J., Fink, A. H., Methven, J., Schlueter, A., Sielmann, F., & Wheeler, M. C. (2022). The intricacies of identifying equatorial waves. *Quarterly Journal of the Royal Meteorological Society*, *148*(747), 2814–2852. https://doi.org/10.1002/qj.4338

Kousky, V. E. (1979). Frontal Influences on Northeast Brazil. *Monthly Weather Review*, *107*(9), 1140–1153. https://doi.org/10.1175/1520-0493(1979)107<1140:FIONB>2.0.CO;2

Liebmann, B., & Hendon, H. H. (1990). Synoptic-Scale Disturbances near the Equator. *Journal of the Atmospheric Sciences*, *47*(12), 1463–1479. https://doi.org/10.1175/1520-0469(1990)047<1463:SSDNTE>2.0.CO;2

Lin, P., Held, I., & Ming, Y. (2019). The Early Development of the 2015/16 Quasi-Biennial Oscillation Disruption. *Journal of the Atmospheric Sciences*, *76*(3), 821–836. https://doi.org/10.1175/JAS-D-18-0292.1

Lindzen, R. S. (1974). Wave-CISK in the Tropics. *Journal of the Atmospheric Sciences*, *31*(1), 156–179. https://doi.org/10.1175/1520-0469(1974)031<0156:WCITT>2.0.CO;2

Magaña, V., & Yanai, M. (1995). Mixed Rossby–Gravity Waves Triggered by Lateral Forcing. *Journal of the Atmospheric Sciences*, *52*(9), 1473–1486. https://doi.org/10.1175/1520-0469(1995)052<1473:MRWTBL>2.0.CO;2

Mak, M.-K. (1969a). Laterally Driven Stochastic Motions in the Tropics. *Journal of the Atmospheric Sciences*, *26*(1), 41–64. https://doi.org/10.1175/1520-0469(1969)026<0041:LDSMIT>2.0.CO;2

Mak, M.-K. (1969b). Laterally Driven Stochastic Motions in the Tropics. *Journal of the Atmospheric Sciences*, *26*(1), 41–64. https://doi.org/10.1175/1520-0469(1969)026<0041:LDSMIT>2.0.CO;2

Matsuno, T. (1966). Quasi-Geostrophic Motions in the Equatorial Area. *Journal of the Meteorological Society of Japan. Ser. II*, *44*(1), 25–43. https://doi.org/10.2151/jmsj1965.44.1_25

McIntyre, M. E., & Palmer, T. N. (1983). Breaking planetary waves in the stratosphere. *Nature*, *305*(5935), 593–600. https://doi.org/10.1038/305593a0

Moore, B. J., Keyser, D., & Bosart, L. F. (2019). Linkages between Extreme Precipitation Events in the Central and Eastern United States and Rossby Wave Breaking. *Monthly Weather Review*, *147*(9), 3327–3349. https://doi.org/10.1175/MWR-D-19-0047.1

Pelly, J. L., & Hoskins, B. J. (2003). A New Perspective on Blocking. *Journal of the Atmospheric Sciences*, *60*(5), 743–755. https://doi.org/10.1175/1520-0469(2003)060<0743:ANPOB>2.0.CO;2

Postel, G. A., & Hitchman, M. H. (1999). A Climatology of Rossby Wave Breaking along the Subtropical Tropopause. *Journal of the Atmospheric Sciences*, *56*(3), 359–373. https://doi.org/10.1175/1520-0469(1999)056<0359:ACORWB>2.0.CO;2

Pritchard, M. S., & Yang, D. (2016). Response of the Superparameterized Madden–Julian Oscillation to Extreme Climate and Basic-State Variation Challenges a Moisture Mode View. *Journal of Climate*, *29*(13), 4995–5008. https://doi.org/10.1175/JCLI-D-15-0790.1

Randel, W. J. (1992). Upper Tropospheric Equatorial Waves In Ecmwf Analyses. *Quarterly Journal of the Royal Meteorological Society*, *118*(504), 365–394. https://doi.org/10.1002/qj.49711850409

Ripa, P. (1983). General stability conditions for zonal flows in a one-layer model on the β-plane or the sphere. *Journal of Fluid Mechanics*, *126*, 463–489. https://doi.org/10.1017/S0022112083000270

Riehl, H. (1945). Waves in the easterlies and the polar front in the tropics. University of Chicago, *Misc. Rep.* 17, 79.

Riehl, H. (1977). Venezuelan rain systems and the general circulation of the summer tropics I: Rain systems. *Monthly Weather Review*, *105(11)*, 1402-1420.

Riehl, H. (1977). Venezuelan rain systems and the general circulation of the summer tropics II: Relations between low and high latitudes. *Monthly Weather Review*, *105(11)*, 1421-1433.

Roundy, P. E., & Frank, W. M. (2004). A Climatology of Waves in the Equatorial Region. *Journal of the Atmospheric Sciences*, *61*(17), 2105–2132. https://doi.org/10.1175/1520-0469(2004)061<2105:ACOWIT>2.0.CO;2

Sakaeda, N., & Roundy, P. E. (2014). The Role of Interactions between Multiscale Circulations on the Observed Zonally Averaged Zonal Wind Variability Associated with the Madden–Julian Oscillation. *Journal of the Atmospheric Sciences*, *71*(10), 3816–3836. https://doi.org/10.1175/JAS-D-13-0304.1

Salby, M. L. (1984). Survey of planetary‐scale traveling waves: The state of theory and observations. *Reviews of Geophysics*, *22*(2), 209–236. https://doi.org/10.1029/RG022i002p00209

Schlueter, A., Fink, A. H., Knippertz, P., & Vogel, P. (2019). A Systematic Comparison of Tropical Waves over Northern Africa. Part I: Influence on Rainfall. *Journal of Climate*, *32*(5), 1501–1523. https://doi.org/10.1175/JCLI-D-18-0173.1

Scott, R. K., & Cammas, J.-P. (2002). Wave Breaking and Mixing at the Subtropical Tropopause.

Journal of the Atmospheric Sciences, *59*(15), 2347–2361. https://doi.org/10.1175/1520-0469(2002)059<2347:WBAMAT>2.0.CO;2

Shreya, K., & Suhas, E. (2024). A survey of westward‐propagating mixed Rossby–Gravity waves and quantification of their association with extratropical disturbances. *Quarterly Journal of the Royal Meteorological Society*, *150*(760), 1752–1770. https://doi.org/10.1002/qj.4668

Straub, K. H., & Kiladis, G. N. (2003). Extratropical Forcing of Convectively Coupled Kelvin Waves during Austral Winter. *Journal of the Atmospheric Sciences*, *60*(3), 526–543. https://doi.org/10.1175/1520-0469(2003)060<0526:EFOCCK>2.0.CO;2

Streten, N. A. (1973). Some Characteristics of Satellite-Observed Bands Of Persistent Cloudiness Over the Southern Hemisphere. *Monthly Weather Review*, *101*(6), 486–495. https://doi.org/10.1175/1520-0493(1973)101<0486:SCOSBO>2.3.CO;2

Strong, C., & Magnusdottir, G. (2008). Tropospheric Rossby Wave Breaking and the NAO/NAM. *Journal of the Atmospheric Sciences*, *65*(9), 2861–2876. https://doi.org/10.1175/2008JAS2632.1

Suhas, E., Neena, J. M., & Jiang, X. (2020). Exploring the Factors Influencing the Strength and Variability of Convectively Coupled Mixed Rossby–Gravity Waves. *Journal of Climate*, *33*(22), 9705–9719. https://doi.org/10.1175/JCLI-D-20-0218.1

Sun, J., & Wu, Z. (2020). Isolating spatiotemporally local mixed Rossby-gravity waves using multi-dimensional ensemble empirical mode decomposition. *Climate Dynamics*, *54*(3–4), 1383–1405. https://doi.org/10.1007/s00382-019-05066-8

Takasuka, D., & Satoh, M. (2020). Dynamical Roles of Mixed Rossby–Gravity Waves in Driving Convective Initiation and Propagation of the Madden–Julian Oscillation: General Views.

Journal of the Atmospheric Sciences, *77*(12), 4211–4231. https://doi.org/10.1175/JAS-D-20-0050.1

Takasuka, D., & Satoh, M. (2021). Diversity of the Madden–Julian Oscillation: Initiation Region Modulated by the Interaction between the Intraseasonal and Interannual Variabilities. *Journal of Climate*, *34*(6), 2297–2318. https://doi.org/10.1175/JCLI-D-20-0688.1

Takasuka, D., Satoh, M., & Yokoi, S. (2019). Observational Evidence of Mixed Rossby‐Gravity Waves as a Driving Force for the MJO Convective Initiation and Propagation. *Geophysical Research Letters*, *46*(10), 5546–5555. https://doi.org/10.1029/2019GL083108

Takayabu, Y. N., Kiladis, G. N., & Magaña, V. (2016). Michio Yanai and Tropical Waves. *Meteorological Monographs*, *56*, 3.1-3.21. https://doi.org/10.1175/AMSMONOGRAPHS-D-15-0019.1

Takayabu, Y. N., & Nitta, T. (1993). 3-5 Day-Period Disturbances Coupled with Convection over the Tropical Pacific Ocean. *Journal of the Meteorological Society of Japan. Ser. II*, *71*(2), 221–246. https://doi.org/10.2151/jmsj1965.71.2_221

Takayabu, Y. N. (1994a). Large-Scale Cloud Disturbances Associated with Equatorial Waves: Part I: Spectral Features of the Cloud Disturbances. *Journal of the Meteorological Society of Japan. Ser. II*, *72*(3), 433–449. https://doi.org/10.2151/jmsj1965.72.3_433

Takayabu, Y. N. (1994b). Large-Scale Cloud Disturbances Associated with Equatorial Waves: Part II: Westward-Propagating Inertio-Gravity Waves. *Journal of the Meteorological Society of Japan. Ser. II*, *72*(3), 451–465. https://doi.org/10.2151/jmsj1965.72.3_451

Thomas, B., Kunchala, R. K., Singh, B. B., & Kumar, K. N. (2023). Climatology of Rossby Wave Breaking Over the Subtropical Indian Region. *Journal of Geophysical Research:*

Atmospheres, *128*(9), e2022JD038344. https://doi.org/10.1029/2022JD038344

Tomas, R. A., & Webster, P. J. (1994). Horizontal and Vertical Structure of Cross-Equatorial Wave Propagation. *Journal of the Atmospheric Sciences*, *51*(11), 1417–1430. https://doi.org/10.1175/1520-0469(1994)051<1417:HAVSOC>2.0.CO;2

Trenberth, K. E. (1976). Spatial and temporal variations of the Southern Oscillation. *Quarterly Journal of the Royal Meteorological Society*, *102*(433), 639–653. https://doi.org/10.1002/qj.49710243310

Vishnupriya, S., Suhas, E., & Sandeep, S. (2022). Extratropical Stratospheric Air Intrusions Over the Western North Pacific and the Genesis of Downstream Monsoon Low‐Pressure Systems. *Geophysical Research Letters*, *49*(23), e2022GL100976. https://doi.org/10.1029/2022GL100976

Wang, B., & Xie, X. (1996). Low-Frequency Equatorial Waves in Vertically Sheared Zonal Flow. Part I: Stable Waves. *Journal of the Atmospheric Sciences*, *53*(3), 449–467. https://doi.org/10.1175/1520-0469(1996)053<0449:LFEWIV>2.0.CO;2

Waugh, D. W., & Polvani, L. M. (2000). Climatology of intrusions into the tropical upper troposphere. *Geophysical Research Letters*, *27*(23), 3857–3860. https://doi.org/10.1029/2000GL012250

Webster, P. J., & Chang, H.-R. (1988). Equatorial Energy Accumulation and Emanation Regions: Impacts of a Zonally Varying Basic State. *Journal of the Atmospheric Sciences*, *45*(5), 803–829. https://doi.org/10.1175/1520-0469(1988)045<0803:EEAAER>2.0.CO;2

Webster, P. J., & Holton, J. R. (1982). Cross-Equatorial Response to Middle-Latitude Forcing in a Zonally Varying Basic State. *Journal of the Atmospheric Sciences*, *39*(4), 722–733. https://doi.org/10.1175/1520-0469(1982)039<0722:CERTML>2.0.CO;2

Wernli, H., & Sprenger, M. (2007). Identification and ERA-15 Climatology of Potential Vorticity Streamers and Cutoffs near the Extratropical Tropopause. *Journal of the Atmospheric Sciences*, *64*(5), 1569–1586. https://doi.org/10.1175/JAS3912.1

Wheeler, M., & Kiladis, G. N. (1999). Convectively Coupled Equatorial Waves: Analysis of Clouds and Temperature in the Wavenumber–Frequency Domain. *Journal of the Atmospheric Sciences*, *56*(3), 374–399. https://doi.org/10.1175/1520-0469(1999)056<0374:CCEWAO>2.0.CO;2

Wheeler, M., Kiladis, G. N., & Webster, P. J. (2000). Large-Scale Dynamical Fields Associated with Convectively Coupled Equatorial Waves. *Journal of the Atmospheric Sciences*, *57*(5), 613–640. https://doi.org/10.1175/1520-0469(2000)057<0613:LSDFAW>2.0.CO;2

Wilson, J. D., & Mak, M. (1984). Tropical Response to Lateral Forcing with a Latitudinally and Zonally Nonuniform Basic State. *Journal of the Atmospheric Sciences*, *41*(7), 1187–1201. https://doi.org/10.1175/1520-0469(1984)041<1187:TRTLFW>2.0.CO;2

Woollings, T., Hoskins, B., Blackburn, M., & Berrisford, P. (2008). A New Rossby Wave–Breaking Interpretation of the North Atlantic Oscillation. *Journal of the Atmospheric Sciences*, *65*(2), 609–626. https://doi.org/10.1175/2007JAS2347.1

Yanai, M., Chen, B., & Tung, W. (2000). The Madden–Julian Oscillation Observed during the TOGA COARE IOP: Global View. *Journal of the Atmospheric Sciences*, *57*(15), 2374–2396. https://doi.org/10.1175/1520-0469(2000)057<2374:TMJOOD>2.0.CO;2

Yanai, M., & Lu, M.-M. (1983). Equatorially Trapped Waves at the 200 mb Level and Their Association with Meridional Convergence of Wave Energy Flux. *Journal of the Atmospheric Sciences*, *40*(12), 2785–2803. https://doi.org/10.1175/1520-0469(1983)040<2785:ETWATM>2.0.CO;2

Yanai, M., & Maruyama, T. (1966). Stratospheric Wave Disturbances Propagating over the Equatorial Pacific. *Journal of the Meteorological Society of Japan. Ser. II*, *44*(5), 291–294. https://doi.org/10.2151/jmsj1965.44.5_291

Yanai, M., Maruyama, T., Nitta, T., & Hayashi, Y. (1968). Power Spectra of Large-Scale Disturbances over the Tropical Pacific. *Journal of the Meteorological Society of Japan. Ser. II*, *46*(4), 308–323. https://doi.org/10.2151/jmsj1965.46.4_308

Yang, D., & Ingersoll, A. P. (2011). Testing the Hypothesis that the MJO is a Mixed Rossby–Gravity Wave Packet. *Journal of the Atmospheric Sciences*, *68*(2), 226–239. https://doi.org/10.1175/2010JAS3563.1

Yang, G., Feng, X., & Hodges, K. (2023). Seasonal and interannual variation of equatorial waves in ERA5 and GloSea5. *Quarterly Journal of the Royal Meteorological Society*, *149*(752), 1109–1134. https://doi.org/10.1002/qj.4460

Yang, G., & Hoskins, B. J. (2016). ENSO‐related variation of equatorial MRG and Rossby waves and forcing from higher latitudes. *Quarterly Journal of the Royal Meteorological Society*, *142*(699), 2488–2504. https://doi.org/10.1002/qj.2842

Yang, G.-Y., & Hoskins, B. (2013). ENSO Impact on Kelvin Waves and Associated Tropical Convection. *Journal of the Atmospheric Sciences*, *70*(11), 3513–3532. https://doi.org/10.1175/JAS-D-13-081.1

Yang, G.-Y., & Hoskins, B. J. (1996). Propagation of Rossby Waves of Nonzero Frequency. *Journal of the Atmospheric Sciences*, *53*(16), 2365–2378. https://doi.org/10.1175/1520-0469(1996)053<2365:PORWON>2.0.CO;2

Yang, G.-Y., Hoskins, B., & Slingo, J. (2003). Convectively Coupled Equatorial Waves: A New Methodology for Identifying Wave Structures in Observational Data. *Journal of the*

Atmospheric Sciences, *60*(14), 1637–1654. https://doi.org/10.1175/1520-0469(2003)060<1637:CCEWAN>2.0.CO;2

Yang, G.-Y., Hoskins, B., & Slingo, J. (2007a). Convectively Coupled Equatorial Waves. Part I: Horizontal and Vertical Structures. *Journal of the Atmospheric Sciences*, *64*(10), 3406–3423. https://doi.org/10.1175/JAS4017.1

Yang, G.-Y., Hoskins, B., & Slingo, J. (2007b). Convectively Coupled Equatorial Waves. Part II: Propagation Characteristics. *Journal of the Atmospheric Sciences*, *64*(10), 3424–3437. https://doi.org/10.1175/JAS4018.1

Yasunaga, K. (2011). Seasonality and Regionality of the Madden-Julian Oscillation and Convectively Coupled Equatorial Waves. *SOLA*, *7*, 153–156. https://doi.org/10.2151/sola.2011-039

Zangvil, A., & Yanai, M. (1981). Upper Tropospheric Waves in the Tropics. Part II. Association with Clouds in the Wavenumber-Frequency Domain. *Journal of the Atmospheric Sciences*, *38*(5), 939–953. https://doi.org/10.1175/1520-0469(1981)038<0939:UTWITT>2.0.CO;2

Zhang, C. (1993). Laterally Forced Equatorial Perturbations in a Linear Model. Part II: Mobile Forcing. *Journal of the Atmospheric Sciences*, *50*(6), 807–821. https://doi.org/10.1175/1520-0469(1993)050<0807:LFEPIA>2.0.CO;2

Zhang, C., & Webster, P. J. (1989). Effects of Zonal Flows on Equatorially Trapped Waves. *Journal of the Atmospheric Sciences*, *46*(24), 3632–3652. https://doi.org/10.1175/1520-0469(1989)046<3632:EOZFOE>2.0.CO;2

Zhang, C., & Webster, P. J. (1992). Laterally Forced Equatorial Perturbations in a Linear Model. Part I: Stationary Transient Forcing. *Journal of the Atmospheric Sciences*, *49*(7), 585–607. https://doi.org/10.1175/1520-0469(1992)049<0585:LFEPIA>2.0.CO;2

Zhou, X., & Wang, B. (2007). Transition from an eastern Pacific upper‐level mixed Rossby‐gravity wave to a western Pacific tropical cyclone. *Geophysical Research Letters*, *34*(24), 2007GL031831. https://doi.org/10.1029/2007GL031831

Received: 7 February 2023 | Revised: 22 December 2023 | Accepted: 8 January 2024

DOI: 10.1002/qj.4668

Quarterly Journal of the Royal Meteorological Society RMetS

RESEARCH ARTICLE

A survey of westward-propagating mixed Rossby–Gravity waves and quantification of their association with extratropical disturbances

K. Shreya | E. Suhas

Earth and Climate Science, Indian Institute of Science Education and Research Pune, Pune, India

Correspondence
E. Suhas, Earth and Climate Science, Indian Institute of Science Education and Research Pune, Dr. Homi Bhaba Road, Pune 411008, Maharashtra, India.
Email: suhas@iiserpune.ac.in

Funding information
Ministry of Earth Sciences

Abstract

In this study we have conducted a survey of westward-propagating mixed Rossby–Gravity (MRG) wave events in the upper troposphere and quantified their association with the intrusions of extratropical disturbances for the period 1979–2019. MRG wave events are identified by imposing the meridional structure of theoretical MRG waves onto the equatorial meridional winds at 200 hPa. In all, 2390 MRG wave events are identified and the majority (61%) of them occurred during the months of May–October, and 65% of the total MRG wave events occurred over the central–east Pacific and Atlantic Ocean domains. Not only the frequency of occurrence but also the amplitude, wavenumber and trapping scale of the MRG wave events are found to exhibit a clear seasonality. MRG wave events associated with intrusions of extratropical disturbances are identified as when the potential vorticity on the 350-K isentropic surface at 15° latitude exceeded 1 Potential Vorticity Unit (PVU) in the vicinity of the MRG wave events. We find that 37% of the MRG wave events are intrusion MRG wave events and a large majority (88%) of such events occurred over the central–east Pacific and Atlantic Ocean domains. It is also noteworthy that nearly 70% of such intrusions occurred in the winter hemisphere where the westerly wind ducts are well developed. Over the central–east Pacific during northern hemispheric (NH) winter, it is observed that the intrusion MRG wave events have a bigger amplitude and have a larger meridional extent compared to non-intrusion MRG wave events. They also exhibit a similar spatial scale as the extratropical disturbances implying that resonant interactions may be a primary mechanism for the genesis of MRG wave events. During NH summer, on the other hand, MRG wave events are primarily triggered by convective processes and the extratropical disturbances may be instrumental in amplifying their amplitude.

KEYWORDS

equatorial waves, mixed Rossby–Gravity waves, synoptic-scale variability, tropical–extratropical interactions

1 INTRODUCTION

Mixed Rossby–Gravity (MRG) waves are synoptic-scale westward-propagating disturbances observed in dynamic and convective fields over the equatorial region (Hendon & Liebmann, 1991; Kiladis et al., 2016; Suhas et al., 2020; Takayabu, 1994a; Takayabu & Nitta, 1993; Takayabu et al., 2016; Wheeler & Kiladis, 1999). Pronounced cross-equatorial meridional winds and vortices distributed symmetrically about the equator are the prominent features of MRG waves. MRG waves are more frequently observed over the Pacific domain during boreal summer and fall (Hendon & Liebmann, 1991; Kiladis et al., 2016; Magaña & Yanai, 1995; Suhas et al., 2020; Yasunaga, 2011). Several studies have shown that the MRG waves are sensitive to the dynamic and convective background fields in which they are embedded (Wang & Xie, 1996; Zhang & Webster, 1989, 1992). MRG waves are found to be more frequent during the La Niña phase of the El Niño Southern Oscillation (ENSO) and they are confined to the upper troposphere when there is westerly vertical shear or to the lower troposphere when there is easterly vertical shear (Feng et al., 2016; Kiladis et al., 2016; Takayabu & Nitta, 1993; Wang & Xie, 1996).

MRG waves play a pivotal role in dictating the variability and predictability of tropical weather. For example, MRG waves originating over the central or east Pacific often transition to tropical depressions and cyclones over the west Pacific (WP) (Aiyyer & Molinari, 2003; Feng et al., 2016; Takayabu & Nitta, 1993; Zhou & Wang, 2007). Recent studies indicate that MRG dynamics play a major role in initiating large-scale organised convection over the Indian Ocean (IO) (Takasuka et al., 2019; Takasuka & Satoh, 2020, 2021). Contribution of easterly momentum via vertically propagating MRG waves is vital for the quasi-biennial oscillation (QBO), a dominant mode of stratospheric circulation (Holton & Lindzen, 1972; Yanai et al., 1968). MRG waves were identified to be one of the factors that caused the disruption in QBO activity during 2015–2016 period (Lin et al., 2019). Recent theoretical and observational studies point out that dry dynamics is as important as moist dynamics in explaining the initiation, structure and propagation of the Madden–Julian Oscillations (MJO) and MRG wave is a core part of such theories (Pritchard & Yang, 2016; Takasuka et al., 2019; Takasuka & Satoh, 2020; Yang & Ingersoll, 2011). Since MRG waves bear the character of both Rossby and inertia–gravity waves, understanding the dynamics of MRG waves is crucial for improving the method of initialisation and thereby the skill in predicting tropical weather.

Since the advent of satellite observations, many studies have been conducted to understand the structure, propagation and excitation mechanisms of MRG waves (Hendon & Liebmann, 1991; Kiladis et al., 2016; Takayabu & Nitta, 1993; Yanai & Lu, 1983; Zangvil & Yanai, 1981; Zhang & Webster, 1992). Tropical convection, lateral forcing of extratropical disturbances, underlying sea surface temperature (SST) configuration, hydrodynamical instability and wave–wave interactions are suggested as possible mechanisms that can excite MRG waves (Hendon & Liebmann, 1991; Kiladis et al., 2009; Magaña & Yanai, 1995; Randel, 1992; Ripa, 1983). Many of the studies that tried to address the properties of MRG waves and their interactions with other modes of variability often focused on the convectively coupled MRG waves (Kiladis et al., 2016; Suhas et al., 2020; Wheeler et al., 2000; Wheeler & Kiladis, 1999). However, not all MRG wave activity may have a direct association with convection. For example, over the eastern Pacific and Atlantic domains, even while the synoptic-scale perturbation kinetic energy is high, the large-scale convection–circulation coupling strength is weak and hence a large fraction of MRG waves over these regions may not have a direct association with convection (Chen et al., 2016; Yang & Hoskins, 2016). Theoretical and observational studies recognise extratropical wave intrusions as one of the main sources of synoptic-scale variability over such regions where the probability of the occurrence of organised convection is less (Charney, 1963; Tomas & Webster, 1994; Webster & Holton, 1982). Linear wave theory identifies the presence of the upper-tropospheric westerly wind ducts as an important condition that would permit the intrusions of extratropical disturbances (Webster & Holton, 1982). Many observational studies show that extratropical intrusions through the upper-tropospheric westerly ducts can trigger tropical convection and equatorial waves (Kiladis, 1998; Yang & Hoskins, 2016). Wave energy accumulation and dispersion of energy from other locations can also induce synoptic-scale variability over regions where organised convective activity is less active (Hoskins & Yang, 2016; Webster & Chang, 1988; Yang & Hoskins, 2016). Hence a convection-based (e.g., using outgoing longwave radiation [OLR], precipitation, brightness temperature, etc.) identification of MRG wave activity would be an underestimate, as there might be several MRG wave events that might not have a strong signature in convective fields. Therefore, in order to have a comprehensive understanding of the MRG wave activity and their properties, it is important to use a method that is equally sensitive to all categories of MRG waves.

In this study we plan to conduct a climatological survey of MRG waves and characterise them over the whole tropics and separately over different geographical domains. Several past studies that brought out the characteristics of the MRG waves adopted a case study-based approach, which were mostly conducted over localised regions using data of limited sample size (Hendon & Liebmann, 1991; Liebmann & Hendon, 1990; Takayabu, 1994b; Takayabu & Nitta, 1993). Another set of studies extracted the climatological properties of MRG waves over a wider domain using a combination of wavenumber–frequency filtering and linear regression methods (Kiladis et al., 2009, 2016; Suhas et al., 2020; Wheeler et al., 2000). Since the observed MRG waves are localised in space and time, a Fourier-based wave isolation method might not be ideal for bringing out the local characteristics of the waves, as Fourier transform employs the assumption that the MRG waves are global in nature and are continuous. Alternately, wavelet and windowed wavenumber–frequency spectral analysis are used to capture the localised equatorial wave events (Dias & Kiladis, 2014; Kikuchi, 2014). However, these approaches are also not very effective in capturing the episodic MRG events. In order to better capture the spatial and temporal inhomogeneous nature of MRG wave activity, we use an event-based MRG wave identification method proposed by Au-Yeung and Tam (2018).

Since the main objective of the study is to characterise the MRG waves of all kinds, we chose the 200-hPa meridional wind as the primary variable to identify the MRG wave events. The upper-tropospheric winds capture both convectively coupled MRG waves over the Pacific and IO domains and dry MRG waves over the central and east Pacific and Atlantic domains (Kiladis et al., 2016; Magaña & Yanai, 1995; Randel, 1992; Wheeler & Kiladis, 1999; Yanai & Lu, 1983; Yang et al., 2003). The MRG signal in the lower atmosphere is mainly contaminated by the tropical depressions (TD), as it is very difficult to separate out these disturbances (Au-Yeung & Tam, 2018; Takasuka & Satoh, 2020; Takayabu & Nitta, 1993). However, the MRG event identification method based on upper-tropospheric winds is less likely to be contaminated by TD, as the influence of TD is largely confined to the lower to middle troposphere (Feng et al., 2016). Recent studies bring out observational evidence for the role of upper-tropospheric MRG waves in triggering lower-level MRG waves and their subsequent transition to TD and tropical cyclones (Au-Yeung & Tam, 2018; Zhou & Wang, 2007). The intrusion of extratropical disturbances over certain tropical regions is also considered as a triggering mechanism for MRG waves (Kiladis et al., 2016; Magaña & Yanai, 1995; Mak, 1969; Yang & Hoskins, 2016; Zhang & Webster, 1992). According to linear wave theory, extratropical disturbances are more likely to intrude over tropical regions where the background winds are westerly (Webster & Holton, 1982). There exists a direct link between the strength of the mean westerly winds and the intensity of energy carried by the extratropical disturbances. The observation of a stronger westerly wind duct in the upper troposphere over the central and east Pacific and Atlantic domains makes 200-hPa meridional wind an ideal parameter for quantifying MRG events associated with extratropical intrusions. Although many previous studies brought out observational evidence for the role of extratropical forcing in triggering MRG waves (Kiladis et al., 2016; Magaña & Yanai, 1995; Randel, 1992; Yang & Hoskins, 2016; Zangvil & Yanai, 1981), the relative contribution of such a forcing has not been quantified.

It is expected that a detailed climatology of the MRG events and their characterisation over different geographical domains will provide an observational basis for a complete assessment of MRG excitation mechanisms. It will also serve as a testbed for evaluating the skill of climate models in simulating the MRG waves. Since the MRG waves are unique to the tropics and they play an active role in tropical-scale interactions, realistic simulation of MRG waves is crucial for ensuring the reliability of models in simulating the weather and climate variability. It has been noted that extratropical disturbances could modulate the tropical synoptic-scale variability (Charney, 1963; Mak, 1969). A recent study by Vishnupriya et al. (2022) showed that about 15% of the monsoon low-pressure systems are triggered by extratropical air intrusions over the Pacific. A set of recent studies revealed that equatorward-propagating extratropical Rossby waves from the Northern (NH) and Southern (SH) hemispheres and their association with MRG waves contribute nearly half of the wave forcing that caused disruption in the westerly phase of the QBO (Kang et al., 2020; Kang & Chun, 2021; Lin et al., 2019). These results demonstrate the close association between tropical and extratropical dynamics and highlight the importance of quantifying the contribution of extratropical disturbances in modulating the MRG waves. Since QBO is considered a source of predictability on the seasonal time-scales, a comprehensive understanding on the relative role of extratropical disturbances in modulating the MRG wave events is also crucial for improving the prediction skill of extratropical seasonal forecasts (Gray et al., 2018). We believe that analysis of MRG events using 40 years of reanalysis data will help address the long-standing issue of the degree of involvement of extratropical disturbances in determining the MRG waves in the tropics.

2 | DATA AND METHODOLOGY

European Centre for Medium-Range Weather Forecasts Re-Analysis (ERA-Interim) six-hourly $0.5° \times 0.5°$ horizontal-resolution zonal and meridional components of the winds at 200 hPa and daily $2.5° \times 2.5°$ horizontal-resolution potential vorticity (PV) on the 350-K isentropic surface from 1 January 1979 to 31 August 2019

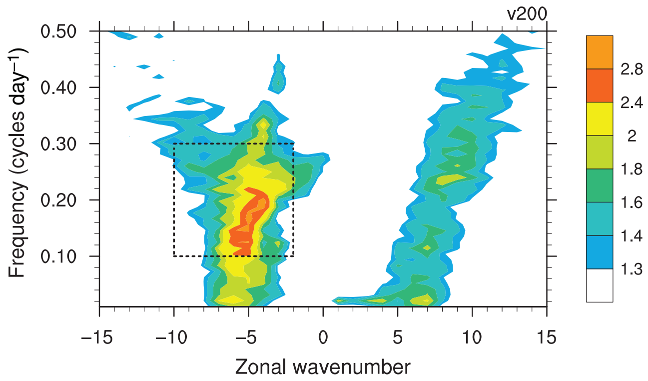

FIGURE 1 Symmetric/background zonal wavenumber–frequency power spectra of 200 hPa meridional wind (v200) in the tropics (15° S–15° N). The black dashed box isolates the wavenumbers and frequencies corresponding to the westward-propagating mixed Rossby–Gravity (MRG) wave activity. Shaded regions are statistically significant at the 99% confidence level. [Colour figure can be viewed at wileyonlinelibrary.com]

are the primary data used in this study (Dee et al., 2011). Figure 1 shows the symmetric wavenumber–frequency power spectra of 200-hPa meridional wind in the tropics (15° S–15° N) normalised by the red background (Wheeler & Kiladis, 1999). MRG wave power is prominently distributed in westward-propagating wavenumbers −10 to −2 in the 3–10-day period. It is interesting to note the presence of significant spectral peaks in the eastward wavenumbers as well. Some part of the eastward spectral power might be a result of Doppler shifting of $n = 2$ equatorial Rossby (ER) and MRG waves by the zonal flow (Yang et al., 2023; Yang & Hoskins, 2016) and some fraction of the eastward spectral power might be contributed by the intrusion of extratropical disturbances (Kiladis, 1998). Even though the spectral power associated with eastward-propagating MRG waves is less than that associated with westward-propagating MRG waves, it contributes to a large fraction of the eastward-propagating synoptic-scale variability in the western hemisphere (Yang & Hoskins, 2016). However a proper investigation of eastward-propagating MRG waves demands a separate study and in this study, we focus on westward-propagating MRG waves. In the following sections westward-propagating MRG waves are referred to simply as MRG waves.

MRG wave events at the 200-hPa level are identified by following the methodology of Au-Yeung and Tam (2018). The method is ideal for capturing the episodic behaviour of the MRG wave events. Westward-propagating strong equatorial meridional winds are the typical signature of the MRG waves and the MRG wave event identification methodology was designed by exploiting this property. The method estimates the instantaneous properties of the MRG waves such as the amplitude, trapping scale, frequency, wavelength and phase speed during the entire duration of an event. The crux of the methodology is based on the imposition of the theoretical meridional structure of MRG waves onto the meridional wind anomalies (Matsuno, 1966). The meridional wind anomalies are estimated by filtering meridional winds in the westward wavenumbers 2–10 and 3–10-day periodicity. Since the meridional winds associated with MRG waves are symmetrically distributed about the equator, only the symmetric meridional wind anomalies are imposed onto the theoretical meridional structure. The MRG event identification methodology involves multiple steps. At first, the longitudes marking the centres of the MRG wave events are located by identifying the local maxima and minima of the meridional wind anomaly at the equator for each time instant. Only the longitudes where the meridional wind anomalies exceed a value equal to 20% of the maximum, meridional wind amplitude are recorded to avoid very weak MRG wave events. Secondly, the meridional structure of the MRG waves is estimated at all those longitude locations by fitting the meridional wind anomalies at the equator onto the theoretical meridional structure of MRG waves using the equation given below.

$$v_{\text{fitted}}(x, y, t) = v_{\text{data}}\left(x, y = 0^0, t\right)D_0(y), \quad (1)$$

$$D_0(y) = e^{-\left(\frac{y}{2y_0}\right)^2}, \quad (2)$$

where v_{fitted} is the meridional wind of MRG waves and v_{data} is the meridional wind anomaly, x, y, t represent the longitude, latitude and time points, respectively, $D_0(y)$ is the $n = 0$ parabolic cylindrical function which describes the meridional structure of the $n = 0$ equatorial wave mode (Yang et al., 2003) and y_0 represents the trapping scale or idealised representation of meridional extent of the MRG wave. y_0 is a free parameter and MRG meridional winds are estimated for y_0 ranging from 0.5° to 20°.

The error associated with the estimation of MRG meridional winds is quantified as follows:

$$E(x, t) = \frac{\sqrt{\frac{1}{n}\sum_{y=0^0}^{y=20^0}\left(v_{\text{data}}(x, y, t) - v_{\text{fitted}}(x, y, t)\right)^2}}{\left|v_{\text{data}}\left(x, y = 0^0, t\right)\right|} \quad (3)$$

where E represents the error as a function of longitude and time and n represents the number of latitude points between 0° and 20°.

Finally, the observed maximum (minimum) of meridional wind anomaly at a longitude and time step is considered as a part of an MRG event only if it is linked to the next time step in a way that the maximum (minimum) of meridional wind anomaly should be observed within 20°

west of the previous longitude point. A cluster of longitude and time points that satisfy the above criteria for a duration ranging from two to eight days with at least one point exhibiting an error value less than or equal to 5% is classified as an MRG wave event. To avoid double counting, we have identified the MRG wave events by considering only the positive phase of the meridional wind anomaly.

Even though the wave-fitting method employed in the study is derived from the wave projection methodology of Yang et al. (2003), there are significant differences between the two approaches. In the wave projection method parabolic cylindrical functions are used as the basis function and since the parabolic cylindrical functions are orthogonal, the projection of dynamical fields onto the theoretical structure of equatorial waves does not permit the mixing of different equatorial waves, whereas in the wave-fitting method, the imposition of meridional wind anomalies[1] onto the meridional structure of MRG waves, while capturing the equatorially trapped and equatorially symmetric character of MRG waves, also allows for the mixing of MRG waves with the other equatorial waves of similar characteristics (e.g., $n = 2$ equatorial Rossby waves). However, it is expected that the limited wavenumber and frequency filtering range (2–10 westward wavenumbers and 3–10-day periodicity) used for extracting the meridional wind anomalies would minimise the possibility of mixing MRG waves with the $n = 2$ and higher even-number meridional modes of ER waves that exhibit a low-frequency character. It has been recognised that the presence of background circulation can modulate the restoring force of equatorial waves, which in turn can cause variability in the trapping scale of equatorial waves (Zhang & Webster, 1989). Since easterly and westerly winds are observed in the tropical upper troposphere, we do expect notable differences in the trapping scales of MRG wave events. Unlike the wave projection method, the wave-fitting method treats the trapping scale as a variable parameter and it enables estimating the instantaneous value of the trapping scale (Au-Yeung & Tam, 2018). There is a possibility that the intrusion of extratropical disturbances over the westerly ducts might lead to an overestimation of the trapping scale and in turn impact the identification of MRG wave events. However, the close similarity between the MRG wave events identified using wave-fitting and wave projection methods (figure not shown), gives more confidence in the wave-fitting-based approach used in the study. A recent study by Knippertz and co-authors (2022) provides a comprehensive review on the subject of equatorial wave identification techniques.

We have identified 2390 MRG wave events at 200 hPa for the 1979–2019 period. Important dynamical properties of the MRG waves during different time instances of an MRG wave event are estimated as follows. The maximum of meridional wind anomaly at the equator is taken as the amplitude of the MRG wave. The trapping scale is estimated from the y_0 values which show minimum error. The instantaneous wavenumber of an MRG wave event is estimated by applying Fourier transform in space. Instantaneous phase speed of an MRG wave event is estimated using the fourth-order Runge–Kutta finite difference method. Statistical significance of the differences in wave properties of the MRG wave events are tested by conducting Student's t and F tests.

The presence of extratropical disturbances over the subtropical and tropical region during MRG wave events is identified by following the methodology of Waugh and Polvani (2000). Waugh and Polvani (2000) traced the intrusion of extratropical air into the tropical region by exploiting the PV conservation in the absence of diabatic processes. By following a similar strategy, PV on the 350-K isentropic surface is used as a tracer to identify the extratropical wave intrusions during MRG wave events. Since the 350-K isentropic surface lies in the lower stratosphere in the extratropics and in the upper troposphere in the tropics (close to 200 hPa), the observation of higher PV on the 350-K isentropic surface over the tropical region suggests the presence of extratropical air in the tropics. An MRG wave event is grouped as the one associated with extratropical wave intrusions only when the criteria involving amplitude and duration of the PV at 350 K over a region where the MRG waves are active, are satisfied. It is noted that the extratropical disturbances can intrude into the tropics by taking NH and SH pathways. First, the amplitude of the PV at 350 K must be greater than 1 Potential Vorticity Unit (PVU; 1 PVU = $10^{-6}\ m^2 \cdot s^{-1} \cdot kg^{-1}$) at 15° N or 15° S within 40° east or west of the longitude at which the meridional wind of MRG waves exhibits a maximum. Second, the above condition must be satisfied for at least two days before the peak MRG wave activity and the high PV amplitude should be persistent over a longitudinal extent of 10°. If an MRG event satisfies these two criteria, such an MRG event is classified as an intrusion MRG event.

3 | RESULTS AND DISCUSSIONS

The equatorial wave characteristics, including that of MRG waves, are known to be sensitive to the mean zonal winds (Wang & Xie, 1996; Yang & Hoskins, 2016; Zhang & Webster, 1989, 1992). In addition to Doppler shifting of the intrinsic frequency, mean zonal winds can modulate the dynamics of MRG waves and restrict MRG wave activity either to the upper or the lower troposphere (Wang & Xie, 1996; Zhou & Wang, 2007). Figure 2 shows the longitude–pressure distribution of

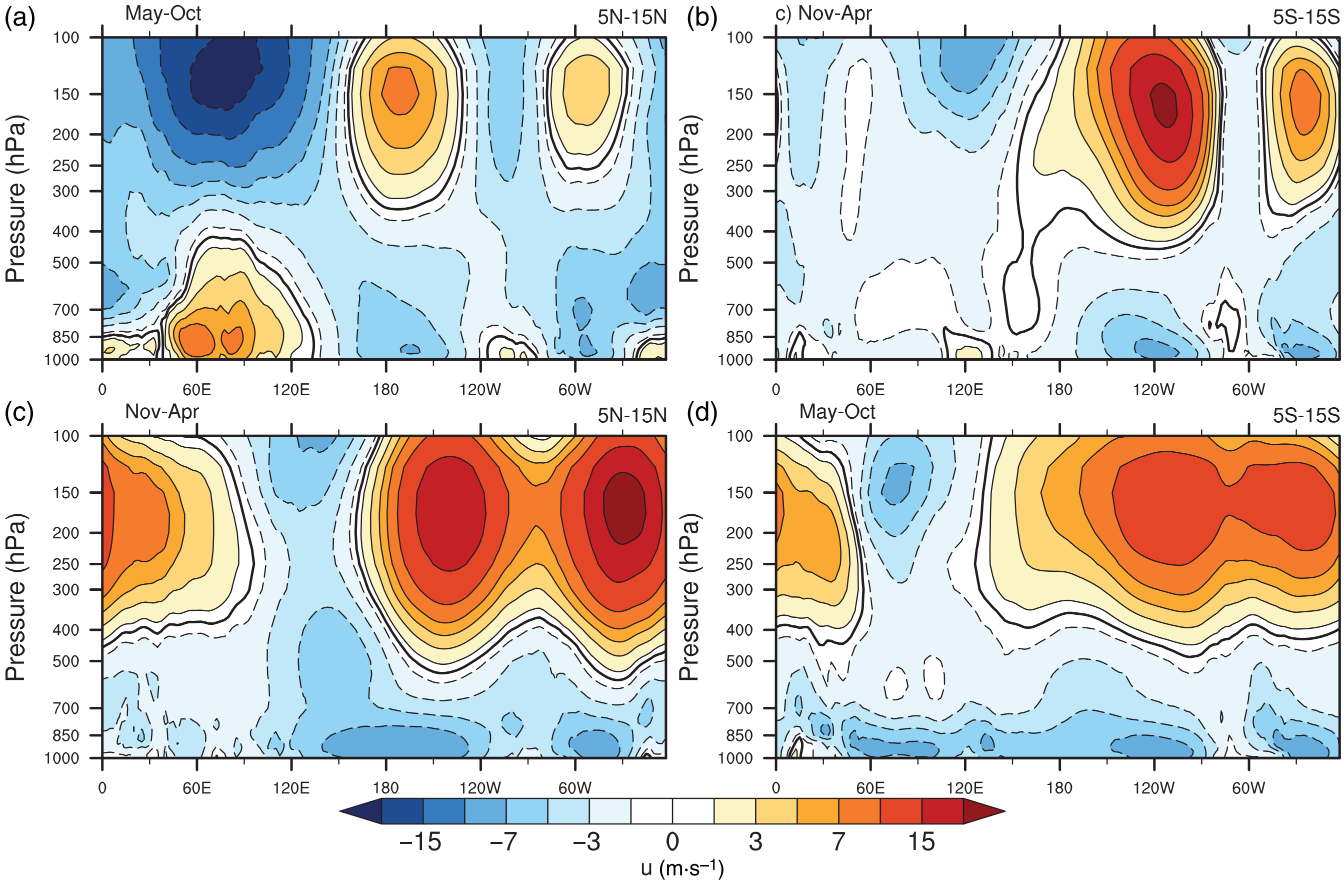

FIGURE 2 Longitude–pressure distribution of zonal winds (m·s^{-1}) averaged over: (a) 5° N–15° N latitudes for northern hemispheric summer seasons (May–October); (b) 5° N–15° N latitudes for northern hemispheric winter seasons (November–April); (c) 5° S–15° S latitudes for northern hemispheric winter seasons (November–April); and (d) 5° S–15° S latitudes for northern hemispheric summer seasons (May–October). [Colour figure can be viewed at wileyonlinelibrary.com]

mean zonal winds averaged over the NH (5° N–15° N) and SH (5° S–15° S) tropical regions, during NH summer and winter seasons. Westerly ducts are known to support extratropical–tropical interactions which might result in the excitation of MRG waves (Magaña & Yanai, 1995; Randel, 1992; Webster & Holton, 1982). Several previous studies have brought out observational evidence for the NH and SH pathways of extratropical intrusions and the subsequent interactions with MRG waves (Kiladis et al., 2016; Magaña & Yanai, 1995; Yang et al., 2007; Yang & Hoskins, 2016). Well-developed westerly wind ducts are observed in the upper troposphere over the central–east Pacific and Atlantic domains in the winter hemispheres (Figure 2b,d), while the westerly wind ducts are weak and mostly confined to a smaller region in the summer hemisphere (Figure 2a,c). It implies the higher likelihood of upper-tropospheric intrusions of extratropical disturbances during winter seasons. On the other hand, in the lower troposphere, westerly winds are observed only during NH summer, its amplitude is weak and is limited to the NH IO domain. The dominance of easterly zonal wind regime in the lower troposphere indicates that the lower troposphere is less conducive for the extratropical intrusions and the upper-tropospheric wind fields are chosen for quantifying the MRG–extratropical interactions.

Since MRG waves belong to the class of synoptic-scale variability, the synoptic-scale (3–10 day) spectral variance of zonal winds is examined for the NH (5° N–15° N) and SH (5° S–15° S) tropical regions during summer and winter seasons. Synoptic-scale spectral variance is estimated by computing the power spectra for multiple 90-day segments and averaging it for 3–10-day periodicity. The longitude–pressure distribution of synoptic-scale variance of zonal winds exhibits similar seasonal and geographical preferences as the zonal mean winds (Figure 3). Strong synoptic-scale variance is observed in the mid to upper troposphere mostly in the western hemisphere, and the synoptic-scale disturbances are more prominent over the winter hemisphere (Figure 3b,c). The longitude–pressure distribution of synoptic-scale variance of meridional winds is similar to that of the zonal winds (figure not shown). The regions of strong synoptic-scale wind variance represent

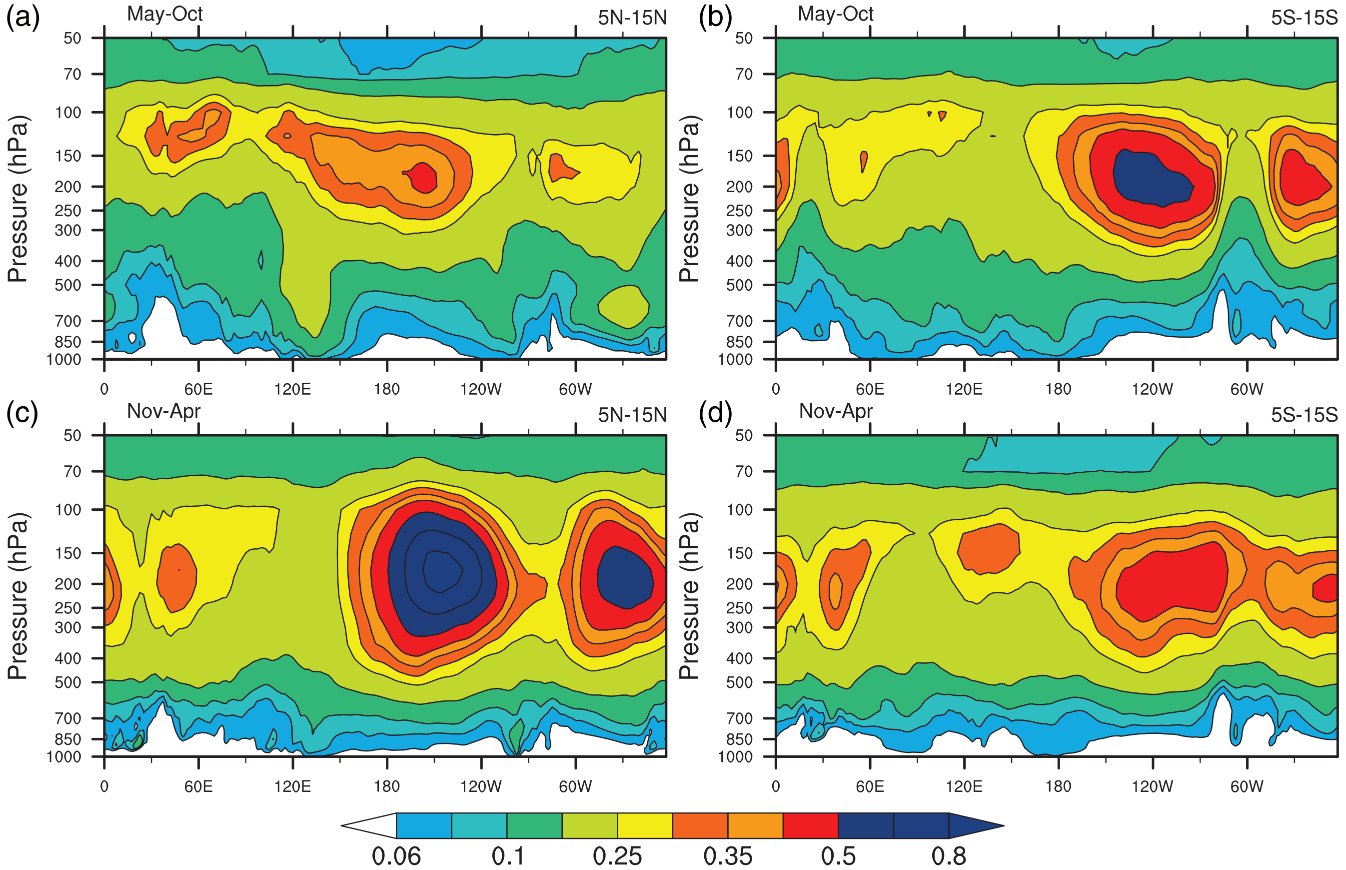

FIGURE 3 Longitude–pressure distribution of 3–10-day power spectra in zonal winds ($m^2 \cdot s^{-2}$) averaged over: (a) 5° N–15° N latitudes for northern hemispheric summer seasons (May–October); (b) 5° N–15° N latitudes for northern hemispheric winter seasons (November–April); (c) 5° S–15° S latitudes for southern hemispheric winter seasons (May–October); and (d) 5° S–15° S latitudes for southern hemispheric summer seasons (November–April). [Colour figure can be viewed at wileyonlinelibrary.com]

the regions of maximum perturbation kinetic energy (PKE). The observed colocation of westerly wind ducts and the PKE maxima corroborates the findings of many previous studies (Arkin & Webster, 1985; Chen et al., 2016; Webster & Chang, 1988; Webster & Holton, 1982). The available potential energy (APE) to PKE conversions is examined by calculating the cospectra between pressure vertical velocity and temperature for NH summer and winter seasons (Figure 4). A positive co-spectral power is an indicator of APE to PKE conversions and it can be used as a measure of convection-wave coupling strength (Chen et al., 2016; Yanai et al., 2000). From the longitude–pressure distribution of synoptic-scale (3–10 day) co-spectral power (Figure 4a), it is evident that the generation of synoptic-scale motions through convection is predominant in the entire tropical upper troposphere during the summer season, while the upper-tropospheric APE to PKE conversion is weak in the western hemisphere during the winter season and it is noticeably absent over the central and east Pacific (EP) and Atlantic Ocean (AO) (Figure 4b). While the westerly wind ducts are collocated with the synoptic-scale PKE maxima, the conspicuous absence of APE to PKE conversions over the westerly wind duct locations implies that the synoptic-scale motions over such regions are likely to be caused by dynamical processes or extratropical forcing (Charney, 1963; Holton, 2004). Recent studies based on the one-dimensional wave propagation theory rule out the variation of zonal flow and wave energy accumulation as the source of synoptic-scale PKE maxima in the western hemisphere (Hoskins & Yang, 2016; Yang & Hoskins, 2016).

In a nutshell, analysis of the mean zonal winds, synoptic-scale variance and conversion of APE to PKE implies that the excitation mechanisms of upper-tropospheric MRG waves can differ regionally and can have seasonal preferences. Examining the number of occurrences of MRG wave events as a function of longitude and months would help in understanding whether the MRG wave events exhibit any spatial and temporal clustering. Using the methodology of Au-Yeung and Tam (2018), the spatial–temporal distribution of MRG events is analysed by calculating the monthly frequency

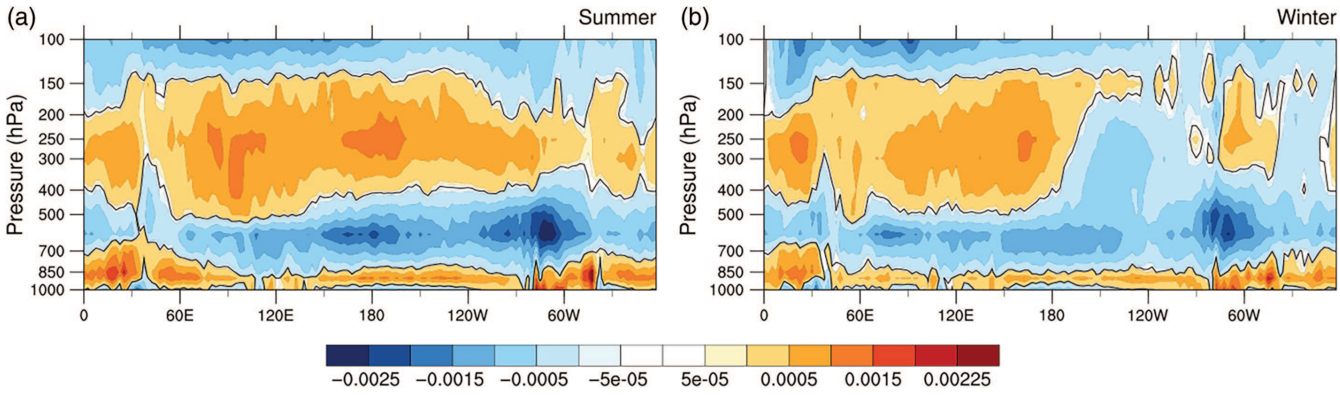

FIGURE 4 Longitude–pressure distribution of 3–10-day cospectra of temperature and vertical pressure velocity averaged over the tropics (15° S–15° N) for (a) northern hemispheric summer seasons (May–October); and (b) northern hemispheric winter seasons (November–April). Temperature and vertical pressure velocity anomalies are normalised with respect to their respective standard deviation before estimating the cross-spectra. [Colour figure can be viewed at wileyonlinelibrary.com]

of occurrence of MRG wave events in 30° longitude bins. Figure 5a shows the climatological distribution of 200-hPa MRG wave events during the months of January to December for the period 1979 to 2019. The analysis shows that MRG wave events occur over all the major ocean basins and exhibit a clear seasonality. More than 60% of the total MRG wave events are observed during NH summer season. A major fraction of MRG wave events over the Indian, Pacific and Atlantic Ocean domains occur during NH summer and secondary maxima of MRG wave events are observed during the NH winter season over the central–east Pacific and IO domains.

Based on the spatial distribution of MRG wave events, we have identified four preferred domains of MRG activity – IO (covers 50° E to 109.5° E), WP (covers 110° E to 179.5° E), EP (covers 180° E to 89.5° W) and AO (covers 90° W to 49.5° E) domains. The statistics of MRG wave events over different domains are summarised in Table 1. As indicated by many previous studies, about 65% of the MRG wave events are observed over the EP and AO domains (Kiladis et al., 2016; Randel, 1992; Suhas et al., 2020; Yang & Hoskins, 2016). It is interesting to note that about two-thirds of the total MRG wave events are equally distributed over the EP and AO domains. The robustness of the method of identification of MRG wave events is confirmed by examining the MRG wave event composites of dynamical fields over the four domains. Figure 6 shows the MRG wave event composites of 3–15-day filtered 200-hPa wind and stream function anomalies over the IO, WP, EP and AO domains. The composites are constructed with respect to the reference longitudes around which the largest number of MRG wave events is observed in each domain. The selected reference longitude for the IO, WP, EP and AO domains are 70° E, 120° E, 135° W and 40° W, respectively. Although the horizontal structure of the MRG waves appears to be similar over all the domains, some differences in their properties are observed over the different domains. For example, the amplitude, wavelength and meridional extent of the MRG waves are larger over the EP domain (Figure 6c). It is also evident that the convection–circulation coupling strength of MRG wave events varies over different domains. The observation of stronger convection–circulation coupling over the IO and WP domains suggestis the prevalence of moist dynamics.

The differences in important wave properties such as the amplitude, wavenumber, trapping scale, phase speed and duration of the individual MRG wave events over all the four domains are further evaluated. Figure 7 shows the range, mean and 90th- and 10th-percentile values of the MRG wave properties over the different domains during summer and winter seasons. Clear seasonality in the major MRG wave properties is observed across all domains. The amplitude of MRG waves is higher during NH summer and the largest- and smallest-amplitude MRG wave events are observed over the EP and AO domain, respectively (Figure 7a). It is noted that the difference in the distribution of amplitude of the MRG waves during summer and winter over the WP and AO domains are statistically significant at the 95% confidence level. In other words, compared to the other domains, the amplitudes of the MRG wave events over the IO and EP domain exhibit less seasonal variability. Summer–winter differences in the distribution of wavenumbers over the EP and AO domains are statistically significant at the 90% confidence level. The MRG wave events exhibit a shorter wavelength (larger wavenumber) during the NH summer season (Figure 7b). The MRG convection–circulation coupling strength is stronger during the NH summer (Suhas et al., 2020) and studies (Aiyyer & Molinari, 2003; Zhou & Wang, 2007) indicate that the MRG scale selection is strongly tied to the active feedback between frictional

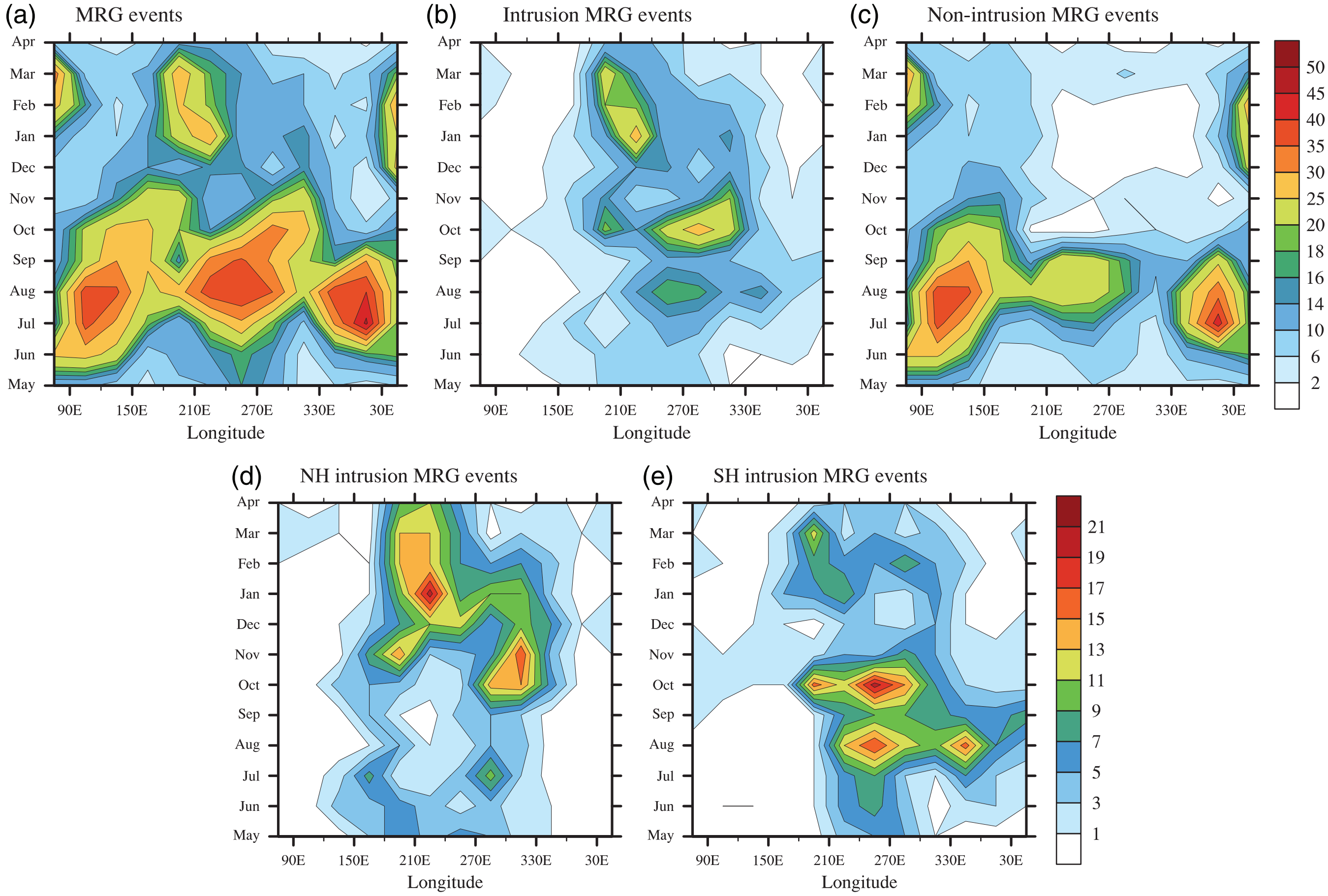

FIGURE 5 Month–longitude distribution of number of occurrences of mixed Rossby–Gravity (MRG) wave events at 200 hPa observed for the period 1979–2019. (a) Total number of occurrences of MRG wave events; (b) number of occurrences of MRG wave events that are associated with the intrusions of extratropical disturbances; (c) number of occurrences of MRG wave events that are not associated with the intrusions of extratropical disturbances, number of occurrences of MRG wave events that are associated with the intrusions of extratropical wave disturbances via (d) the northern hemisphere and (e) the southern hemisphere. [Colour figure can be viewed at wileyonlinelibrary.com]

TABLE 1 Number of occurrence of intrusion mixed Rossby–Gravity (MRG) events, non-intrusion mixed Rossby–Gravity (MRG) events and total MRG events observed over the Indian Ocean, West Pacific Ocean, central–east Pacific Ocean and Atlantic Ocean domains for the period 1979–2019.

MRG event category	Indian Ocean (50° E–110° E)	West Pacific Ocean (110° E–180° E)	central–east Pacific Ocean (180° E–90° W)	Atlantic Ocean (90° W–50° E)	Total MRG events
Intrusion MRG events	29	77	480	314	900 (37%)
Non-intrusion MRG events	361	387	276	466	1490 (63%)
Total MRG events	390 (16%)	464 (19%)	756 (32%)	780 (33%)	2390

Note: Fraction (%) of the total MRG events observed over different domains are shown in parentheses.

convergence and convective processes. The shorter wavelength observed during NH summer might be related to a stronger feedback between frictional convergence and convection (Zhou & Wang, 2007). The relatively smaller trapping scale of MRG wave events over the IO and WP domains (Figure 7c) suggests that probably convection plays a dominant role in triggering the MRG waves over these domains (Figure 6a,b). Tropical organised convection makes the atmosphere less stable and decreases the effective equivalent depth which in turn reduces the

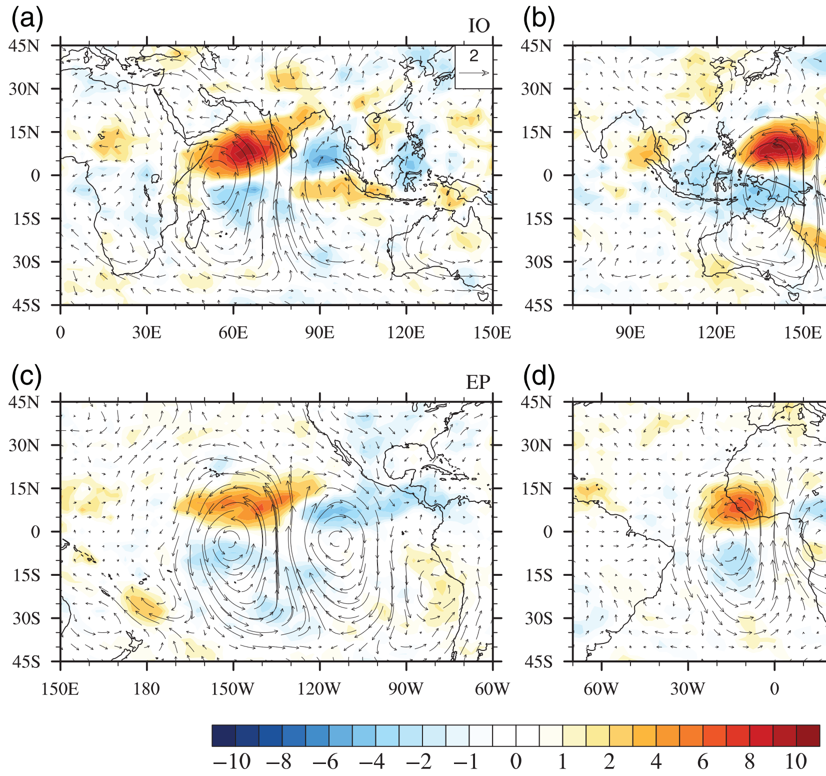

FIGURE 6 Composites of mixed Rossby–Gravity (MRG) wave events constructed using 3–15-day bandpass-filtered 200 hPa wind ($m\cdot s^{-1}$) and outgoing longwave radiation (OLR; $W\cdot m^{-2}$) anomalies over: (a) the Indian Ocean (IO); (b) West Pacific Ocean (WP); (c) central–east Pacific Ocean (EP); and (d) Atlantic Ocean (AO) domains. While compositing the wind and OLR anomalies are longitudinally translated to a reference longitude corresponding to maximum occurrence of MRG wave events for each domain.

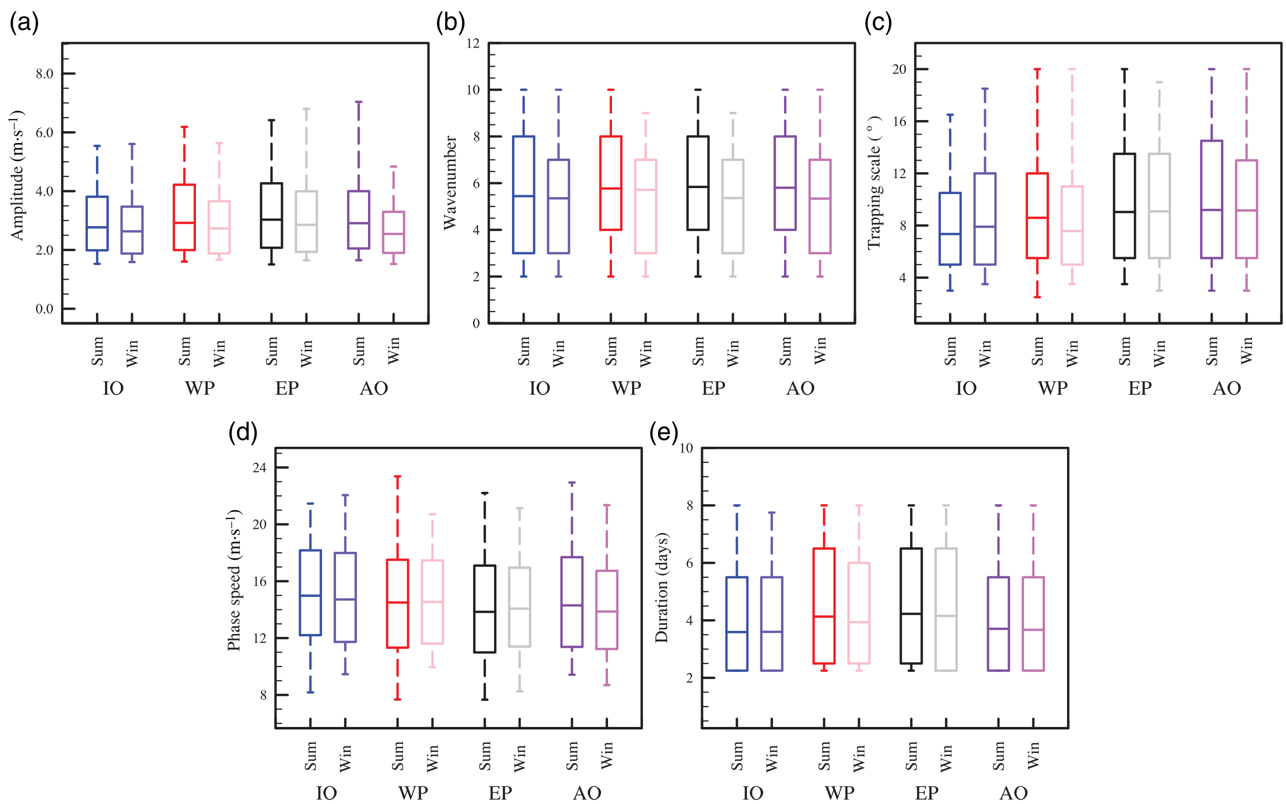

FIGURE 7 Range (maxima, minima), 90th percentile, mean, and 10th percentile of: (a) amplitude ($m\cdot s^{-1}$); (b) wavenumber; (c) trapping scale (°); (d) phase speed ($m\cdot s^{-1}$); and (e) duration (days) of mixed Rossby–Gravity (MRG) wave events observed over the Indian Ocean (IO, blue), West Pacific (WP, red), central–east Pacific (EP, black) and Atlantic Ocean (AO, purple) domains during northern hemispheric summer (Sum, dark colour) and northern hemispheric winter (Win, light colour).

trapping scale of wave disturbances (Kiladis et al., 2009). A relatively larger trapping scale is observed over the less convectively active EP and AO domains (Figure 7c). Zonal mean winds and extratropical forcing also play a role in determining the trapping scale of MRG waves (Zhang & Webster, 1989, 1992). The larger trapping scale might be indicative of the role of wave–mean flow interactions and intrusions of extratropical disturbances in triggering MRG wave events over these domains. The MRG wave phase speeds range from 12 to 17 $m\cdot s^{-1}$ and in contrast to the other parameters, they do not show much seasonality and variations across the different domains (Figure 7d). The duration of MRG wave events is also not very sensitive to the season. However, longer-duration MRG wave events are observed over the Pacific domain (Figure 7e).

The possible link between MRG wave events and intrusions of extratropical disturbances are investigated by examining the PV on the 350-K isentropic surface. Using the intrusion identification methodology described above, we find that about 37% of the MRG wave events are associated with intrusions of extratropical disturbances (Table 1) and the majority (54%) of such MRG wave events occur during NH winter (Table 2). The longitudinal distribution of monthly frequency of occurrence of MRG wave events associated with and without intrusions of extratropical disturbances is shown in Figure 5b,c. It is indicated in Table 1 that a significant fraction of intrusion MRG wave events (88%) occurs over the EP and AO domains, and about half of the MRG wave events over these domains are associated with intrusions of extratropical disturbances. On the other hand, a large fraction of the MRG wave events (86%) over the IO and WP domains is not associated with intrusions of extratropical disturbances, consistent with the existence of an upper-level easterly basic state that would preclude the propagation of Rossby wave energy into those regions.

Intrusion MRG wave events are further classified as NH (SH) intrusion MRG wave events in the case when extratropical air intrusions occur in the NH (SH), respectively. In rare cases, when intrusions are observed in both hemispheres, the event is classified based on the strength of the PV. The statistics and seasonality of the NH and SH intrusion MRG events and non-intrusion MRG events over the four domains are summarised in Table 2. The longitudinal distribution of monthly frequency of occurrence of NH and SH intrusion MRG wave events is shown in Figure 5d,e. The analysis reveals that intrusion of extratropical disturbances from both the NH and the SH is equally important in the genesis of MRG wave events. Except Yang and Hoskins (2016) and Kiladis et al. (2016), all other past studies only reported the association between the intrusion of extratropical disturbances via SH and MRG wave events (e.g., Magaña & Yanai, 1995; Suhas et al., 2020). The NH intrusion MRG wave events exhibit a

TABLE 2 Number of occurrences of northern hemispheric (NH) intrusion mixed Rossby–Gravity (MRG) events, SH intrusion events, co-occurrence of NH and SH intrusion MRG events and non-intrusion MRG events observed during NH summer and winter seasons for the period 1979–2019.

MRG event category	Indian Ocean (50° E–110° E)			West Pacific Ocean (110° E–180° E)			central–east Pacific Ocean (180° E–90° W)			Atlantic Ocean (90 W–50° E)			Total
	NH intrusion	SH intrusion	NH & SH intrusion	NH intrusion	SH intrusion	NH & SH intrusion	NH intrusion	SH intrusion	NH & SH intrusion	NH intrusion	SH intrusion	NH & SH intrusion	
Intrusion: NH summer	0	8	0	36	3	0	68	154	6	50	113	10	448 (19%)
Intrusion: NH winter	10	10	1	22	12	4	162	73	17	85	44	12	452 (19%)
Non-intrusion: NH summer	209			266			220			333			1028 (43%)
Non-intrusion: NH winter	152			121			56			133			462 (19%)
Total	390 (16%)			464 (19%)			756 (32%)			780 (33%)			2390

maxima over the EP during December–January and over the AO during October–November. Likewise, a large number of SH intrusion MRG wave events is observed during SH winter. Consistent with the inferences made from the distribution of mean zonal winds, the winter hemisphere with the westerly wind ducts seem to provide a favourable environment for the occurrence of intrusion MRG wave events (Figure 2b,d). About 70% of the intrusion MRG wave events over the EP and AO domains are observed in the winter hemisphere.

Spatial–temporal evolution of the upper-tropospheric tropical and extratropical dynamical fields during MRG wave events is examined for further validating the intrusion and non-intrusion MRG wave event classification. Lead–lag composites of dynamical fields associated with MRG wave events are constructed by identifying the day and longitudinal location of the amplitude maxima corresponding to each MRG wave event and translating the longitudinal locations to a reference longitudinal location and separately averaging the dynamical fields two days before, two days after and on the day of the MRG amplitude maxima. Figure 8 shows the lead–lag composites of 3–15-day filtered wind and stream function anomalies at 200 hPa associated with the intrusion MRG wave events over the EP domain. Statistical significance of the composites of MRG wave events are tested by conducting *t*-tests. Northwest–southeast-oriented stream function anomalies propagating from the NH extratropical to tropical region are found in the composites of NH intrusion MRG wave events during summer and winter (Figure 8a–f). At the same time, southwest–northeast-oriented eastward-propagating wave trains composed of alternate cyclonic and anticyclonic wind anomalies arching towards the equator are found in the SH in the composites of SH intrusion MRG wave events during summer and winter (Figure 8g–l). The observation of differences in the amplitude of the intruding extratropical disturbances two days before (stronger) and two days after (weaker) the MRG wave event amplitude maxima indicates the role of extratropical disturbances in triggering the MRG wave events. Weakening of the intruding extratropical disturbances a few days after the MRG amplitude maxima could be explained based on the PV–convection relationship. Past studies showed the occurrence of convection downstream of the intruding extratropical disturbances over the EP (Kiladis, 1998). Diabatic heating associated with convection can induce anticyclonic anomalies in the upper level which in turn can weaken the pre-existing cyclonic anomalies through destructive interference and thereby weaken the wave trains.

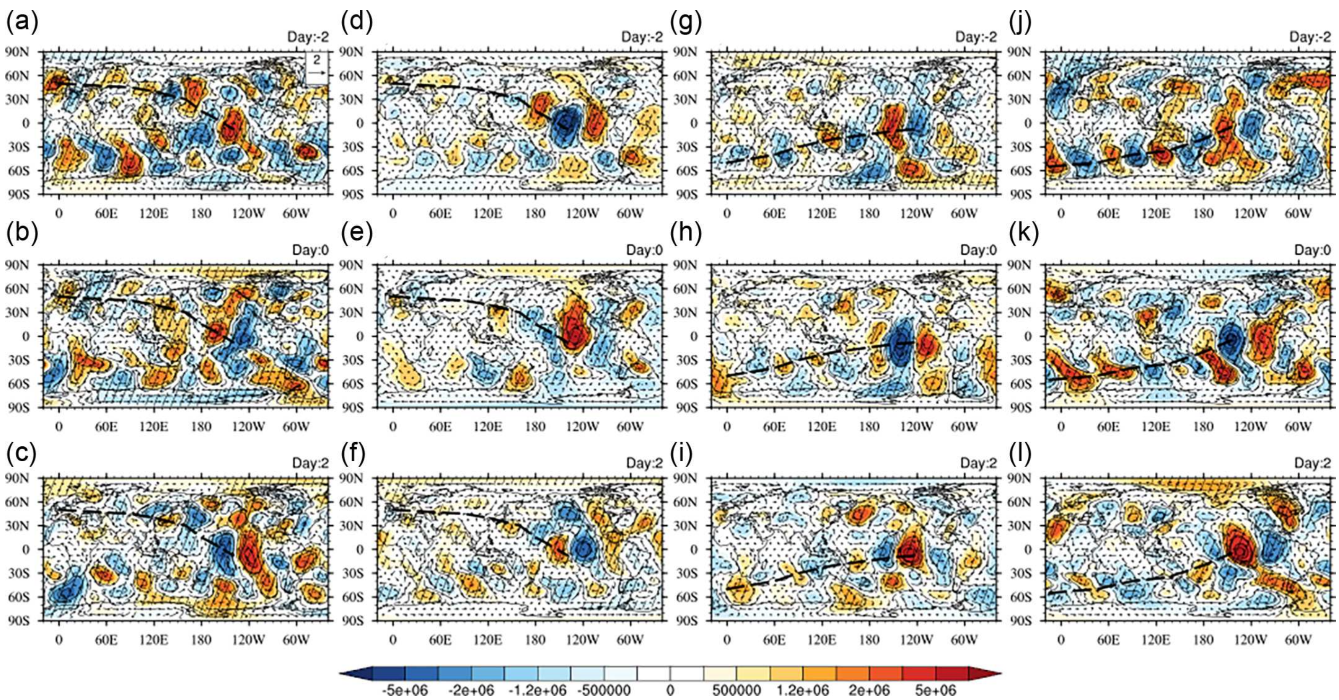

FIGURE 8 Lead–lag composites of intrusion MRG wave events over the central-east Pacific Ocean domain, constructed using 3–15-day bandpass-filtered 200 hPa wind (m·s^{-1}) and stream function (m^2·s^{-1}) anomalies. Positive (negative) lag represents the number of days after (before) the maximum mixed Rossby–Gravity (MRG) wave amplitude. (a–c) NH intrusion MRG wave events during NH summer; (d–f) NH intrusion MRG wave events during NH winter; (g–i) SH intrusion MRG wave events during NH summer; and (j–l) SH intrusion MRG wave events during NH winter. Black dashed curves highlight the intrusions of extratropical disturbances. Stippled regions are statistically significant at the 95% confidence level. [Colour figure can be viewed at wileyonlinelibrary.com]

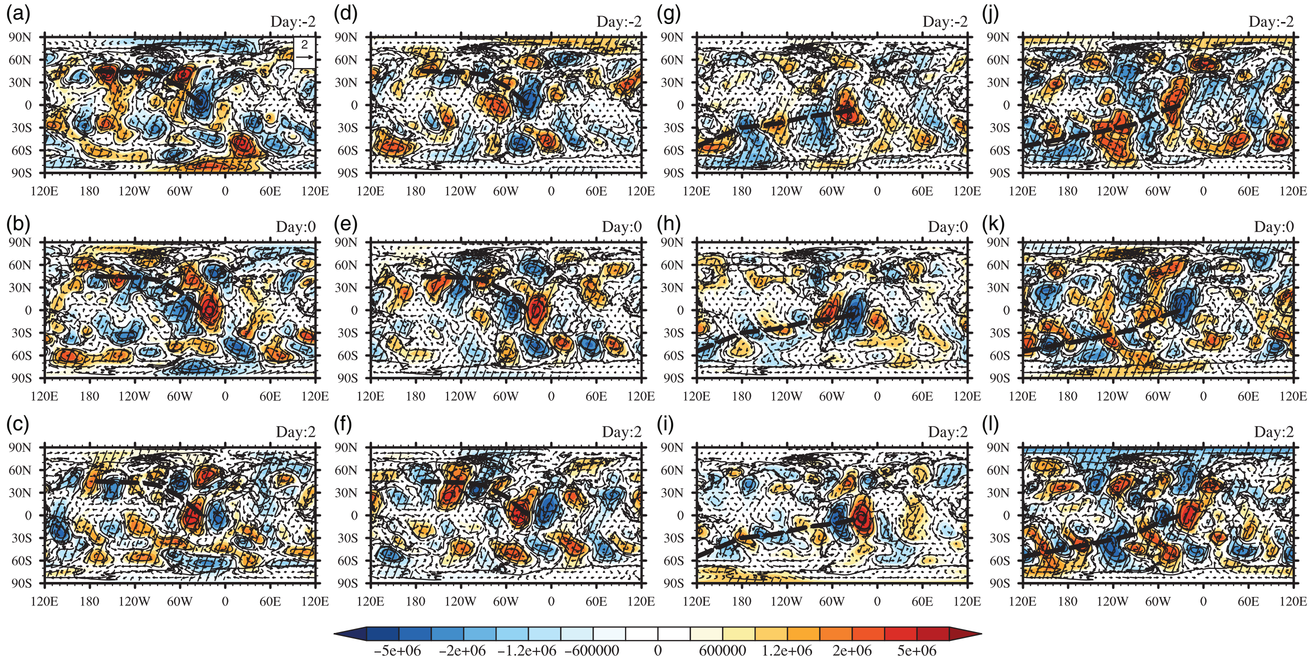

FIGURE 9 Lead–lag composites of intrusion mixed Rossby–Gravity (MRG) wave events over the Atlantic Ocean domain, constructed using 3–15-day bandpass-filtered 200 hPa wind ($m \cdot s^{-1}$) and stream function ($m^2 \cdot s^{-1}$) anomalies. Positive (negative) lag represents the number of days after (before) the maximum MRG wave amplitude. (a–c) NH intrusion MRG wave events during NH summer. (d–f) NH intrusion MRG wave events during NH winter; (g–i) SH intrusion MRG wave events during NH summer; and (j–l) SH intrusion MRG wave events during NH winter. Black dashed curves highlight the intrusions of extratropical disturbances. Stippled regions are statistically significant at the 95% confidence level. [Colour figure can be viewed at wileyonlinelibrary.com]

Similar to life cycle composites of the intrusion MRG wave events over the EP domain, northwest–southeast-oriented and southwest–northeast-oriented equatorward and eastward-propagating extratropical disturbances are observed over the AO domain during summer and winter (Figure 9). It seems that the inter-hemispheric propagation of extratropical disturbances is more likely over the AO domain (Figure 9a–f). It can be deduced from the lead–lag composites that the intruding extratropical disturbances exhibit wavenumbers in the range of 4–7 (Figures 8, 9).

Figure 10 represents the composites of 3–15-day filtered 200-hPa wind and stream function anomalies of non-intrusion MRG wave events over the IO, WP, EP and AO domains during summer and winter. The composites are created for the day of the maximum MRG amplitude of non-intrusion MRG wave events. As expected, the composites of MRG non-intrusion wave events show that extratropical disturbances are either absent or weak and do not intrude into the tropics during NH summer and winter over all the domains (Figure 10). The results of the composite analyses for intrusion and non-intrusion MRG wave events validate the robustness of the method employed in classifying the MRG wave events.

Some previous studies based on idealised modelling experiments argued that lateral forcing and different configurations of mean winds can induce differences in the properties of MRG waves (Mak, 1969; Wang & Xie, 1996; Zhang & Webster, 1992). To explore whether the intrusion and non-intrusion MRG wave events exhibit notable differences in their properties, the statistical modes of the amplitude, wavenumber, trapping scale, phase speed and duration of the two groups of MRG wave events are examined during summer and winter (Figure 11). The analysis is restricted to the EP and AO domains since approx. 88% of the intrusion MRG wave events are observed over these domains. The non-intrusion MRG wave events exhibit a larger amplitude during the summer season compared to winter over both domains (Figure 11a,f), consistent with the larger MRG amplitude observed during summer (Figure 7a). Over the EP domain, where the largest-amplitude MRG wave events are observed, during the winter season, intrusion MRG wave events exhibit a larger amplitude than the non-intrusion MRG wave events and during the summer season, the amplitude of non-intrusion MRG wave events exceeds that of intrusion MRG wave events. This explains the low seasonal variability in MRG amplitude over the EP domain. Zhang and Webster (1992) hypothesised that the MRG waves would exhibit stronger amplitudes in the regions of westerly mean zonal winds, under the influence of lateral intrusions. As seen in Figure 2,

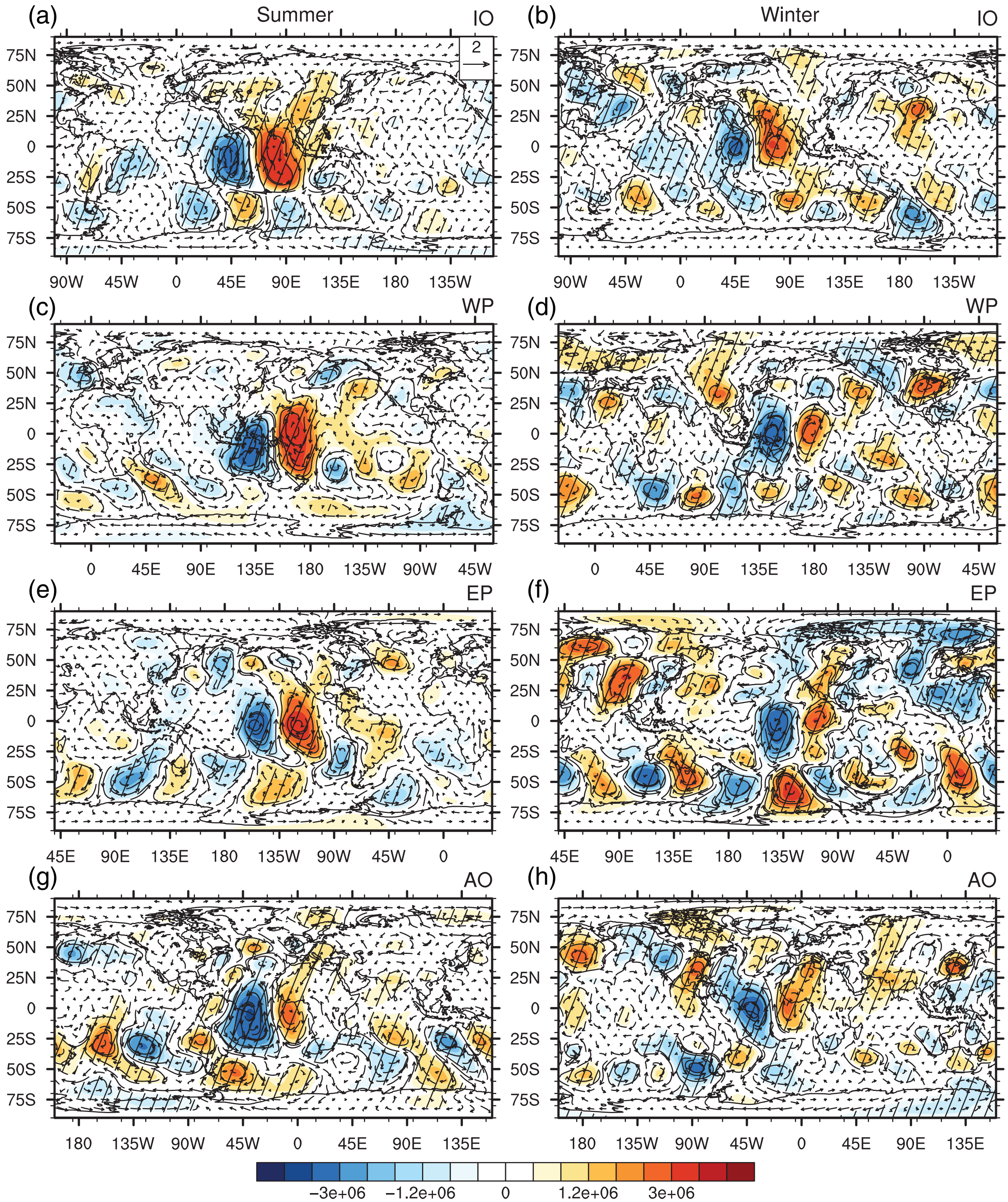

FIGURE 10 Composite non-intrusion mixed Rossby–Gravity (MRG) wave events constructed using 3–15-day bandpass-filtered 200 hPa wind ($m \cdot s^{-1}$) and stream function ($m^2 \cdot s^{-1}$) anomalies over the composites of 3–15-day bandpass-filtered 200 hPa wind ($m \cdot s^{-1}$) and stream function ($m^2 \cdot s^{-1}$) anomalies of non-intrusion MRG events occurring over: (a,b) the Indian Ocean; (c,d) West Pacific; (e,f) central–east Pacific; and (g,h) Atlantic Ocean domains during NH summer (left column) and winter (right column). Stippled regions are statistically significant at the 95% confidence level. [Colour figure can be viewed at wileyonlinelibrary.com]

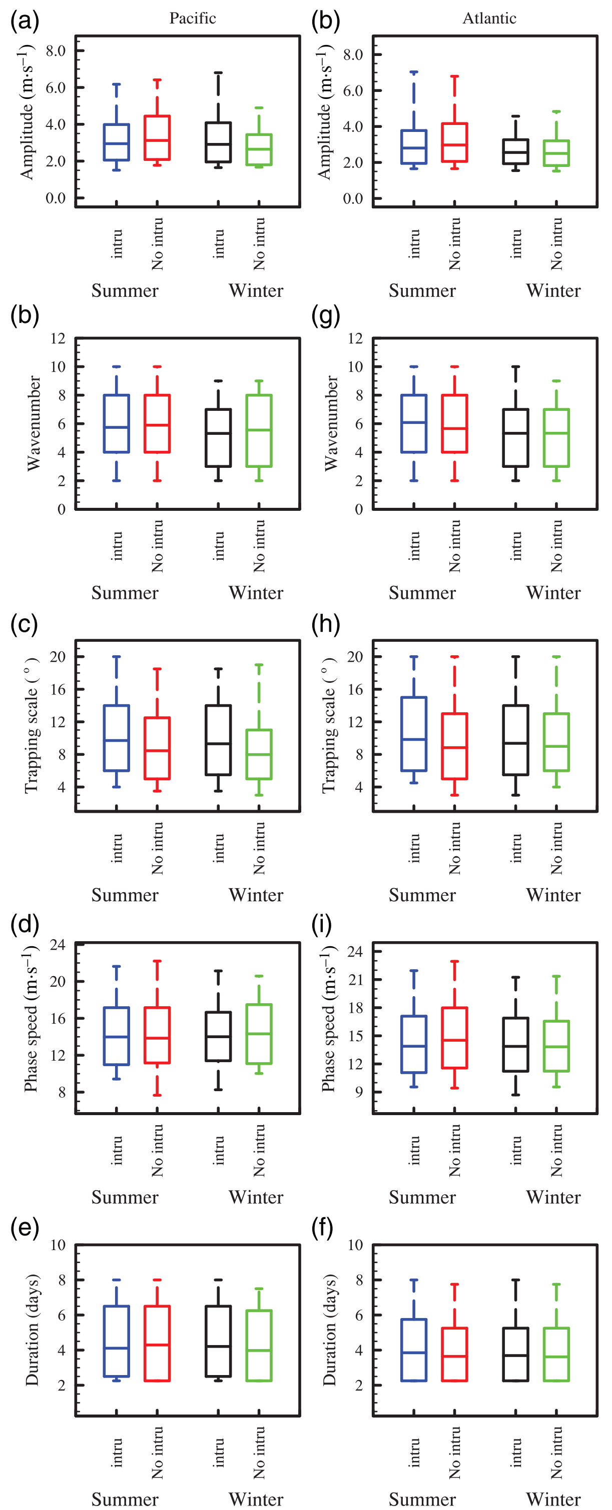

FIGURE 11 Range (maxima, minima), 90th percentile,mean, and 10th percentile of: (a,f) amplitude (m·s^{-1}); (b,g) wavenumber; (c,h) trapping scale (∘); (d,i) phase speed (m·s^{-1}); and(e,j) duration (days) of intrusion and non-intrusion mixedRossby–Gravity (MRG) wave events occurring over the central–eastPacific (left column) and Atlantic Ocean (right column) domains during NH summer and winter. Grey and black boxes represent intrusion and non-intrusion MRG wave events, respectively for NH summers and NH winters. [Colour figure can be viewed at wileyonlinelibrary.com]

the upper-tropospheric westerly wind ducts are well developed over the EP and AO domains only during the winter season. Consistent with this, the amplitude of intrusion MRG wave events is higher than that of the non-intrusion MRG wave events over the EP domain during the winter season (statistically significant at the 95% confidence level) (Figure 11a). Over the AO domain, where the smallest-amplitude MRG wave events are observed, the summer intrusion MRG wave events exhibit a larger amplitude compared to their winter counterparts (Figure 11f). Even though the MRG wave events prefer to have higher wavenumbers during NH summer over the EP and AO domains, the wavenumbers of intrusion and non-intrusion MRG wave events do not exhibit a clear separation except over the EP domain during NH winter (Figure 11b,g). Unlike the distribution of amplitudes and wavenumbers, statistical modes of trapping scales of intrusion and non-intrusion MRG wave events exhibit a clear separation over the EP and AO domains and it is evident from Figure 11c,h that the intrusion MRG events are less trapped to the equator (statistically significant at the 90% confidence level). However, the phase speeds and duration of the intrusion and non-intrusion MRG wave events do not show a noticeable difference in their distributions over the EP and AO domains (Figure 11d,e,i,j).

The whisker plots provide some insights on the role of extratropical disturbances in the genesis of MRG waves over the EP. According to linear wave theory, lateral forcing by eastward-moving extratropical disturbances cannot cause resonance in westward-propagating MRG waves (Yang & Hoskins, 2016). However, contrasting differences in the wave properties of intrusion and non-intrusion MRG wave events over the EP during NH winter indicate the possibility of resonant interactions. For example, the intrusion MRG wave events have a stronger amplitude and a larger meridional extent compared to non-intrusion MRG wave events (statistically significant at the 90% confidence level) (Figure 11a,c). The intrusion MRG wave events also exhibit a spatial scale similar to that of the extratropical disturbances (wavenumber 4–7) implying that resonant interactions may be a primary mechanism for the genesis of MRG wave events during NH winter. During NH summer, on the other hand, extratropical disturbances seemingly act as a catalytic factor in intensifying the MRG wave events. Past studies have shown observational evidence for the decisive role of intrusion of extratropical disturbances in determining the strength of the MRG waves during NH summer (Magaña & Yanai, 1995; Suhas et al., 2020). It can be deduced from the shorter wavelengths, smaller trapping scales (Figure 11b,c), and stronger convection–circulation coupling strength (Suhas et al., 2020) exhibited by the MRG wave events during NH summer that they could be primarily triggered by convective processes. However, the observed weakening of the strength of MRG waves in the absence of intrusion of extratropical disturbances via the SH suggests that lateral forcing may be instrumental in amplifying their amplitude.

4 | SUMMARY AND CONCLUSIONS

In this study we have conducted a survey of westward-propagating MRG wave events at 200 hPa and quantified their association with the intrusions of extratropical disturbances using ERA-I reanalysis data for the period 1979–2019. MRG wave events are identified by imposing the theoretical meridional structure of MRG waves onto the equatorial meridional wind anomalies (Au-Yeung & Tam, 2018). The method is ideal for capturing the episodic nature of MRG waves and it also provides the instantaneous values of its amplitude, phase speed, wavenumber and trapping scale. We have identified 2390 MRG wave events in the upper troposphere and the majority (61%) of them occurred during the months of May–October (Figure 5). As pointed out by many previous studies, MRG wave events over the EP and AO domains account for a major chunk (65%) of the total MRG wave events (Table 1). Statistical modes of wave properties of the MRG wave events over the IO, western Pacific, EP and AO reveal that not only the frequency of occurrence but also the amplitude, wavenumber and trapping scale of the MRG wave events exhibit a clear seasonality (Figure 7). MRG wave events exhibit higher amplitudes and shorter wavelengths during the NH summer. MRG wave events observed over the IO domain are more closely trapped to the equator during NH summer. The MRG wave events observed in the western hemisphere are lesser trapped to the equator and it is also noted that the trapping scales do not exhibit significant seasonal variability. The phase speeds of the MRG wave events do not exhibit significant variability.

MRG wave events are classified as intrusion MRG wave events if the PV on the 350-K isentropic surface at 15° N/S latitude in the spatial–temporal neighbourhood of the MRG wave events is greater than 1 PVU. Such events are further classified as NH intrusion or SH intrusion MRG wave events based on the hemisphere where the intrusions of extratropical disturbances are observed. We find that 37% of the MRG wave events are associated with intrusions of extratropical disturbances and a large majority (88%) of such events occur over the EP and AO domains. Larger numbers of NH (SH) intrusion MRG wave events are found to occur during the NH (SH) winter. Although the intrusions of extratropical disturbances occur in both hemispheres over the EP and AO domains, it is interesting to note that nearly 70% of the intrusions of extratropical disturbances associated with the MRG wave events occur in the winter hemisphere. The predominant preference of the winter hemispheric route of intruding extratropical disturbances corroborates the extratropical–tropical interaction theory of Webster and Holton (1982). Detailed analysis reveals that the amplitude, wavenumber and trapping scale of intrusion and non-intrusion MRG wave events are distinctly different only over the EP during NH winter (Figure 11). The intrusion MRG wave events exhibit higher amplitudes, lower wavenumbers, and larger trapping scales compared to the non-intrusion MRG wave events. Coherent evolution of extratropical and tropical disturbances is evident in the intrusion MRG wave events life cycle composites (Figures 8, 9) validating the classification of MRG wave events into intrusion and non-intrusion categories. Equatorward-propagating extratropical disturbances show northwest–southeast and southwest–northeast tilt in the NH and the SH, respectively. It is inferred from the life cycle composites that extratropical disturbances associated with the MRG wave events have wavenumbers in the range of 4–7. Stronger extratropical disturbances a few days before the MRG amplitude maxima and weakening of extratropical disturbances a few days after the MRG amplitude maxima indicate the possibility that such MRG wave events might be forced by the extratropical disturbances.

The study reveals that 37% of the MRG wave events are associated with intrusions of extratropical disturbances. It implies that external forcing of MRG waves is as important as their in-situ genesis mechanisms. Even though the diagnostic analyses may be insufficient to clearly establish the impact of lateral forcing via extratropical disturbances in exciting MRG wave events, probable scenarios can be deduced from the analyses. The observation of stronger amplitudes and larger trapping scales exhibited by intrusion MRG wave events and the similarity in spatial scales of the MRG wave events and extratropical disturbances suggest the role of resonant interactions between these two modes over the EP during NH winter. Past studies showed that the intrusions of extratropical disturbances is a crucial factor governing the strength of MRG waves during NH summer and fall (Magaña & Yanai, 1995; Suhas et al., 2020). However, the absence of a clear difference in the amplitudes of intrusion and non-intrusion MRG wave events over the EP and AOdomains during NH summer rules out the possibility of resonant interactions. It could be possible that the MRG waves are excited by random convective perturbations over the EP and Atlantic domains which in turn might be amplified by the intruding extratropical disturbances (Salby and Garcia, 1987). Without such amplification by intrusions of extratropical disturbances, the growth of the MRG perturbations induced by convective processes may be limited.

ACKNOWLEDGEMENTS

We are grateful to Dr George Kiladis for his feedback and comments. The study is a part of K. Shreya's PhD dissertation. E. Suhas acknowledges the Ministry of Earth Science, Government of India, for the REACHOUT grant.

DATA AVAILABILITY STATEMENT

All the data used in this study are freely available from public data repositories. ERA-interim reanalysis data (Dee et al., 2011) can be accessed from: https://apps.ecmwf.int/datasets/data/interim-full-daily/levtype=sfc/. Daily NOAA interpolated OLR data (Liebmann & Hendon, 1990) can be accessed from: https://psl.noaa.gov/data/gridded/data.interp_OLR.html.

ENDNOTE

[1] Although the wave-fitting methodology can be used as an approximation of wave projection methodology in identifying the MRG wave events, it should be noted that the wave-fitting methodology works only with the meridional winds since the zonal winds of MRG waves are identified by two parabolic cylindrical functions.

ORCID

E. Suhas https://orcid.org/0000-0002-4813-613X

REFERENCES

Aiyyer, A. & Molinari, J.E. (2003) Evolution of mixed Rossby–gravity waves in idealized MJO environments. *Journal of Atmospheric Science*, 60(23), 2837–2855. Available from: https://doi.org/10.1175/1520-0469(2003)060<2837:EOMRWI>2.0.CO;2

Arkin, P.A. & Webster, P.J. (1985) Annual and interannual variability of tropical–extratropical interaction: an empirical study. *Monthly Weather Review*, 113(9), 1510–1523. Available from: https://doi.org/10.1175/1520-0493(1985)113<1510:AAIVOT>2.0.CO;2

Au-Yeung, A.Y.M. & Tam, C.Y. (2018) Dispersion characteristics and circulation associated with boreal summer westward-traveling mixed Rossby-gravity wave-like disturbances. *Journal of Atmospheric Science*, 75(2), 513–533. Available from: https://doi.org/10.1175/JAS-D-16-0245.1

Charney, J.G. (1963) A note on large-scale motions in the tropics. *Journal of Atmospheric Science*, 20(6), 607–609. Available from: https://doi.org/10.1175/1520-0469(1963)020<0607:ANOLSM>2.0.CO;2

Chen, B., Tung, W.-W. & Yanai, M. (2016) Multiscale temporal mean features of perturbation kinetic energy and its budget in the tropics: review and computation. *Meteorological Monographs*, 56(1), 8.1–8.23. Available from: https://doi.org/10.1175/AMSMONOGRAPHS-D-15-0017.1

Dee, D.P., Uppala, S.M., Simmons, A.J., Berrisford, P., Poli, P., Kobayashi, S. et al. (2011) The ERA-interim reanalysis: configuration and performance of the data assimilation system. *Quarterly Journal of Royal Meteorological Society*, 137(656), 553–597. Available from: https://doi.org/10.1002/qj.828

Dias, J. & Kiladis, G.N. (2014) Influence of the basic state zonal flow on convectively coupled equatorial waves. *Geophysical Research Letters*, 41(19), 6904–6913. Available from: https://doi.org/10.1002/2014GL061476

Feng, T., Yang, X.Q., Zhou, W., Huang, R., Wu, L. & Yang, D. (2016) Synoptic-scale waves in sheared background flow over the western North Pacific. *Journal of Atmospheric Science*, 73(11), 4583–4603. Available from: https://doi.org/10.1175/JAS-D-16-0064.1

Gray, L.J., Anstey, J.A., Kawatani, Y., Lu, H., Osprey, S. & Schenzinger, V. (2018) Surface impacts of quasi biennial oscillation. *Atmospheric Chemistry and Physics*, 18(11), 8227–8247.

Hendon, H.H. & Liebmann, B. (1991) The structure and annual variation of antisymmetric fluctuations of tropical convection and their association with Rossby–gravity waves. *Journal of Atmospheric Science*, 48(19), 2127–2140. Available from: https://doi.org/10.1175/1520-0469(1991)048<2127:TSAAVO>2.0.CO;2

Holton, J.R. (2004) *Introduction to dynamic meteorology*, 4th edition. Amsterdam: Elsevier Academic Press, p. 535.

Holton, J.R. & Lindzen, R.S. (1972) An updated theory for the quasi-biennial cycle of the tropical stratosphere. *Journal of Atmospheric Science*, 29(6), 1076–1080. Available from: https://doi.org/10.1175/1520-0469(1972)029<1076:AUTFTQ>2.0.CO;2

Hoskins, B.J. & Yang, G.-Y. (2016) The longitudinal variation of equatorial waves due to propagation on a varying zonal flow. *Journal of Atmospheric Science*, 73(2), 605–620. Available from: https://doi.org/10.1175/JAS-D-15-0167.1

Kang, M.-J. & Chun, H.-Y. (2021) Contributions of equatorial planetary waves and small-scale convective gravity waves to the 2019/20 QBO disruption. *Atmospheric Chemistry and Physics*, 21(12), 9839–9857. Available from: https://doi.org/10.5194/acp-2021-85

Kang, M.-J., Chun, H.-Y. & Garcia, R.R. (2020) Role of equatorial waves and convective gravity waves in the 2015/16 quasi-biennial oscillation disruption. *Atmospheric Chemistry and Physics*, 20(23), 14669–14693. Available from: https://doi.org/10.5194/acp-20-14669-2020

Kikuchi, K. (2014) An introduction to combined Fourier–wavelet transform and its application to convectively coupled equatorial waves. *Climate Dynamics*, 43, 1339–1356. Available from: https://doi.org/10.1007/s00382-013-1949-8

Kiladis, G.N. (1998) Observations of Rossby waves linked to convection over the eastern tropical Pacific. *Journal of Atmospheric Science*, 55(3), 321–339. Available from: https://doi.org/10.1175/1520-0469(1998)055<0321:OORWLT>2.0.CO;2

Kiladis, G.N., Dias, J. & Gehne, M. (2016) The relationship between equatorial mixed Rossby–gravity and eastward inertio-gravity waves part I. *Journal of Atmospheric Science*, 73(5), 2123–2145. Available from: https://doi.org/10.1175/JAS-D-15-0230.1

Kiladis, G.N., Wheeler, M.C., Haertel, P.T., Straub, K.H. & Roundy, P.E. (2009) Convectively coupled equatorial waves. *Reviews of Geophysics*, 47(2), RG2003. Available from: https://doi.org/10.1029/2008RG000266

Knippertz, P. et al. (2022) The intricacies of identifying equatorial waves. *Quarterly Journal of Meteorological Society*, 148(747), 2814–2852. Available from: https://doi.org/10.1002/qj.4338

Liebmann, B. & Hendon, H.H. (1990) Synoptic-scale disturbances near the equator. *Journal of Atmospheric Science*, 47(12), 1463–1479. Available from: https://doi.org/10.1175/1520-0469(1990)047<1463:SSDNTE>2.0.CO;2

Lin, P., Held, I. & Ming, Y. (2019) The early development of the 2015/16 quasi-biennial oscillation disruption. *Journal of Atmospheric Science*, 76(3), 821–836. Available from: https://doi.org/10.1175/JAS-D-18-0292.1

Magaña, V. & Yanai, M. (1995) Mixed Rossby–gravity waves triggered by lateral forcing. *Journal of Atmospheric Science*, 52(9), 1473–1486. Available from: https://doi.org/10.1175/1520-0469(1995)052<1473:MRWTBL>2.0.CO;2

Mak, M.K. (1969) Laterally driven stochastic motions in the tropics. *Journal of Atmospheric Science*, 26(1), 41–64. Available from: https://doi.org/10.1175/1520-0469(1969)026<0041:LDSMIT>2.0.CO;2

Matsuno, T. (1966) Quasi-geostrophic motions in the equatorial area. *Journal of the Meteorological Society of Japan. Ser. II*, 44(1), 25–43. Available from: https://doi.org/10.2151/jmsj1965.44.1_25

Pritchard, M.S. & Yang, D. (2016) Response of the superparameterized madden–Julian oscillation to extreme climate and basic-state variation challenges a moisture mode view. *Journal of Climate*, 29(13), 4995–5008. Available from: https://doi.org/10.1175/JCLI-D-15-0790.1

Randel, W.J. (1992) Upper tropospheric equatorial waves in ECMWF analyses. *Quarterly Journal of Royal Meteorological Society*, 118(504), 365–394. Available from: https://doi.org/10.1002/qj.49711850409

Ripa, P. (1983) General stability conditions for zonal flows in a one-layer model on the beta-plane or sphere. *Journal of Fluid Mechanics*, 126, 463–489. Available from: https://doi.org/10.1002/qj.504

Suhas, E., Neena, J.M. & Jiang, X. (2020) Exploring the factors influencing the strength and variability of convectively coupled mixed Rossby–gravity waves. *Journal of Climate*, 33(22), 9705–9719. Available from: https://doi.org/10.1175/JCLI-D-20-0218.1

Takasuka, D. & Satoh, M. (2020) Dynamical roles of mixed Rossby-gravity waves in driving convective initiation and propagation of the madden-Julian oscillation: general views. *Journal of the Atmospheric Sciences*, 77(12), 4211–4231. Available from: https://doi.org/10.1175/JAS-D-20-0050.1

Takasuka, D. & Satoh, M. (2021) Diversity of the madden–Julian oscillation: initiation region modulated by the interaction between the Intraseasonal and interannual variabilities. *Journal of Climate*, 34(6), 2297–2318. Available from: https://doi.org/10.1175/JCLI-D-20-0688.1

Takasuka, D., Satoh, M. & Yokoi, S. (2019) Observational evidence of mixed Rossby-gravity waves as a driving force for the MJO convective initiation and propagation. *Geophysical Research Letters*, 46(10), 5546–5555. Available from: https://doi.org/10.1029/2019GL083108

Takayabu, Y.N. (1994a) Large-scale cloud disturbances associated with equatorial waves. Part I: spectral features of the cloud disturbances. *Journal of the Meteorological Society of Japan. Ser. II*, 72(3), 433–449. Available from: https://doi.org/10.2151/jmsj1965.72.3_433

Takayabu, Y.N. (1994b) Large-scale cloud disturbances associated with equatorial waves. Part II: westward-propagating inertio-gravity waves. *Journal of the Meteorological Society of Japan. Ser. II*, 72(3), 451–465. Available from: https://doi.org/10.2151/jmsj1965.72.3_451

Takayabu, Y.N., Kiladis, G.N. & Magaña, V. (2016) Michio Yanai and tropical waves. *Meteorological Monographs*, 56(1), 3.1–3.21. Available from: https://doi.org/10.1175/AMSMONOGRAPHS-D-15-0019.1

Takayabu, Y.N. & Nitta, T. (1993) 3–5 day-period disturbances coupled with convection over the tropical Pacific Ocean. *Journal of the Meteorological Society of Japan. Ser. II*, 71(2), 221–246. Available from: https://doi.org/10.2151/jmsj1965.71.2_221

Tomas, R. & Webster, P.J. (1994) Vertical and horizontal structure of cross-equatorial wave propagation. *Journal of Atmospheric Science*, 51(11), 1417–1430. Available from: https://doi.org/10.1175/1520-0469(1994)051<1417:HAVSOC>2.0.CO;2

Vishnupriya, S., Suhas, E. & Sandeep, S. (2022) Extratropical stratospheric air intrusions over the Western North Pacific and the genesis of downstream monsoon low-pressure systems. *Geophysical Research Letters*, 49(23), e2022GL100976. Available from: https://doi.org/10.1029/2022GL100976

Wang, B. & Xie, X. (1996) Low-frequency equatorial waves in vertically sheared zonal flow. Part I: stable waves. *Journal of Atmospheric Science*, 53(3), 449–467. Available from: https://doi.org/10.1175/1520-0469(1996)053<0449:LFEWIV>2.0.CO;2

Waugh, D.W. & Polvani, L.M. (2000) Climatology of intrusions into the tropical upper troposphere. *Geophysical Research Letters*, 27(23), 3857–3860. Available from: https://doi.org/10.1029/2000GL012250

Webster, P.J. & Chang, H.R. (1988) Equatorial energy accumulation and emanation regions: impacts of a zonally varying basic state. *Journal of the Atmospheric Sciences*, 45(5), 803–829. Available from: https://doi.org/10.1175/1520-0469(1988)045<0803:EEAAER>2.0.CO;2

Webster, P.J. & Holton, J.R. (1982) Cross-equatorial response to midlatitude forcing in a zonally varying basic state. *Journal of Atmospheric Science*, 39(4), 722–733. Available from: https://doi.org/10.1175/1520-0469(1982)039<0722:CERTML>2.0.CO;2

Wheeler, M. & Kiladis, G.N. (1999) Convectively coupled equatorial waves: analysis of clouds and temperature in the wavenumber–frequency domain. *Journal of Atmospheric Science*, 56(3), 374–399. Available from: https://doi.org/10.1175/1520-0469(1999)056<0374:CCEWAO>2.0.CO;2

Wheeler, M., Kiladis, G.N. & Webster, P.J. (2000) Large-scale dynamical fields associated with convectively coupled equatorial waves. *Journal of Atmospheric Science*, 57(5), 613–640. Available from: https://doi.org/10.1175/1520-0469(2000)057<0613:LSDFAW>2.0.CO;2

Yanai, M., Chen, B. & Tung, W.-W. (2000) The madden–Julian oscillation observed during the TOGA COARE IOP: global view. *Journal of Atmospheric Science*, 57(15), 2374–2396. Available from: https://doi.org/10.1175/1520-0469(2000)057<2374:TMJOOD>2.0.CO;2

Yanai, M. & Lu, M.M. (1983) Equatorially trapped waves at the 200 mb level and their association with meridional convergence of wave energy flux. *Journal of Atmospheric Science*, 40(12), 2785–2803. Available from: https://doi.org/10.1175/1520-0469(1983)040<2785:ETWATM>2.0.CO;2

Yanai, M., Maruyama, T., Nitta, T. & Hayashi, Y. (1968) Power spectra of large-scale disturbances over the tropical Pacific. *Journal of the Meteorological Society of Japan. Ser. II*, 46(4), 308–323. Available from: https://doi.org/10.2151/jmsj1965.46.4_308

Yang, D. & Ingersoll, A.P. (2011) Testing the hypothesis that the MJO is a mixed Rossby–gravity wave packet. *Journal of Atmospheric Science*, 68(2), 226–239. Available from: https://doi.org/10.1175/2010JAS3563.1

Yang, G.Y., Feng, X. & Hodges, K. (2023) Seasonal and interannual variation of equatorial waves in ERA5 and GloSea5. *Quarterly Journal of Royal Meteorological Society*, 149(752), 1109–1134. Available from: https://doi.org/10.1002/qj.4460

Yang, G.Y. & Hoskins, B.J. (2016) ENSO related variation of equatorial MRG and Rossby waves and forcing from higher latitudes. *Quarterly Journal of Royal Meteorological Society*, 142(699), 2488–2504. Available from: https://doi.org/10.1002/qj.2842

Yang, G.Y., Hoskins, B.J. & Slingo, J. (2003) Convectively coupled equatorial waves: a new methodology for identifying wave structures in observational data. *Journal of Atmospheric Science*, 60(14), 1637–1654. Available from: https://doi.org/10.1175/1520-0469(2003)060<1637:CCEWAN>2.0.CO;2

Yang, G.Y., Hoskins, B.J. & Slingo, J. (2007) Convectively coupled equatorial waves: part III: synthesis structures and extratropical forcing. *Journal of Atmospheric Science*, 64, 3438–3451.

Yasunaga, K. (2011) Seasonality and regionality of the madden–Julian oscillation and convectively coupled equatorial waves. *Scientific Online Letters in the Atmosphere (SOLA)*, 7, 153–156. Available from: https://doi.org/10.2151/sola.2011-039

Zangvil, A. & Yanai, M. (1981) Upper tropospheric waves in the tropics. Part II: association with clouds in the wave number-frequency domain. *Journal of Atmospheric Science*, 38(5), 939–953. Available from: https://doi.org/10.1175/1520-0469(1981)038<0939:UTWITT>2.0.CO;2

Zhang, C. & Webster, P.J. (1989) Effects of zonal flows on equatorially trapped waves. *Journal of Atmospheric Science*, 46(24), 3632–3652. Available from: https://doi.org/10.1175/1520-0469(1989)046<3632:EOZFOE>2.0.CO;2

Zhang, C. & Webster, P.J. (1992) Laterally forced equatorial perturbations in a linear model. Part I: stationary transient flow. *Journal of Atmospheric Science*, 49(7), 585–607. Available from: https://doi.org/10.1175/1520-0469(1992)049<0585:LFEPIA>2.0.CO;2

Zhou, X. & Wang, B. (2007) Transition from an eastern Pacific upper-level mixed Rossby-gravity wave to a western Pacific tropical cyclone. *Geophysical Research Letters*, 34(24), L24801. Available from: https://doi.org/10.1029/2007GL031831

How to cite this article: Shreya, K. & Suhas, E. (2024) A survey of westward-propagating mixed Rossby–Gravity waves and quantification of their association with extratropical disturbances. *Quarterly Journal of the Royal Meteorological Society*, 1–19. Available from: https://doi.org/10.1002/qj.4668